TOJSAT
The Online Journal of Science and Technology

ISSN 2146-7390

The Online Journal of Science and Technology

Volume 8 Issue 4
October 2018

www.tojsat.net
October 2018

Published in TURKEY

Contact Address:

Prof. Dr. Mustafa Şahin Dündar - TOJSAT, Editor Sakarya-Turkey

Message from the Editor-in-Chief

Dear Colleagues,

TOJSAT welcomes you. TOJSAT would like to thank you for your online journal interest. The online journal system has been diffused very fast for last eight years. We are delighted that academicians, scientists, educators, teachers, and students from around the world have visited TOJSAT. It means that TOJSAT has continued to diffuse new trends in science and technology to all over the world for eight years. We hope that the volume 8, issue 4 will also successfully accomplish our global science and technology goal.

TOJSAT is confident that readers will learn and get different aspects on science and technology. Any views expressed in this publication are the views of the authors and are not the views of the Editor and TOJSAT.

TOJSAT thanks and appreciate the editorial board who have acted as reviewers for one or more submissions of this issue for their valuable contributions.

TOJSAT will organize ISTEC 2019 conference. The ISTEC 2019 conference book will be published at **http://www.iste-c.net/istecpubs**

For any suggestions and comments on the international online journal TOJSAT, please do not hesitate to send e-mail.

Call for Papers
TOJSAT invites you article contributions. Submitted articles should be about all aspects of science and technology. The articles should be original, unpublished, and not in consideration for publication elsewhere at the time of submission to TOJSAT. Manuscripts must be submitted in English.

TOJSAT is guided by it's editors, guest editors and advisory boards. If you are interested in contributing to TOJSAT as an author, guest editor or reviewer, please send your cv to tojsateditor@gmail.com.

October 01, 2018
Prof. Dr. Aytekin ISMAN
Sakarya University

Message from the Editor

Dear Readers,

Eight volume of the Online Journal of Science and Technology (Tojsat) is published since 2011. Audiences and readers of the journal is widening throughout the World and increasing especially after the conference series of Science and Technology. Tojsat journal is now indexed with Doaj, Dergipark, Cite Factor, Index Copernicus, and Google Scholar and will be cited by Scopus index soon.

The journal favours papers addressed to inter-disciplinary and multi-diciplinary articles shown in the section of scopes. In this issue of on line journal, selected papers such as Identifying Predictive Genes for Classification using Artificial Immune Recognition System, Depollution of Olive Mill Wastewater Through Electrocoagulation and Advanced Oxidation, Evaluation of Polyethylene Based Insulation Material in Textile Dyeing Machines, The reflection of Urban Poverty on Child Poverty, The Neutron Macroscopic Cross Sections Calculation of Some Minerals By Using Fluka Monte Carlo Method, etc. will be published.

I will thank to the readers for their supports by sending their valuable scientific works to publish in this journal.

Prof.Dr. Mustafa S. Dundar

Editor

Table of Contents

COMPARISON OF QUALITY PARAMETERS FOR RING AND OPEN-END ROTOR SPUN YARNS

Suat CANOGLU[1], S.Muge YUKSELOGLU[1], Nagihan KUCUK[2]
[1]Marmara University, Faculty of Technology, Department of Textile Engineering, Istanbul, TURKEY
[2] LC Waikiki Mağazacılık Hizmetleri Tic. A.Ş., Istanbul,TURKEY
scanoglu@marmara.edu.tr

Abstract: Spinning is a major part of the textile manufacturing process where among all these are ring spinning and open-end rotor spinning which are widely used in production of textiles. In this study, cotton (CO) and polyester (PES) fibers were used with various blends to produce both ring and open-end rotor spun yarns. These 3 different blends (33/67% PES/CO, 50/50 % PES/CO and 67/33 PES/ CO) of Ne 30/1 yarns were later knitted on a plain knitting machine. The physical properties of these produced spun yarns were studied i.e. evenness, hairiness, breaking strength and elongation with additionally pilling properties of the produced fabrics. It was observed that as the blend ratio of the PES fiber increases within the yarn structure the both breaking strength and elongation gets higher on the ring-spun and open-end rotor spun yarns. Among all these produced blended spun yarns, the highest breaking strength and elongation is 21.79 cN/tex and 8.96% respectively. Evenness test results showed that ring spun yarns presented better values than the open-end rotor spun yarns; the lowest %CV %90 was obtained on the %67/33 PES/CO ring spun yarns. Both imperfection values and hairiness gets better as the PES ratio increases within the both yarn types. On the other hand, better pilling resistance was obtained on the OE-rotor spun than the ring spun yarns. The pilling values also indicate that as the PES fiber ratio increases within the open-end rotor spun yarns it shows better pilling (pilling scale 4-5).
Keywords: Ring, Open-end, Rotor, Imperfections, Mechanical properties, Hairiness

Introduction

Staple yarns are constructed from the bundle of fibers, which are twisted together during the spinning process. The widely used ones are ring spinning and open-end rotor spinning technologies. If one would like to have a brief look to these techniques are given below:

The ring spinning machine was first invented by Thorp in 1828 and later Jenk added the traveler rotating around the ring in 1830. In the intervening period of more than 170 years the ring spinning machine has undergone considerable modification in detail, but the basic concept has remained the same. For many years any noteworthy further development hardly seemed possible, yet a significant process of evolution took place during this time (Ahmed, 2016). The principle of ring spinning is illustrated in Figure 1. A bundle of parallel fibers which are roving slivers fed to the drafting zone. The difference in surface velocity are obtained with the help of roller speeds; the front roller is faster and back roller is slower ones, hence drafting rollers will attenuate the roving to a thinner strand of parallel fibers, under the control of the double aprons. The thin strand of parallel fibers emerging from the front rollers is then simultaneously twisted and wound onto a yarn package (i.e., cop) mounted on a driven spindle. The twisted thin strand of fibers, now called a yarn, is threaded through a traveller and a yarn guide and balloons out between these two elements during spinning. The twisted yarn is then wound onto the bobbin or yarn package (Tang, 2006).

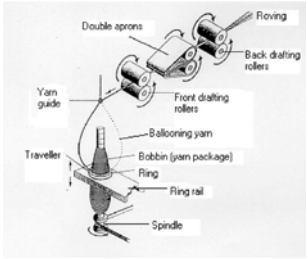

Figure1. The ring spinning process (Tang, 2006)

On the other hand, commercial open end-rotor spinning was first developed in 1967 in Czechoslovakia. Open-end rotor spinning has been characterized from the outset by incomparably higher production potential than ring spinning. This potential has been increased by the higher rotor speeds and winding up speeds and also there is no

need for roving process. Therefore, rotor-spun yarns are also can manufactured much cheaper than the ring-spun yarns. Rotor spinning combines in two process stages namely spinning and winding at the same single machine. Additionally the rotor spinning system is able to process carded or draw frame slivers directly. Last but not least, the rotor spinning system has benefited from the fact that operator functions on the rotor spinning machine were much easier to automate than those on the ring spinning machine. After the sliver has been opened on the opening roller are fed through the fiber transport channel individually to the collecting groove of the rotor itself. The rotor itself is also a twisting device of this spinning system. Since the individual fibers are released from a compact fiber bundle to the individually ones, this can here refer to an open-end yarn. This brief explanation of the process is also presented in the Figure 2.

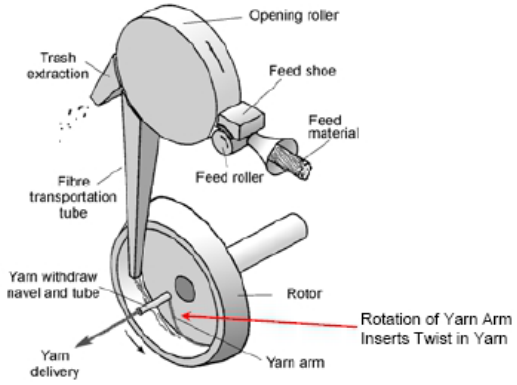

Figure 2. Principle of Rotor spinning (Sheikh and Emeritus, 2013)

One of the major distinctions between OE-rotor-spun yarns and ring spun yarns is the difference between the hairiness in the yarn. This was also studied by Tyagi et. al.(Tyagi, 2009) and they observed that open-end rotor spun yarns show less hairiness than the ring spun yarns which is related to twist factor. Strumillo et. al. (Strumillo, 2007) worked on quality parameters that may affect from different linear densities of cotton yarns on both ring and open-end rotor spun yarns; they determined various mathematical models on tenacity, elongation at break, unevenness, hairiness and the number of faults on the yarn's linear density.

Materials and Methods

In this study, polyester and cotton fibers and its different blends (PES/CO 33/67% -PES/CO 50/50 % - PES/CO 67/33%) were used at twist constant of α_e 3.3 and Ne 20 ring-spun carded yarns and open-end rotor-spun yarns were produced. The yarn tests were carried out at 20 ± 2 ^{0}C, 65% ± 2 RH conditions after the samples reaching equilibrium. The fibers properties of these materials are measured on the Spinlab HVI 900 and their results are given in Table 1, the specification of the machines are all presented in Table 1-5. The produced yarns were then knitted on the Dubied knitted machine with a knitting structure of supreme fabrics.

Table 1: Fiber parameters

Measured fiber parameters	Fiber used in the study	
	Cotton	Polyester
Cotton fiber fineness (micronaire)	4.74	-
Fiber length (ML) (mm)	28.2	-
Fiber strength (g/tex)	32.9	-
Fiber elongation (%)	9.4	-
(UR%)	50.4	-
Polyester fiber fineness (denier)	-	1.4
Fiber length (mm)	-	38

Table 2: Carding machine specifications

Technological/machine set parameters	Values
Main cylinder speed (rpm)	650
Production rate (m/min)	210
Sliver count (Ne)	0.120

Table 3: Draw-frame machine specifications

Technological/machine set parameters	Values
Rotor speed (rpm)	86000
Total draft	8
Roller Distance in break-draft zone (mm)	52
Number of fed slivers	8
Sliver count (Ne)	0.120

Table 4: Ring machine specifications

Technological/machine set parameters	Values
Ring yarn type	Conventional
Spindle speed (rev/min)	14500
Ring diameter (mm)	42
Type of traveler and ISO No	C1 UL udr and 31.5
Theoretical twist coefficient (α_e)	3.5
Theoretical twist (turns/inch)	19

Table 5: OE-Rotor machine specifications

Technological/machine set parameters	Values
Rotor speed (rev/min)	86000
Rotor diameter (mm)	32
Nozzle	Plain with 8 groves, ceramic (KK8K)

Results and Discussion

1. Yarn count, twist parameters, yarn breaking tenacity and elongation

In this study, 3 different blends of materials were produced on the ring and OE-rotor spinning machines with the total of 6 yarns at the same your count Ne 30. Table 6 presents the parameters of these produced yarns.

Table 6: Yarn parameters

Yarn abbreviations	Yarn count	Production type	Yarn types
M	Ne 30	Ring	PES/CO (33/67%)
N			PES/CO (50/50%)
O			PES/CO (67/33%)
P		OE-Rotor	PES/CO (33/67%)
R			PES/CO (50/50%)
S			PES/CO (67/33%)

Yarn counts, twist parameters and yarn breaking tenacity with elongation are tabulated in the Table 7. Breaking tenacity and elongation of these yarns were determined according to TS 245 standard by using Uster Tensojet 4. All tests were carried out in the standard atmosphere conditions (20 ± 2 C^0 and % 65 ± 2 RH) after 48 hours of equilibrium was reached.

Table 7: Yarn specifications

Yarn type	Abbreviations	Measured yarn count (Ne)	Measured yarn twist (turns/inch)	Measured breaking strength (cN/tex)	Measured elongation (%)
Ring	M	30.6	19,4	15.20	6.01
	N	30.4	19.8	19.39	7.54
	O	30.8	19.6	21.19	8.96
OE-Rotor	P	30.7	-	11.80	5.04
	R	30.5	-	12.10	7.02
	S	30.6	-	12.92	8.02

It can be seen from the results that as the PES ratio increases the breaking strength and elongation gets better. It is thought that PES is much stronger fiber than the cotton, therefore as the PES ratio increases within the blended yarns the overall fiber length also increases.

2. Yarn irregularity, imperfections and hairiness

Yarn irregularity, imperfections and hairiness were tested on the USTER TESTER 3. All samples run through the tester at 400 m/min. The results of these yarns are listed in the Table 8.

Table 8: Yarn irregularity, imperfections and hairiness values

Yarn type	Yarn Abbreviations	Mean linear irregularity, (U)	Thin places, (-50%)	Thick places, (+50%)	Neps,	Hairiness, (H)
Ring	M	12.92	11	208	250	4.64
	N	12.52	10	148	151	4.24
	O	12.18	8	102	120	3.94
OE-Rotor	P	14.80	230	300	988	4.44
	R	13.96	150	213	902	4.00
	S	13.18	105	185	671	3.77

It can be seen from the results that as the PES ratio increases the imperfections, irregularity and the hairiness of the yarns have shown improved parameters; this is due to the PES fiber length increment which is all same lengths of bundle in the blended yarns of cotton/polyester.

3. Fabrics production and pilling

The knitted supreme fabrics were measured on the Nu-Martindale tester for their pilling. The samples were conditioned under the standard atmosphere for 48 hours. Testing period was set 2000 rubs and later the samples were compared with the K3 EMPA Standard photographs [SN. 1985-25] for their pilling. Pilling values of the knitted fabrics are classified from worse to best as 1-3, 2-3, 3-4, 4-5 and the images of these samples are given as an example at the Figure 3. The pilling test results of these samples are given in Table 9.

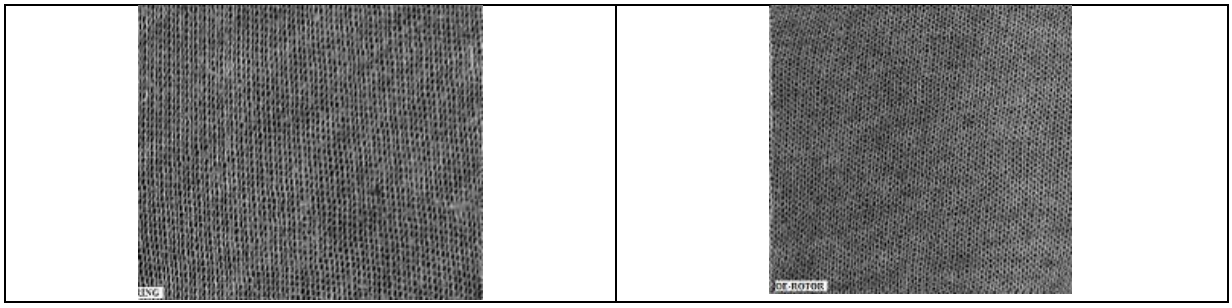

Ring knitted fabric OE-Rotor knitted fabric

Figure 3. 67/33 % PES/CO ring and OE-rotor knitted fabric pilling images

Table 9: Pilling data of the knitted fabrics

Yarn type	Yarn Abbreviations	Pilling values
Ring	M	1-2
	N	1-2
	O	2-3
OE-Rotor	P	3-4
	R	3-4
	S	4-5

From both Figure 3 and Table 9, it can be seen that as the PES ratio increases the hairiness of the yarns gets less hairy therefore the fiber protruding ends are much lesser on the surface of the yarn structure and this leads to less pilling on the knitted fabric surfaces.

Conclusion

The overall results are presented at the following conclusions:

1. Generally, as the PES ratio increases slight lower values occur on the linear irregularity of the yarns. This indicates that the produced yarns improved in means of regularity.

2. Overall ring and OE-rotor yarns presented enhance imperfection results as the PES ratio increases within the blends of the yarns.

3. All the ring and OE-rotor yarns offered an increase on both breaking strength and elongation of the samples as the PES ratio increases within the blends.

4. Ring yarns have lower irregularity than the OE-Rotor yarns.

5. Ring yarns have lower thick places (+ 50%), thin places (-50%) and neps than the OE-Rotor yarns.

6. Both ring and OE-Rotor yarns presented low hairiness values as the PES ratio increases.

7. Both ring and OE-Rotor yarns offered low neps values as the PES ratio increases.

8. Ring yarns produced better breaking strength and elongation values than the OE-rotor yarns.

9. OE-Rotor yarns presented better pilling than the ring yarns.

10. Both ring and OE-Rotor yarns show higher pilling values as PES ratio increases within the blends; this points out that the knitted fabrics do present better pillings.

Acknowledgements

The authors would like to thank to BAPKO (Scientific Research Project Commission of Marmara University) for funding the project FEN-D-070617-0386.

References

Ahmed, S., Syduzzaman, Md., Sultan Mahmud, Md., Ashique, S.M. & Rahman, M.M.(2016), Comparative study on ring, rotor and air-jet spun yarn, *European Scientific Journal* , Vol.11 , No.3 (pp411-424)

Sheikh & Emeritus (2013) , Development of open-end rotor spinning system, *Pakistan Textile Journal*, Vol.3

Strumillo, L.J., Cyniak, D., Czekalski, J & Jackowski, T (2007), Quality of cotton yarns spun using ring-compact-and rotor spinning machines as a function of selected spinning process parameters, *FIBRES & TEXTILES in Eastern Europe*, vol.15, No.1 (pp24-30)

Tang,Z.X., Wang, X., Fraser, W.B. & Wang, L.(2006), Simulation and experimental validation of a ring spinning process, *Simulation Modelling Practice and Theory*,Vol.14 (pp.809-816)

Tyagi, G.K., Bhattacharya, S.& Gupta, S. (2009), Pretreatment dependence of mechanical and surface properties of cotton ring- and OE rotor-spun yarns, *Indian Journal of Fibre and Textile Research*, Vol.34, March (pp.20-25)

TS245(ISO 2026).: "Tekstil-Paketlerden Alınan İplikler- Tek İpliğin Kopma Mukavemeti ve Uzamasının Tayini", Türk Stadartları Enstitüsü,Ankara, Türkiye (1996)

SN1985-25.: Empa Kumaş Boncuklanma(pilling) Standartları

CREEP BEHAVIOR PREDICTION OF ALUMINUM-TITANIUM DIBORIDE (Al-TiB_2) METAL MATRIX COMPOSITE USING FINITE ELEMENT SIMULATION

Mine USLU UYSAL
Yildiz Technical University, Department of Mechanical Engineering, Istanbul- Turkey
mineuslu@yildiz.edu.tr

Abstract: Metal matrix composites are widely preferred for engineering applications, especially aluminum is used as a matrix because of its unique mechanical properties in naval and aerospace industries. In the present paper, the creep behavior of an aluminum based metal matrix composite reinforced with TiB_2 particles was studied for various over temperature range and stress levels. Aluminum 6061 was selected to be the metal matrix which has high strength to weight ratio and it is reinforced with TiB_2 which has extremely thermal stability. TiB_2 powder is added into the aluminum by varying the percentage of the powder by volume in order of 3,6 and 9 percent, respectively. The finite element analysis software package ANSYS® is used to obtain the creep behavior of the composite material. The influence of the over temperature rates, stress levels and volume of the TiB_2 powders on the creep behavior were studied by using simple finite element model. Using such a simple composite model, remarkable savings in time and identifying the correct combination of the TiB_2 powder can be obtained for creep conditions.

Keywords: Finite Element Simulation, Creep Prediction, Metal Matrix Composite, Al-TiB_2 Reinforcement

Introduction

Metal matrix composites (MMCs) are widely used because of their superior properties as compared to those of most conventional materials. They have high specific strength, wear resistant and stiffness. Nowadays, main focus is given to aluminum alloy because of using for commercial applications in the construction, engineering industries and transportation. Especially, aerospace industries raise the demand for the new materials which perform efficiently in very tough environment. Although a variety of matrix materials used for making metal matrix composites (MMCs), the biggest emphasis is on the development of lighter metal matrix composites using aluminum and titanium alloys. Because they have the significant potential in the weight ratio and at the same time the material posses low density, high thermal conductivity, low thermal expansion and high modulus for the aerospace and space engines. The aluminum-based metal matrix composites serve these purposes and also new light aluminum alloys have received considerable attention in the literature (Ioannidis et al., 1989, McShane et al., 1990). Despite of the superior properties of the MMCs, they have lower ductility and fracture toughness than unreinforced alloys (Lloyd, 1994, Srivatsa et al., 1991).

The employ of intermetallic particles (such as titanium aluminides) as suitable reinforcement for aluminum and titanium alloys were proposed as least two decades (Yamada and Unakoshi, 1983, Larrouy et al., 2001). Ceramic particles contribute a pure structural build up for the metal matrix composites. The addition of ceramic particle such as SiC, Al_2O_3, TiB_2 to an aluminum matrix doesn't considerably change the density of the material but instead it leads to a major rise in specific strength and modulus of composite and this plays a good role use in structural applications (Yue et al., 1999). The physical properties such as friction resistance, friction co-efficient and thermal conductivity also changes. This due to fact that TiB_2 have outstanding features such as high elastic modulus (530 x 10^3 GPa) , high melting point (2790°C), high hardness (86 HRA or 960 HV) and good thermal stability (Tjong et al., 2005, Mandal et al., 2007, Kumar et al., 2010, Lakshmi et al., 1998). TiB_2 particles don't react with molten aluminum, thereby avoiding formation of brittle reaction products at the reinforcement-matrix interfaces. So the Al-TiB_2 composites have certain useful and unique characteristics. For example; the wear resistance of the aluminum matrix reinforced with titanium diboride (TiB_2) increases as the volume fraction of the TiB_2 increased, when compared to the pure aluminum (Popoola et al., 2010). The tensile and ultimate strength of the Al increases with increase in the amount of TiB_2 (Suresh et al., 2014). The addition of TiB_2 particles increases the hardness value when the formed TiB_2 particles have a mix up of cubic, spherical and hexagonal shaped particles (Rajan et al., 2013).

Relationship between microstructure and mechanical property for TiB_2 reinforced aluminum have been studied by various authors, however in literature it has lack of study about at the behavior of the Aluminium-Titaninum Dibordine (Al-TiB_2) metal matrix composites the high temperatures. For example, creep is an inelastic response

of materials loaded at high temperatures. It has important effect on deformation because defect of microstructure rearrangement process is accelerated at high temperatures. So this process tends to soften material they counteract the hardening produced by plastic deformation. Creep can be resembled viscoelasticity behavior because the resulting strain at constant applied stress is a function of time, but in contrast with viscoelastic behavior permanent deformation remains following creep. Additionally, elasticity and plasticity are mechanical responses to loading which is independent of the time. When the load is applied, the corresponding level of strain set in. But, during creep behavior the mechanical response is time dependent.

The aim of the present study is to investigate the creep behavior of Aluminum-Titanium Dibordine (Al-TiB_2) metal matrix composite over a temperature range at various stress levels. Aluminum 6061 and TiB_2 were selected to be the metal matrix and reinforcement materials respectively. The TiB_2 powder was added to the aluminum matrix a 3%, 6% and 9% vol. The influence of these volume rations, over temperatures rates and stress levels on the creep behavior were investigated. The principal aim of the contribution is to define and describe a simple model of metal matrix composite for the numerical simulation and prediction of creep behaviors. For this purpose, finite element models were developed using ANSYS® software and using this model, saving time and identifying the correct combination of TiB_2 can be obtained.

Description of the Aluminum-Titanium Diboride (Al-TiB_2) Metal Matrix Composite

In this work, Aluminum 6061 was selected to be the metal matrix. Different metal matrix composites are obtained by mixing TiB_2 powder with different percentages of reinforcing particles. The mixtures obtained are aluminum with 3, 6 and 9% in volume of TiB_2. The properties of the metal matrix composites not only depend on the matrix and the volume fractions, but also on distribution of reinforcing particle on the matrix. In practically, there is no doubt that achieving homogeneous distribution is difficult. But in the present MMCs, a certain number of fibers are considered to be unidirectional oriented in the z direction, as shown in Figure 1.

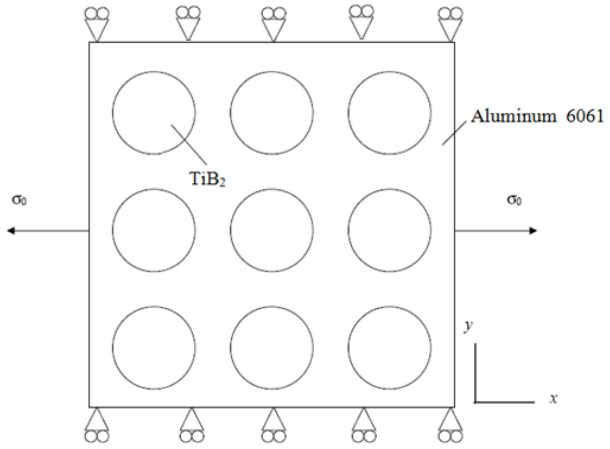

Figure 1. Loading and boundary conditions of Aluminum-Titanium Diboride (Al-TiB_2) metal matrix composite.

The material properties of the matrix Aluminum 6061 and reinforcing particle TiB_2 powder are shown in Table 1.

Table 1: Mechanical properties of Aluminum 6061 and TiB_2 powder (Suresh et al., 2012) [15].

Matrix (Aluminum 6061)	Fiber (TiB_2)
E = 56000 MPa	E= 530000000 MPa
υ = 0.33	υ = 0.33

The standard tension test can be applied to investigate the mechanical response of composite materials deforming at high temperatures. In the present paper the two different high temperatures values were used, they were 232°C and 288°C. The easiest to perform is tension test at constant load and temperature. Using constant loads and temperatures values in this study can be seen in Table 2.

Table 2: Constant temperatures and load value parameters.

Parameters	Temperature (°C)	Load (MPa)
1	T = 232 °C	σ = 27.6 MPa
2	T = 288 °C	σ = 13.8 MPa
3	T = 288 °C	σ = 20.7 MPa
4	T = 288 °C	σ = 27.6 MPa

The resulting strain is measured as a function of time. In this study, time was selected as 2.5 hours (150 minutes). In the creep test, the resulting strain-time curves are called creep curve. The curve in Figure 2 shows the idealized shape of a creep curve. The slope of this curve (de/dt) is referred to as the creep rate. The curve B (dashed line) shows the shape of a constant-stress creep curve. In engineering it is generally the load not the stress that is maintained constant, so a constant-load creep test is more important, but fundamental studies of the mechanism of creep should be carried out under constant-stress conditions.

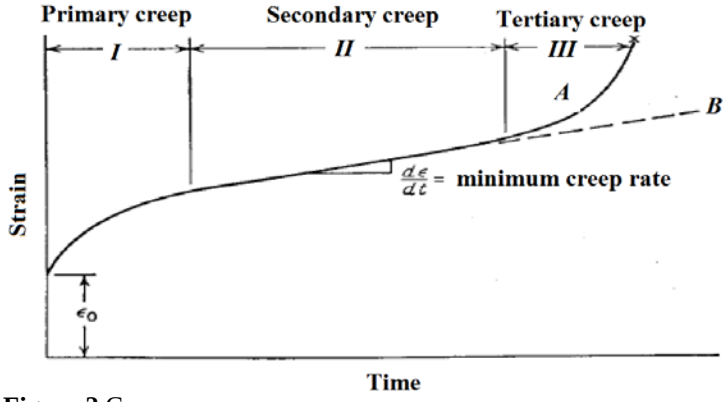

Figure 2. Creep curve.

Strain-time curves obtained from the creep tests at constant load and long periods of time often exhibit three different characteristic stages. These can be defined as below:

- **Primary Creep, I, (Transient Creep);** Following the setting in of the instantaneous elastic strain (ε_0), the material deforms rapidly but at a decreasing rate. The duration of the stage is typically relatively short in relation to the total creep curve.
- **Secondary Creep, II, (Steady-State Creep);** The creep strain rate reaches a minimum value and remains approximately constant over a relatively long period of time.
- **Tertiary Creep, III;** In this stage, the creep strain rate accelerates rapidly.
- **Rupture;** The material in unable to withstand the load anymore and breaks.

In this paper, the matrix (Aluminum 6061) which is a function of tension makes primary (transient) creep and secondary creep (steady-state creep) movement. When an external load is applied, present metal matrix composite materials samples undergoes elastic deformation and then these internal stresses cause creep behavior for the matrix. In calculations, it is assumed that usually only the matrix has been creep and the elastic shape of the fibers has changed but has not been creep behavior. This situation creates creep resistance in the fiber direction. Creep behavior, like other thermo mechanical properties in unidirectional composites, is anisotropy. This is too small in longitudinal direction and can be negligible, but it is worth taking in to account for transverse direction.

Creep Analysis of the Aluminum-Titanium Diboride (Al-TiB_2) Metal Matrix Composite Structure

Finite element models can be simply thought based on to be cylinders placed in the middle of a cube. So the metal matrix composite is modeled as circles arranged symmetrically in a square. An edge length of the square is taken as 1000 units. Finite element analyses were performed using ANSYS® commercial programme. Finite element model of the metal matrix composite structure can be seen in Figure 3(a) and the geometry were meshed by using Plane 182 can be seen in Figure 3(b). Plane 182 element type is used for two dimensional modeling of solid structures. This element is defined by four nodes having two degrees of freedom at each node: translation in the nodal x and y directions. This element is very suitable for studying creep behavior because it can be used in plastic, hyper elastic stress, large deformation and large unit elongation analyses. The ANSYS® package program has 12 different creep relationships that model creep behavior, in this paper it has accepted that matrix material makes

both primary and secondary creep movements. The correlation to be used in this model should be appropriate for this type of behavior. So the creep behavior given in 11th place in the ANSYS package program was chosen suitably.

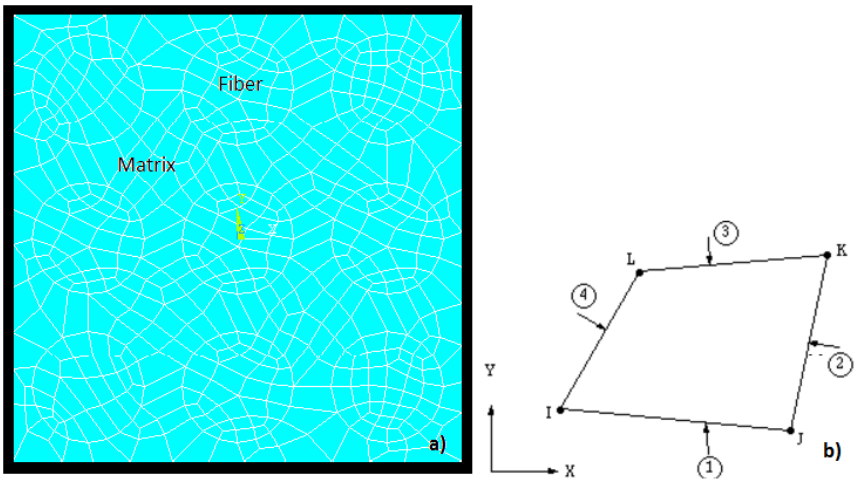

Figure 3.a) Finite element model of the metal matrix composite b) Plane 182 element type.

Analysis Results and Discussion

In this paper, the creep behavior of the aluminum-titanium diboride (Al-TiB_2) metal matrix composite in 150 minutes was investigated. Figure 4 and Figure 5 show the result of the creep analysis performed with the ANSYS at various stress and temperature conditions. Stress is one of the major factors that affect the creep strain. Figure 4 shows that effect of the stress on the creep behavior for the 6% volume of TiB_2. As seen in Figure 4, the creep strain value is 0.027 for T= 288°C, σ = 13.8 MPa conditions. At the same temperatures, when the stress increases 13.8 MPa to 20.7 MPa, the creep strain value increases approximate 2.61 times. Similarly, the creep stain increases nearly 5.38 times when the stress increases 13.8 MPa to 27.6 MPa at the 288°C.

Also, creep behavior for the aluminum-titanium diboride (Al-TiB_2) metal matrix was affected by temperature. At constants 27.6 MPa stress, when 232°C was applied for 6% volume of TiB_2 the creep strain is 0.0017. When the temperature increases from 232°C to 288°C, the creep strain value increases nearly 81.8 times. As seen in Figure 4, the creep strain is 0.1455 for T= 288°C, σ = 27.6 MPa conditions. These result presented that the creep strain of the aluminum-titanium diboride (Al-TiB_2) metal matrix affected for both stress values and temperatures values. Finally, the creep behavior can be significantly controlled by selecting the stress and temperatures as a parameter.

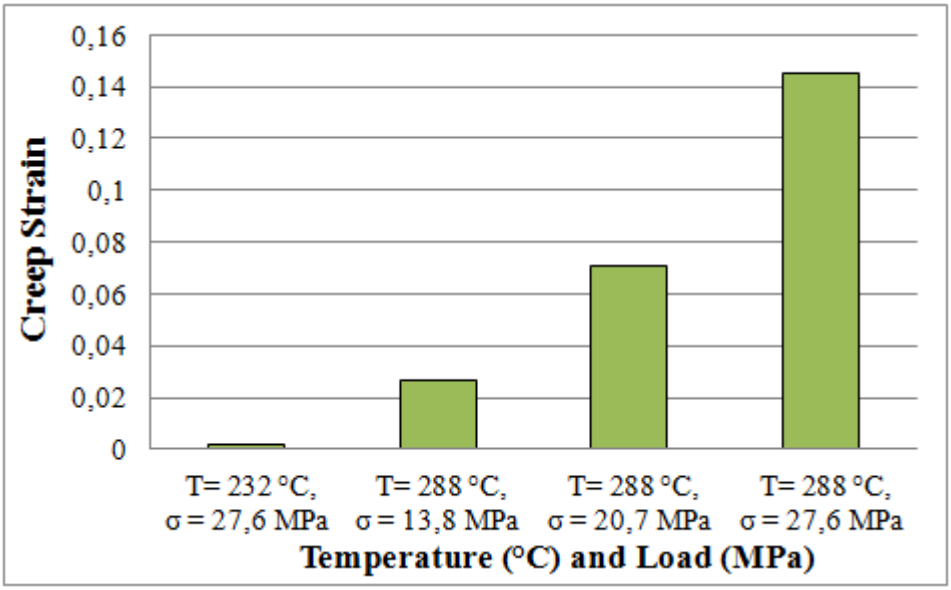

Figure 4. Effect of the temperatures and stress on the creep strain for 6% volume of TiB_2.

From the numerical results, the creep strain of the aluminum-titanium diboride (Al-TiB_2) metal matrix were measured for different design composition of % volume of TiB_2. The plot in Figure 5 clearly shows the benefit provided by the change of the % volume TiB_2. The creep strain values compared for the percentages of TiB_2 volume ratio in Aluminum 6061 in the T= 232°C, σ = 27.6 MPa conditions in Figure 5(a). In Figure 5(b) shows that the creep strain decreases as 30.29% when the percentages of volume ratio of TiB_2 is raised from 3% to 6% for T= 288°C, σ = 13.8 MPa conditions. The maximum change reflecting the differences of the TiB_2 ratio is seen in case of vol. 3% to vol. 9%. For example, in Figure 5(c) for the T= 288°C, σ = 20.7 MPa condition shows that the creep strain decreases nearly 106%. Similarly, when the percentages of volume ratio of TiB_2 is raised from 3% to 9%, the creep strain decreases as 117%, it can be seen in Figure 5(d). These results revealed that composition of the volume %TiB_2 plays a major role in the creep behavior on aluminum-titanium diboride (Al-TiB_2) metal matrix composites. As the % volume ratio of TiB_2 increases, the creep strain values decreases. In other words, the creep resistance can also be said to increase.

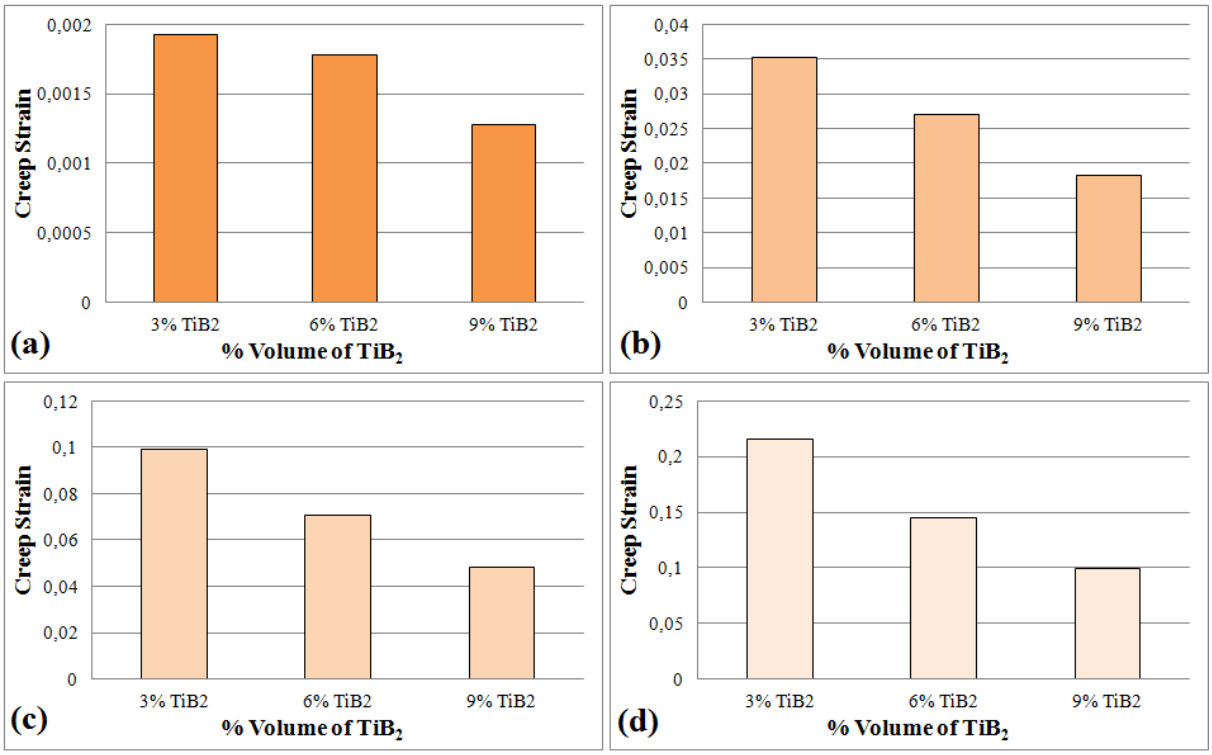

Figure 5. Effect of the volume ratio TiB_2 on the creep strain, a) T= 232°C, σ = 27.6 MPa, b) T= 288°C, σ = 13.8 MPa, c) T= 288°C, σ = 20.7 MPa, d) T= 288°C, σ = 27.6 MPa.

Conclusion

In this study, finite element model was used to estimate the creep behavior of the aluminum-titanium diboride (Al-TiB_2) metal matrix composite for investigating the creep strain values. Firstly, different percentages of reinforcing particles (TiB_2) were chosen as 3, 6 and 9% in volume for obtained different metal matrix composites mixtures and also two different high temperature constant value (232°C and 288°C) were used. Three various stress value (13.8 MPa, 20.7 MPa and 27.6 MPa) were also used for measuring the creep strain which is a function of time. Time was selected as 2.5 hours in this paper. Comparing the obtain results from the numerical investigation, it is seen that the creep strain increases when the temperatures and stress values increase. Also finite element model were investigated for three different percentages of reinforcing particles TiB_2 for obtain the creep behavior. As the % volume ratio of TiB_2 increases, the creep strain values decrease and also it is mean that as the % volume ratio of TiB_2 increases, the creep resistance of metal matrix composite increases. The results indicate that a useful aluminum-titanium diboride (Al-TiB_2) metal matrix composite can be achieved by selecting proper design parameter as a reinforcing particle TiB_2 for high temperatures.

References

Ioannidis, E.K., Marshall, G.J. & Sheppard, T. (1989). *Microstructure and properties of extruded Al–6Mg–3Cr alloy prepared from rapidly solidified powder*, Materials Science and Technology, vol. 5, pp. 56-64.

Kumar, S., Subramanya, S.V. & Murty, B.S. (2010). *High temperature wear behavior of Al-4Cu-TiB_2 in situ composites*, Wear, vol. 268(11), pp. 1266-1274.

Lakshmi, S., Lu, L. & Gupta, M. (1998). *In situ preparation of TiB_2 reinforced Al based composites*, Journal of Materials Processing Technology, vol. 73, pp. 160-166.

Larrouy, T., Fournier, D. & Belague, P. (2001). *Fabrication and properties assessment of HIPed gas atomised titanium aluminides*, Anals of Powder Metallurgy Congress, pp. 427-432.

Lloyd, D.J. (1994). *Particle reinforced aluminium and magnesium matrix composites*, International Materials Reviews, vol. 39, pp. 1-23.

Mandal, A, Chakraborty, M. & Murty, B.S. (2007). *Effect of TiB_2 particles on sliding wear behavior of Al-4Cu alloy*. Wear, vol. 262(1-2), pp. 160-166.

McShane, H.B., Mahmoud, M.S. & Sheppard, T. (1990). *Microstructure and properties of extruded Al–Li–Cr alloy prepared from atomised powder*, Materials Science and Technology, vol. 6, pp. 161-169.

Popoola, A.P., Pityana, S. & Ogunmuyiwa, E. (2010). *Microstructure and wear behaviour of Al/TiB_2 metal matrix composite*, CSIR Research Space, vol. 22(7), pp. 23-26.

Rajan, M.H.B., Ramabalan, S., Dinaharan, I. & Vijay, S.J. (2013). *Synthesis and characterization of in situ formed titanium diboride particulate reinforced AA7075 aluminium alloy cast composites*, Materials and Design, vol. 44(3), pp. 438-445.

Suresh, S., Shenbaga, N. & Moorthi, V. (2012). *Aluminium-Titanium Diboride (Al-TiB_2) metal matrix composites: challenges and opportunities*, Procedia Engineering, vol. 38, pp. 89-97.

Suresh, S., Shenbaga, V.M.N., Vettivel, S.C. & Selvakumar, N. (2014). *Mechanical behavior and wear prediction of stir cast Al-TiB_2 composites using response surface methodology*, Materials and Design, vol. 59(2), pp. 383-396.

Srivatsa, T.S., Ibrahim, I.A., Mohamed, F.A. & Lavernia, E.J. (1991). *Processing techniques for particulate-reinforced metal aluminium matrix composites*, Journal of Materials Science, vol. 26(22), pp. 5965-5978.

Tjong, S.C, Wang, G.S. & Mai, Y-.W. (2005). *High cycle fatigue response of in-situ Al-based composites containing TiB_2 and Al_2O_3 submicron particles*, Composite Science and Technology, vol. 65(10), pp. 1537-1546.

Yamada, M. & Unakoshi, Y. (1983). *Intermetallic compounds*, Tokyo, Japan: Nikkan Kogyo Press.

Yue, N.L, Lu, L. & Lai, M.O. (1999). *Application of thermodynamic calculation in the in-situ process of Al/TiB_2*. Composite Structures, vol. 47, pp. 691-694.

DEPOLLUTION OF OLIVE MILL WASTEWATER THROUGH ELECTROCOAGULATION AND ADVANCED OXIDATION

Hoor JALO[a], Samir EL HAJJAJI[a], Abdelkrim OUARDAOUI[a]*

[a]School of Science and Engineering, Al Akhawayn University, Ifrane, 53000, Morocco
*Corresponding author: a.ouardaoui@aui.ma

Abstract: The goal of the Research described in this paper is to treat Olive Mill Wastewater (OMWW) to cause its decolorization, thus enabling its safe and legal release in main water streams. To this end, two different methods were tested on samples of OMWW collected from Ain Taoujdate, a small town that is located 25 km to the south of Fez, Morocco. These samples were freshly diluted by a factor of 20 prior to a treatment by either electrocoagulation or the photo-Fenton process, a type of advanced oxidation. It was found that an electrocoagulation treatment of two hours, at 22V DC with aluminum plates, was satisfactory to get nearly clear and colorless water (93% decolorization). A phenolic content reduction by 92.4% was obtained using this same technique. Photo-Fenton was tested with the use of H_2O_2/Fe(II), O_2/Fe(II), and H_2O_2/O_2/Fe(II) at a wavelength of 254 nm. With this technique, the best operating conditions afforded 78% decolorization. A discussion on the viability of each technique concludes this study.
Keywords: Wastewater, Pollution, Electrocoagulation, Oxidation, Fenton

Introduction

With an annual production of 140 000 tons of olive oil in 2014-2015, Morocco is ranked the 5th biggest producer of olive oil in the world. Unfortunately, like in nearly all industries, the production of this good is accompanied by the production of wastes that represent a major environmental issue and that must be dealt with. During the olive oil production process, two kinds of residues are generated: a wet solid waste called “crude olive cake” and an aqueous waste called “olive mill wastewater, OMWW”. OMWW is a dark liquid effluent characterized by high concentrations of organic compounds, including organic acids, sugars, tannins, pectins and phenolic substances that makes it phytotoxic and inhibit bacterial activity. In 2014, the amount of OMWW generated in Morocco alone was estimated to be 250-400 000 m^3 per year;[1-2] a sizeable amount given that 1 m^3 of OMWW is equivalent to 100-200 m^3 of domestic sewage.[3] OMWW treatment and disposal is a problem with great complexity due to the strong nature of the waste and several economical, technical, and organizational constraints involved in the olive oil sector. Over the last 60 years, practically all treatment processes developed for domestic and industrial wastewaters have been tested on OMWW but none of them appeared suitable to be generally adopted.[3] These processes include aerobic processes,[4-5] anaerobic processes,[6-11] anaerobic digestion,[12] pH neutralization,[13] coagulation,[12] electro-coagulation,[14] advanced oxidation processes,[15-19] distillation/ evaporation,[11-12] and membrane processes (ultrafiltration, microfiltration, reverse osmosis).[20-22] When not dumped illegally directly into nearby aquatic bodies, i.e. rivers, lakes, or even the sea,[23] nearly all olive mills in Morocco, and around the globe at large, dispose of OMWW in evaporation ponds or storage lakes (lagoons), such as the one shown in **Figure 1a**. This technique consists in storing the waste outdoor and let its water evaporate naturally in ambient air by exposure to sunlight.

Figure 1a: OMWW evaporation pond beside an olive mill in Ain Taoujdate, Morocco (Feb. 2016).

In spite of having low energy costs and being simple to operate, this method has important drawbacks; it requires

a long waste residence time (7-8 months) and a large land surface area (~1 m^2 for each 2.5m^3 of OMWW). Furthermore, it raises several ecological concerns including the possibility of groundwater contamination if the bottom of the pond is not properly lined against infiltration and leakage – as it is often the case – and the emissions of methane in the atmosphere due to the anaerobic fermentation of the waste that occurs in the pond.[3,10,11] Finally, these ponds and lagoons cause serious nuisance to their neighborhood because they attract insects and cause foul smells.

Materials and Methods

Chemicals and Equipment

Sodium hydroxide was supplied by Fluka, Switzerland. Aluminum sulfate was supplied by AppliChem Panreac, Spain. Ferrous sulfate heptahydrate was supplied by Fluka, Switzerland. Oxalic acid monohydrate, 99% pure, was supplied by PanReac Applichem, Germany. Hydrogen peroxide, 110 vol., was supplied by Société Nouvelle Pharmac, Morocco. Ethanol, 96% pure, was supplied by Carlo Erbo, Spain. Anhydrous sodium carbonate was supplied by Sigma-Aldrich. The Folin-Ciocalteu reagent was supplied by Educomptoir, Morocco. Medical grade oxygen gas was supplied by Maghreb Oxygen, Morocco.

For centrifugation, a 5500 rpm centrifuge, *Hettich Zentrifugen* model EBA 30, was used. Vacuum filtrations were performed by means of piston-powered vacuum pump with a pressure of 0.85 atm and an air flow of 38 L/min. Weights were measured by an *AND* balance with a readability of 0.01g model EK610i, an *OHAUS* balance with a readability of 0.0001g model AS120, or a *KERN* balance with a readability of 0.05g model KB10K0.05N. pH and temperature were measured by using a *Hanna* instruments pH meter model HI 9318.
Preparation of solutions for phenolic content determination was done by means of 25 µL and 100µL syringes, supplied by *HAMILTON*, Switzerland. For heating and stirring, digital stirring hotplates were used. Either *DLab* MS-H280-pro or *VWR* VMS-C7 advanced series. For electrocoagulation, a *Tektronix* voltage meter model PS280 was used. For measuring the absorbance, a *Jenway* spectrophotometer model 6320D was used. Wavelength scan was done with a *JASCO* spectrophotometer model V-530. Conductivity was measured with a *YSI* conductivity meter model 33. Ultraviolet light was generated by a *CAMAG* UV transilluminator model CM3 with wavelengths of 254 nm and 366 nm, and a *FOTODYNE* UV transilluminator model C3-3501. A Q.10 *CHANDOS* quartz cuvette was used to perform photo-Fenton reactions.

Phenolic content determination

The determination of total phenolics in treated OMWW samples was based on a micro method reported in the literature.[24] It was performed by spectrophotometry with gallic acid as standard. A calibration curve was plotted by preparing six standards. The latter were made in 4-mL glass vials by mixing 20 µL of gallic acid solution being in the concentration range 0-50-100-150-250-500 mg/L, 1.58 mL of distilled water and 100 µL of Folin-Ciocalteu reagent. After vigorous shaking for 1 min at room temperature, 300 µL of aqueous saturated sodium carbonate solution was added. Next, the solution was shaken again and heated at 40°C for 30 min by means of a bain-marie. The resulting blue solution was transferred entirely into the cuvette of a spectrophotometer and absorbance was measured at a wavelength of 765 nm. A 5000 mg/L aqueous gallic acid stock solution was used to prepare these solutions accurately.

Electrocoagulation experiments

All OMWW samples that were treated by electrocoagulation were first diluted with distilled water by a factor of 20. Next, they were filtered, centrifuged for five minutes at 5500 rpm, and re-filtered in order to measure their absorbance at a wavelength of 395 nm. The applied voltage for all electrocoagulation experiments was 22 V DC unless stated otherwise. Filtrations were done under vacuum over cotton wool.
Four different aluminum cells with various sizes and geometries were constructed and tested in the laboratory (**Figure 1**).

Figure 1: Aluminium cells tested in the electrocoagulation experiments**.**

Characteristics of these cells are given in **Table 1**.

Cell name	*Shape*	*Number of plates*	*Effective surface area (cm^2)*
Cell #1	rectangular	2	139
Cell #2	rectangular	4	256
Cell #3	square	2	783
Cell #4	round	2	2791

Table 1: Aluminium cells tested in the electrocoagulation experiments.

Photo-Fenton experiments

Since photo-Fenton experiments require an exposure to UV light (λ= 254 nm), they were conducted directly in the quartz cuvette of a spectrophotometer having a thickness of 1.0 cm. When performed on a larger scale, experiments were conducted in a 50mL glass beaker placed below a UV lamp. The source of Fe (II) chosen for our experiments is iron (II) oxalate, FeC_2O_4. This compound was made by mixing equal volumes of aqueous solutions of 30 mM iron (II) sulfate, $FeSO_4$ and 5 mM oxalic acid, $C_2H_2O_4$. The photo-Fenton experiment consisted in reacting within a cuvette, 0.5 mL of iron (II) oxalate solution, FeC_2O_4, 1 mL of 8mM hydrogen peroxide solution, H_2O_2, and 1.5mL of OMWW sample. When need be, a gas tubing was inserted in the reacting mixture to allowing bubbling of oxygen gas with a controlled flow rate.

Results and Discussion

Conventional coagulation

Our first attempts to treat OMWW were done by performing conventional coagulation experiments by using two coagulants known to be effective in the field of wastewater treatment: iron (II) sulfate, $FeSO_4$, and aluminum sulfate, $Al_2(SO_4)_3$. In spite of a treatment time as long as 24 h and the testing of different pH conditions, none of our attempts with conventional coagulation was successful. Therefore, in our hands this technique, and these two simple coagulants, did not seem suitable for an effluent as complex as OMWW.

Electrocoagulation

Electrocoagulation differs from conventional coagulation mainly with the fact the coagulant – in our case aluminum hydroxide – is generated in situ. This technique turned out to be very successful when applied on OMWW. **Figure 2** shows the evolution of a sample of OMWW being treated for 19 h with cell#2.

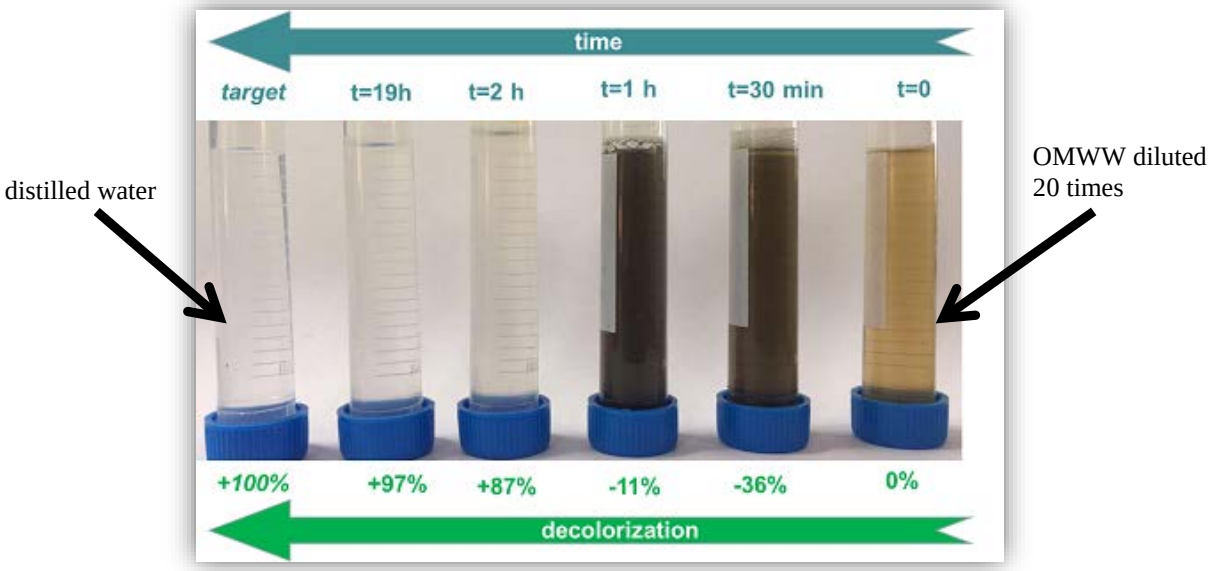

Figure 2: OMWW sample being treated by electrocoagulation with cell #2. Decolorization as a function of treatment time.

As shown in **Figure 2**, the OMWW gets initially darker and darker in the initial stage of the treatment. This phenomenon is presumably caused by the absence of a critical mass of coagulant at the outset. However, once the treatment has been carried out long enough, a high decolorization of the sample is attained (+87% in 2 h). Decolorization starts taking place when flocs are formed and precipitated; however, their particle surface charge are affected by various parameters, one of which is the pH of the solution. Evidence for this explanation was obtained by monitoring the pH and the absorbance simultaneously (**Figure 3**). Indeed, **Figure 3** shows that after 60 min of treatment, the increase of pH causes an immediate drop of the absorbance and therefore a decolorization. This increase in pH, which is typical in electrocoagulation, is caused by the formation of hydroxide ions at the cathode.

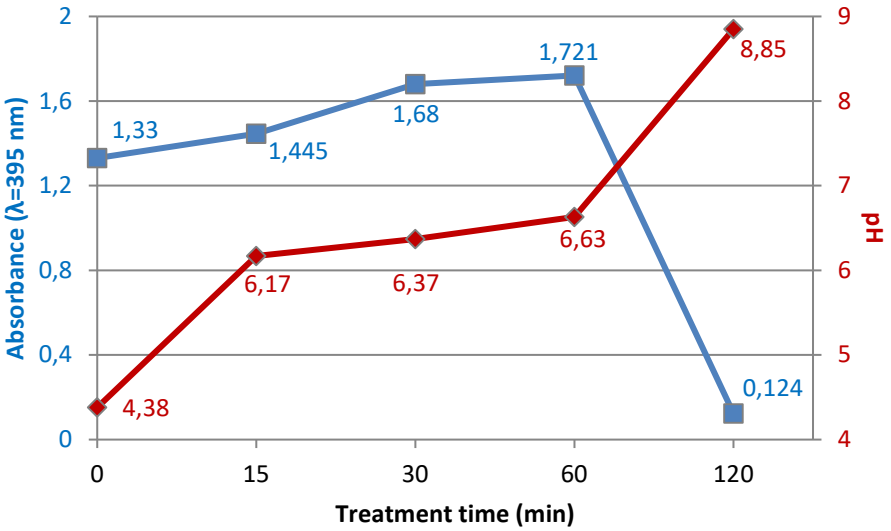

Figure 3: Monitoring of absorbance and pH in the electrocoagulation of OMWW with cell #2.

The effect of pH on decolorization is due to the solubility of the different aluminum hydroxide species in different pH ranges.[25] Indeed, depending on the pH, aluminum hydroxide will exist either as a monomeric species (e.g $Al(OH)^{2+}$, $Al(OH)_2^{+}$, $Al(OH)_4^{-}$), a polymeric species (e.g. $Al_2(OH)_2^{4+}$, $Al_2(OH)_2^{5+}$) or an amorphous and less stable species (e.g. $Al(OH)_3$).[26] Table 2 compares the results obtained with each of the cells employed in our electrocoagulation experiments.

Table 2: Results obtained with cells 1-4 in the electrocoagulation experiments.

Entry	Cell name	Conditions				Results		
		Volume of OMWW treated (L)	Voltage applied (V)	EC[(a)] treatment time (h)	Settling time (days)	Decolorization[(b)]	pH	Conductivity (µS/cm)
1	Cell #1	0.475	22	2.5	0	+84.0%	6.22	690
2	Cell #2	0.790	22	2	2	+ 92.3%	6.13	510
3				19	2	+ 97.4%	-[(c)]	300
4	Cell #3	9	14	15.5	10	+ 93.5%	7.41	550
5	Cell #4	5	11-13	8	10	+ 93.2%	7.65	550

(a) EC: electrocoagulation.
(b) Based on the change of absorbance at λ=395 nm. Sample centrifuged for 5 min beforehand.
(c) Not determined.

Determination of the phenolic content reduction was done for OMWW treated with cell #3. The concentration of polyphenols, expressed as mg of gallic acid equivalent, was found to drop by 92.4%; an excellent result given the detrimental effect of these polyphenols to the environment.

Photo-Fenton

Results obtained in the treatment of OMWW with the Fenton and photo-Fenton process are shown in **Table 3**.

Table 3: Results obtained in the Fenton and photo-Fenton experiments. $[Fe^{2+}]$initial = 3 mM.

Entry	UV light[(a)]	O_2 (g)[(b)]	$[H_2O_2]$	Treatment time	Type of OMWW treated[(c)]	Decolorization[(d)]
1	no	no	5 mM	20h	Untreated	+8.0%
2					Pre-treated by EC	+2.1%
3	no	no	8 mM	20h	Untreated	-3.9%
4					Pre-treated by EC	**+15.6%**
5	yes	no	8 mM	2h	Untreated	-21.3%
6					Pre-treated by EC	-29.1%
7	yes	no	5 mM	5h	Untreated	+4.1%
8					Pre-treated by EC	-13.5%
9	yes	no	5 mM	5h + 15h settling	Untreated	+9.6%
10					Pre-treated by EC	-6.8%
11	yes	yes	0 mM	2h + 15h settling	Pre-treated by EC	-10.9%
12	yes	yes	8 mM	2h	Pre-treated by EC	-17.5%
13				2h + 3 days settling	Pre-treated by EC	**+78.2%**

(a) λ=254 nm.
(b) Flow rate: 40 mL/min.
(c) Untreated = only diluted with distilled water by a factor of 20. EC = electrocoagulation.
(d) Based on the change of absorbance at λ=395 nm. Sample centrifuged for 5 min beforehand.

First, **entries 1-4** show the level of decolorization attained in the Fenton process (i.e. absence of UV light). Under the conditions tested, the best result was obtained in the treatment of OMWW pre-treated by electrocoagulation for 20h with 8mM H_2O_2 and 3mM Fe (II), to afford a color reduction by 15.6%. In the case of untreated OMWW, it was found that a lower concentration of H_2O_2 is favorable to a rapid degradation of organic pollutants (**entry 1** vs **entry 3**); however, the opposite trend is observed when dealing with OMWW pre-treated by electrocoagulation (**entry 2** vs **entry 4**). Therefore, our data seems to indicate that the efficiency of the Fenton process can be fairly variable since it can be affected by both the oxidant concentration and the quality of the effluent to be treated. **Entries 5-13** deal with the photo-Fenton process (i.e. UV-induced degradation). Comparison of **entries 5,7,9** vs **entries 6,8,10** shows that better results are obtained by processing untreated OMWW rather than the pre-treated one. It was found that an increase of the treatment time from 2h to 5h, in spite of a reduction of the oxidant concentration from 8mM to 5mM, leads to a higher level of decolorization (**entry 5** vs **entry 7**). Also, our data shows that settling of the solution over a prolonged period of time is also beneficial to the purification process when used post-treatment (**entry 7** vs **entry 9**). When oxygen gas, O_2, was used either as a replacement of H_2O_2 or as a co-oxidant (**entries 11-12**), poor results were obtained. However, with proper reaction conditions of time and oxidant concentration, the combination of O_2 and H_2O_2 as oxidants afforded an exceptionally high level of decolorization (+78.2%, **entry 13**).

Conclusion

A total of four techniques were tested in our investigation, namely coagulation, electrocoagulation, Fenton, and photo-Fenton. One the one hand, coagulation and Fenton performed poorly in terms of decolorization of OMWW. On the other hand, electrocoagulation and photo-Fenton in presence of oxygen gas both proved to be potent and efficient solutions when performed under the right experimental conditions of time and oxidant concentration. Though electrocoagulation affords the best results in terms of decolorization (>93%) and phenolic content reduction (>92%) at the scale of the laboratory, its utilization at the olive mill scale may be challenging because of the inherent high energy cost of the technique. Consequently, the future of this technique will be largely dependent on its optimization by for example powering it with inexpensive energy sources. Regarding the photo-Fenton process, the identification of unique experimental conditions enabled to reach a decolorization of pre-treated OMWW by more than 78%. This technique is attractive because of its practicality; however, its use at a large scale may be hampered by the cost of usage and maintenance of UV light. This study has clearly shown that the issue of OMWW treatment can be hardly solved by a single method, but that it rather relies on the clever combination of a sequence of finely tuned processes to be operated individually. Electrocoagulation and

photo-Fenton have been proved to be very good examples of such processes.

Acknowledgements
The authors are thankful to Mr. Abdellatif Ouddach and Mr. Driss Wahid for technical assistance and to the School of Science and Engineering of Al Akhawayn University in Ifrane for its support.

References
http://www.libe.ma/Les-margines-une-menace-pour-la-qualite-des-eaux-a-Taounate_a46333.html
http://www.leconomiste.com/article/915526-comment-rentabiliser-les-sous-produits-de-l-olivier
E. Tsagaraki, H. N. Lazarides, K. B. Petrotos, « Utilization of By-Products and Treatment of Waste in the Food Industry », "Chapter 8: Olive Mill Wastewater Treatment", Springer, 2006, p 135.
C. F. Cereti, F. Rossini, F. Federici, D. Quaratino, N. Vassilev, M. Fenice, « Fermentative decolorization of olive mill wastewater by Lactobacillus plantarum », *Bioresour. Technol.*, **2004**, *91*, 135.
R. Lanciotti, A. Gianotti, D. Baldi, R. Angrisani, G. Suzzi, D. Mastrocola, M. E. Guerzoni, « Use of Yarrowia lipolytica strains for the treatment of olive mill wastewater », *Bioresour. Technol.*, **2004**, In Press.
R. Borja, A. Gonzalez, « Comparison of anaerobic filter and anaerobic contact process for olive mill wastewater previously fermented with Geotrichum candidum », *Process Biochem.*, **1994**, *29*, 139.
D. Dalis, K. Anagnostidis, A. Lopez, I. Letsiou, L. Hartmann, « Anaerobic digestion of total raw olive-oil wastewater in a two-stage pilot-plant (up-flow and fixed-bed bioreactors) », *Bioresour. Technol.*, **1996**, *57*, 237.
N. Zouari, « Decolorization of olive oil mill effluent by physical and chemical treatment prior to anaerobic digestion », *J. Chem. Technol. Biotechnol.*, **1998**, *73*, 297.
N. Zouari, R. Ellouz, « Toxic effect of coloured olive compounds on the anaerobic digestion of olive oil mill effluent in UASB-like reactors », *J. Chem. Technol. Biotechnol.*, **1996**, *66*, 414.
N. Azbar, A. Bayram, A. Filibeli, A. Muezzinoglu, F. Sengul, A. Ozer, « A Review of Waste Management Options in Olive Oil Production », *Crit. Rev. Env. Sci. Technol.*, **2004**, *34*, 209.
A. Rozzi, F. Malpei, « Treatment and Disposal of Olive Mill Effluents », *Int. Biodeterioration & Biodegradation*, **1996**, *38*, 135.
M. Niaounakis, C. P. Halvadakis, « Olive-Mill waste management- literature review and patent survey », **2004**, Typothito-George Dardanos, Athens, Greece.
M. Mitrakas, G. Papageorgiou, A. Docoslis, G. Sakellaropoulos, « Evaluation of various pretreatment methods for olive mill wastewaters », *European Water Pollution Control*, **1996**, *6*, 10.
S. Khoufi, F. Feki, S. Sayadi, « Detoxification of olive mill wastewater by electrocoagulation and sedimentation processes », *J. Hazard. Mat.*, **2007**, *142*, 58-67.
W. Gernjak, M. I. Maldonado, S. Malato, J. Caceres, T. Krutzler, A. Glaser, R. Bauer, « Pilot-plant treatment of olive mill wastewater by solar TiO2 photocatalysis and solar photo-Fenton », *Solar Energy*, **2004**, In Press.
J.F. Rivas, F. J. Beltran, G. Gimeno, J. Frades, « Treatment of Olive Oil Mill Wastewater by Fenton's reagent », *J. Agric. Food Chem.*, **2001**, *49*, 1873.
(a) A. Ouardaoui, « Spectroscopic and kinetic studies of the photodegradation of 4-Chlorophenol », Ph.D. Thesis, University of Massachusetts. Lowell, USA, **1996**.
A. Ouardaoui, C.S. Steren, H. Willigen, C. Yang., « FT-EPR study of the photolysis of 4-chlorophenol », *J. Am. Chem. Soc.*, **1995**, 117 (25), 6803-68.
A. Ouardaoui, D.M. Martino, C.A. Steren, H. Van Willigen, « FT-EPR and HPLC study of the mechanism of 4-chlorophenol photolysis », *App. Magn. Reson.*, **1997**, 13 (3), 275-284.
O. Yahiaoui, H. Lounici, N. Abdi, N. Ghaffour, A. Pauss, N. Mameri, « Treatment of olive mill wastewater by the combination of ultrafiltration and bipolar electrochemical reactor processes », *Chem. Eng. Proc. Proc. Inten.*, **2011**, *50*, 37-41.
K. B. Petrotos, T. Lellis, M. I. Kokkora, P. E. Gkoutsidis, « Purification of Olive Mill Wastewater Using Microfiltration Membrane Technology », *J. Memb. Separ. Tech.*, **2014**, *3*, 50-55.
T. Coskun, A. Yildirim, C. Balcik, N. M. Demir, E. Debik, « Performances of Reverse Osmosis Membranes for Treatment of Olive Mill Wastewater », *Clean*, **2013**, *41*, 463-468.
P. Galiatsatou, M. Metaxas, D. Arapoglou, V. Kasselouri-Rigopoulou, « Treatment of olive mill waste water with activated carbons from agricultural by-products », *Waste Management*, **2002**, *22*, 803-812.
A. Waterhouse, «Folin-Ciocalteau Micro Method for Total Phenol in Wine», Department of Viticulture & Enology, University of California, Davis. Link: http://waterhouse.ucdavis.edu/faqs/folin-ciocalteau-micro-method-for-total-phenol-in-wine
P.K. Holt, G.W. Barton, C.A. Mitchell, « The future for electrocoagulation as a localized water treatment technology », *Chemosphere*, **2005**, *59*, 355–367.
K. Bensadok, S. Benammara, F. Lapicque, G. Nezzal, « Electrocoagulation of cutting oil emulsions using aluminium plate electrodes », *J. Hazard. Mat.*, **2008**, *152*, 423-430.

DRILL TOOL FLANK WEAR IN DRILLING OF PURE AND CARBON BLACK REINFORCED HIGH DENSITY POLYETHYLENE

Alper UYSAL
Yildiz Technical University, Department of Mechanical Engineering, Istanbul- Turkey
auysal@yildiz.edu.tr

Abstract: Polymer materials are preferred in various industrial areas such as automotive, manufacturing, aeronautic etc. and their material properties are improved by reinforcing carbon black, carbon fiber, graphite, carbon nanotubes, metal oxides etc. to enhance their usage areas. Additionally, in application areas, drilling operations are required for assembly processes. Therefore, in this experimental study, drill tool flank wear was investigated in drilling of pure and carbon black reinforced HDPE (High Density Polyethylene) materials. In experiments, two cutting speeds, feeds, and drill point angles (120° and 80°-120°) were selected as drilling parameters. Depending on the results, drill tool flank wear increased with increase of cutting speed and decreased with increase of feed. The maximum tool wear values were measured in drilling with standard drill tools (120°) and the double-angled (80°-120°) drill tool design reduced the tool wear. In addition, the carbon black addition improved the material properties of HDPE and this caused an increase in drill tool flank wear during drilling process.
Keywords: Carbon Black, HDPE, Drilling, Drill Tool Wear

Introduction

Polymer materials are consumed more than steel materials and their usage continues to grow so rapidly due to their material properties such as non corrosive nature, high impact resistance, being lighter, good strength to weight ratio etc. (Alauddin et al., 1995, Gulrez et al., 2014). Among the polymer materials, polyethylene has excellent chemical resistance and mechanical properties and it is electrically insulating material. However, the electrical conductivity can be increased by using various conductive fillers to enhance their usage in other applications such as in manufacturing computer chip, fuel tankers, automotive housing etc. In general, carbon black, carbon fibers, metal fibers and carbon nanotubes are commonly preferred to improve the electrical conductivity and these fillers can enhance the modulus and strength of matrix material (Gulrez et al., 2014, Hopmann et al., 2014, Zhijun et al., 2009). Polymer materials are usually shaped using methods such as plastic injection, extrusion etc. but the demand for the machining of them increases. Drilling is one of the most important machining operations that applied on polymer and composite materials to prepare them for joining and assembly (Ahmad, 2009). During drilling of polymer and composite materials, drill tool wears and so drilled part quality is reduced. Lin and Chen (1996) studied the effects of increasing cutting speed on tool wear when drilling carbon fiber reinforced composite material with both multifacet drill and twist drill. Drill tools are worn quickly at high cutting speeds and the multifacet drill tool was not superior when compared with the twist drill. Inoue et al. (1997) carried out drilling experiments in glass fiber reinforced composite material under various feed rates and cutting speeds and the relationship between tool wear and drilled hole quality was examined. Depending on the results, a great number of holes at a constant quality were obtained at high feed rates. Khashaba et al. (2010) performed an experimental study on the effect of drill pre-wear and machining conditions in drilling glass fiber reinforced glass epoxy composites. The results showed that thrust force and surface roughness were affected by the drill pre-wear and this effect became more significant at high cutting speed and feed which increased peel-up and push-out delaminations. Uysal et al. (2012) investigated the effects of cutting parameters on tool wear in drilling of sheet molding compound composite material. Feed was found as the most effective parameter while cutting speed was the least significant parameter on drill tool wear. Wang et al. (2013) aimed to investigate the wear of uncoated, diamond coated and AlTiN (Aluminium Titanium Nitride) coated carbide drills in drilling of carbon fiber reinforced composite material. The diamond coating reduced the edge rounding wear while the AlTiN coating was not effective on reducing the wear due to its oxidation during drilling. Gaugel et al. (2016) performed drilling experiments with uncoated and diamond coated tungsten carbide hard metal twist drills in carbon fiber reinforced polymer laminates. According to the measurement results, it was figured out that there was a correlation between drill tool wear and delamination damage. Uysal and Altan (2015) investigated drill tool wears in drilling of pure and carbon black reinforced polypropylene and polyamide materials with drill tools having different drill point angles. The minimum drill tool wear was observed in drilling with drill tool having small point angle (80°) and it increased with increase of cutting speed. Additionally, drill tool wears were higher in drilling of carbon black reinforced polymer materials than that observed in drilling of pure polymer materials. In literature, the studies about drill tool wears have been generally performed on drilling carbon or glass fiber reinforced polymer composite materials and there are no further works on particle reinforced polymer composite materials. However, in this experimental study, drill tool flank wear was investigated in drilling pure and carbon black reinforced HDPE

(High Density Polyethylene) materials. In experiments, two cutting speeds, feeds and drill point angles were selected as drilling parameters and their effects on the drill tool flank wear were examined.

Experimental Studies

In experimental studies, BPC brand pure HDPE (High Density Polyethylene) and Premix brand PRE-ELEC® PE 1296 model carbon black reinforced HDPE (CBR-HDPE) materials were the workpiece materials and their material properties were given in Table 1.

Table 1: Material properties of pure and carbon black reinforced HDPE.

Properties	Pure HDPE	CBR-HDPE
Specific gravity (gr/cm^3)	0,95	1,12
Yield strength (MPa)	23	24
Flexural modulus (MPa)	800	1100
Elongation at break (%)	>50	40
Elongation at yield (%)	9	12
Impact strength, notched Izod (4 mm thickness, 23°C) (kJ/m^2)	12	29
Deflection temperature (0,45 MPa) (°C)	60-82	80
Volume resistivity (Ωcm)	≥10^{14}	<10^3
Surface resistance (Ω)	≥10^{14}	<10^5

The polymer workpiece materials were injection molded from pure HDPE and CBR-HDPE granules in dimensions of 150x150x10 mm. Before the injection molding process, the granules were dried at 60°C for 2 hours. During the molding process, the granules were melted at 230°C, the mold temperature was 50 ºC and injection pressure was 90 MPa.

Drilling operations were performed by First MCV-300 CNC machining center with HSS (High Speed Steel) twist drill tools as seen in Figure 1. The drilling parameters were given in Table 2.

Figure 1. Drilling operation with HSS twist drill tool using CNC machining center.

Table 2: Drilling parameters.

Parameters	Value	
Cutting speed, V (m/min)	40	120
Feed, f (mm/rev)	0,1	0,2
Drill point angle, α (°)	120°	80°-120° (double-angled)

The drill diameter was 8 mm and the drill point angles were selected as 120°, and 80°-120° (double-angled) as given in Figure 2.

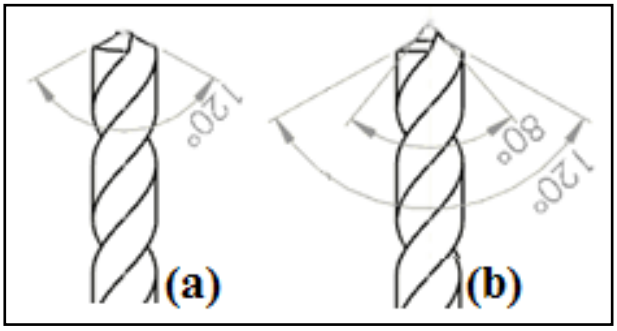

Figure 2. Point angles of selected HSS twist drill tools a) 120°, b) 80°-120° (double-angled).

Drill tool flank wears were viewed by SOIF XJP-6A model trinocular microscope and 9 MP MD90 camera as seen Figure 3. The flank wear values were measured via MShot software after drilling 50 holes and 100 holes. In addition, drill tool SEM (Scanning Electron Microscopy) images were taken by FEI Philips XL30 ESEM-FEG device.

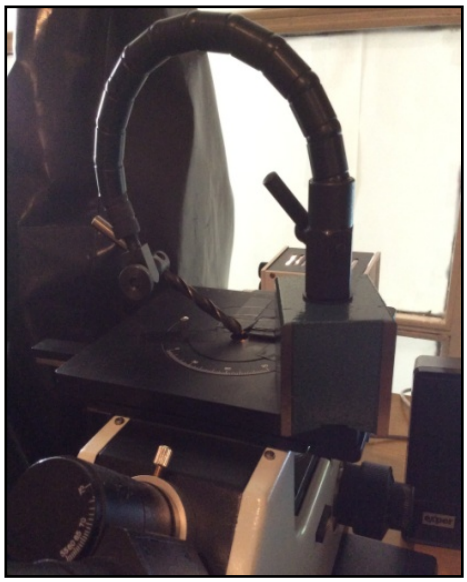

Figure 3. Viewing and measuring of drill tool flank wears by trinocular microscope.

Experimental Results and Discussion

As is known, friction between drill tool and poymer material increases at higher cutting speeds. Therefore, drill tool flank wear increased with increase of cutting speed for both pure HDPE and CBR-HDPE as seen in Figure 4.

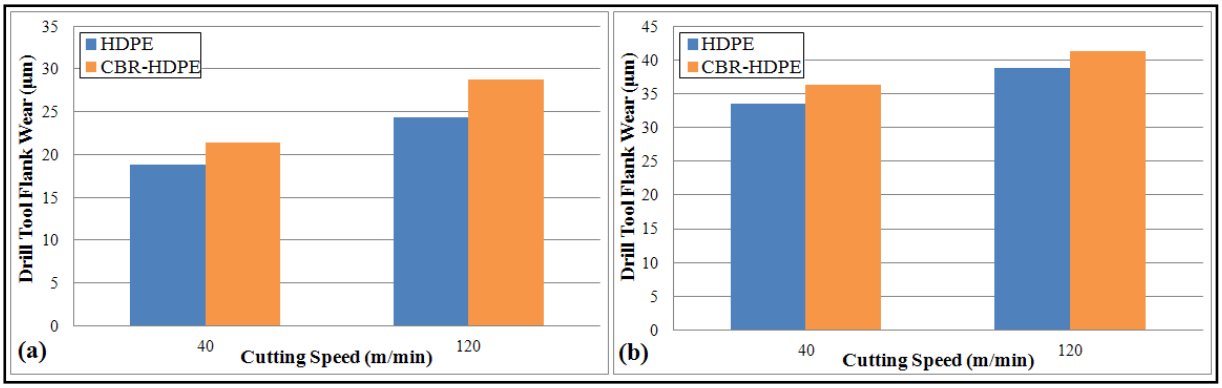

Figure 4. Drill tool flank wear according to the cutting speed (α=120°, f=0,1 mm/rev), after drilling of a) 50 holes and b) 100 holes.

When the double-angled (80°-120°) drill tools were preferred, less drill tool wear occurred as seen in Figure 5. Polymer material can be crashed when high drill point angle (120°) is used and this increases friction and also drill tool wear while sharp pointed tip makes easier the cutting operation.

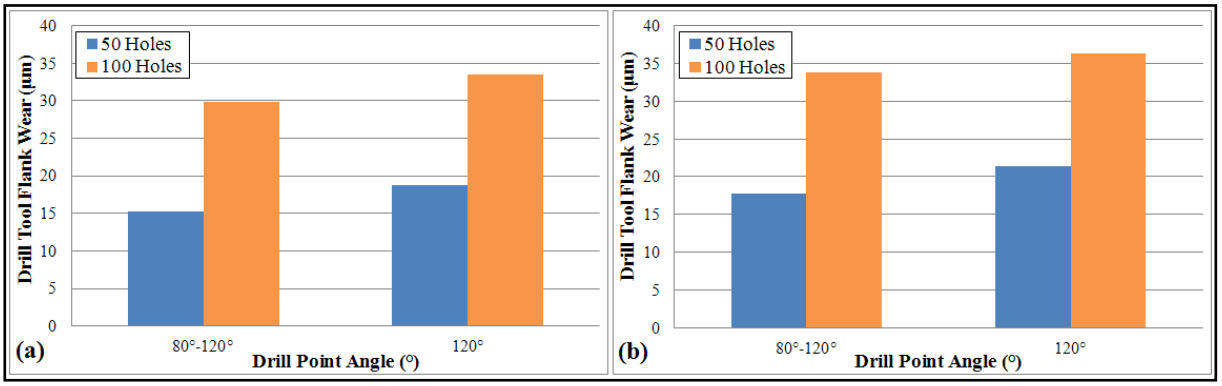

Figure 5. Drill tool flank wear according to the drill point angle (V=40 m/min, f=0,1 mm/rev), a) HDPE and b) CBR-HDPE.

The changing of drill tool flank wear with the feed was given in Figure 6. As increasing the feed, the drilling operation can be performed faster and so it is resulted that the heat based friction decreases. For this reason, less drill tool flank wear values were measured when the feed increased.

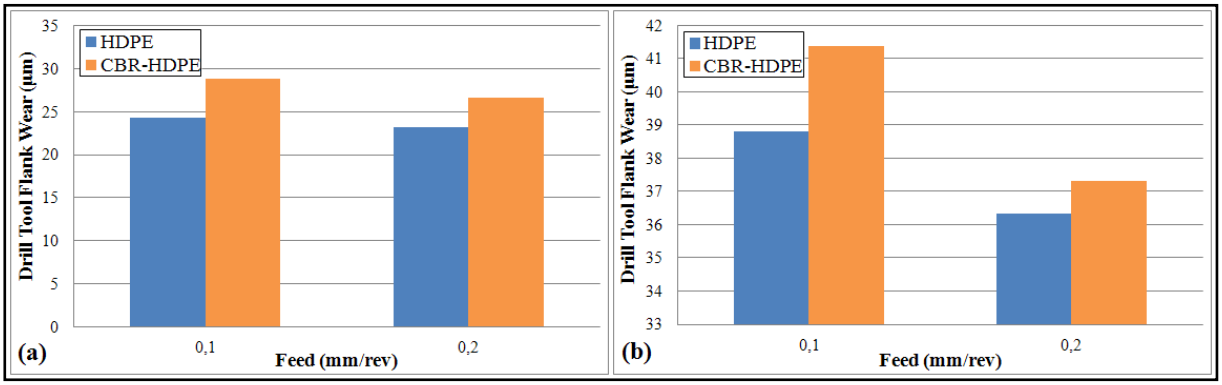

Figure 6. Drill tool flank wear according to the feed (α=120°, V=120 m/min), after drilling of a) 50 holes and b) 100 holes.

Polymer materials have low thermal conductivity and in the machining process, the generated heat is collected at the upper surface of polymer material due to not conducting. However, the carbon black reinforcement increases the thermal conductivity and also it is known that the carbon black particles improve the strength and hardness values of the polymer materials. Therefore, higher drill tool flank wears were measured in the drilling of CBR-HDPE when compared to the drilling of pure HDPE.

After drilling of 100 holes, SEM images of drill tool flank wear were given in Figure 7 and Figure 8. Drill tool were adversely worn in the drilling of CBR-HDPE at the point angle of 120°, the cutting speed of 120 m/min and the feed of 0,1 mm/rev (Figure 7). Less drill tool flank wear was occurred when drilling with the double-angled (80°-120°) drill tool at the cutting speed of 40 m/min and the feed of 0,2 mm/rev (Figure 8). Besides, it was specified that the carbon black reinforcement increased the drill tool flank wear.

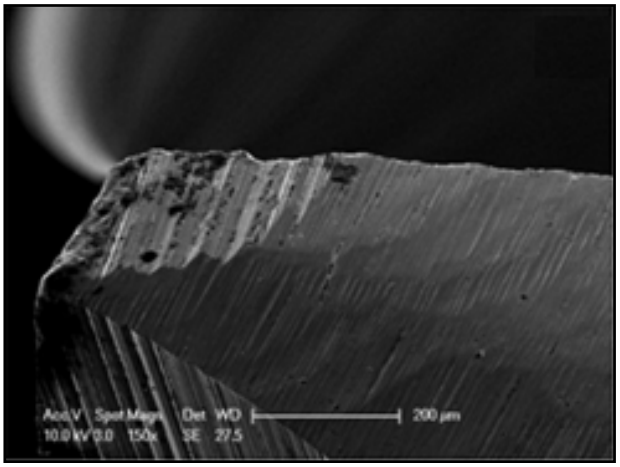

Figure 7.SEM image of drill tool flank wear after drilling of 100 holes on the CBR-HDPE (α=120°, V=120 m/min, f=0,1 mm/rev).

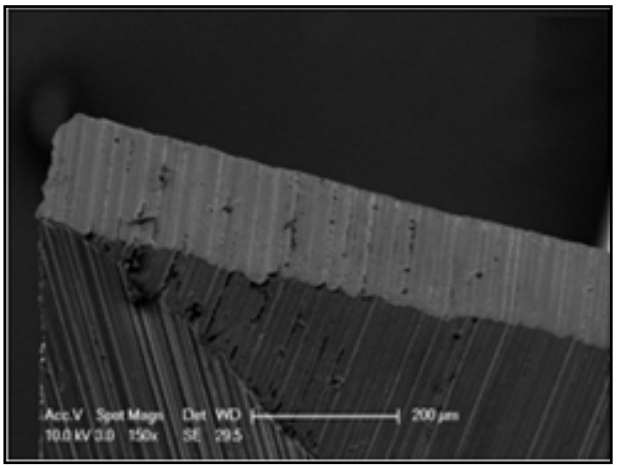

Figure 8.SEM image of drill tool flank wear after drilling of 100 holes on the pure HDPE (α=80°-120°, V=40 m/min, f=0,2 mm/rev).

Conclusion

In this study, pure and carbon black reinforced HDPE materials were drilled with drill tools having different drill point angles at two different cutting speeds and feeds and drill tool flank wear was investigated. The experimental results were given below.

- At higher drill point angles, polymer materials are subjected to plastic deformation with cutting, high drill forces occur to drill a hole and also friction and cutting temperature increase. Therefore, maximum drill tool flank wears were observed in the drilling of pure and carbon black reinforced HDPE with drill tools having drill point angle of 120°.
- The friction between drill tool and polymer material increased with increase of cutting speed and more drill tool flank wear was occurred in drilling both pure and carbon black reinforced HDPE polymer materials.
- Drill tool flank wear values decreased when increasing the feed due to the fact that drilling process was perfomed faster and less heat based on friction was occurred at high feed.
- It has been observed that the heat around the drilling zone is transmitted through the polymer material and the heat does not accumulate in a zone due to the fact that the carbon black reinforcement increases the thermal conductivity of polymer materials. In addition, less softening is observed when compared to pure polymer materials. For these reasons, drill tool flank wear values measured in the drilling of CBR-HDPE were higher than

that observed in the drilling of pure HDPE.

Acknowledgements
This research has been supported by Yıldız Technical University Scientific Research Projects Coordination Department. Project Number: 2014-06-01-GEP01.

References
Ahmad, J.Y.S. (2009). *Machining of polymer composites*, New York: Springer.

Alauddin, M., Choudhury, I.A., Baradie, M.A.E. & Hashmi, M.S.J. (1995). *Plastics and their machining: a review*, Journal of Materials Processing Technology, vol. 54, pp. 40-46.

Gaugel, S., Sripathy, P., Haeger, A., Meinhard, D., Bernthaler, T., Lissek, F., Kaufeld, M., Knoblauch, V. & Schneider, G. (2016). *A comparative study on tool wear and laminate damage in drilling of carbon-fiber reinforced polymers (CFRP)*, Composite Structures, vol. 155, pp. 173-183.

Gulrez, S.K.H, Mohsin, M.E.A., Shaikh, H., Anis, A., Pulose, A.M., Yadav, M.K., Qua, E.H.P. & Al-Zahrani, S.M. (2014). *A review on electrically conductive polypropylene and polyethylene*, Polymer Composites, vol. 35, pp. 900-914.

Hopmann, C., Fragner, J. & Haase, S. (2014). *Development of electrically conductive plastic compounds based on filler combinations*, Journal of Plastics Technology, vol. 10, pp. 49-67.

Inoue, H., Aoyama, E., Hirogaki, T., Ogawa, K., Matushita, H., Kitahara, Y. & Katayama, T. (1997). *Influence of tool wear on internal damage in small diameter drilling in GFRP*, Composite Structures, vol. 39(1-2), pp. 55-62.

Khashaba, U.A., El-Sonbaty, I.A., Selmy, A.I. & Megahed, A.A. (2010). *Machinability analysis in drilling woven GFR/epoxy composites: Part II – effect of drill wear*, Composites: Part A, vol. 41, pp. 1130-1137.

Ling, S.C. & Chen, I.K. (1996). *Drilling of carbon fiber-reinforced composite material at high speed*, Wear, vol. 194, pp. 156-162.

Uysal, A., Altan, M. & Altan, E. (2012). *Effects of cutting parameters on tool wear in drilling of polymer composite by Taguchi method*, International Journal of Advanced Manufacturing Technology, vol. 58, pp. 915-921.

Uysal, A. & Altan, E. (2015). *Tool wear in drilling of pure and carbon black reinforced polypropylene and polyamide materials*, 1st National Plastic Technologies Symposium; Plastics, Polymer Composites, Forming Technologies (UPTS'2015), pp. 181-188, 15-16 October 2015, Istanbul, Turkey (in Turkish).

Wang, X., Kwon, P.Y., Sturtevant, C., Kim, D.D.W. & Lantrip, J. (2013). *Tool wear of coated drills in drilling CFRP*, Journal of Manufacturing Processes, vol. 15, pp. 127-135.

Zhijun, Q., Xingxiang, Z., Ning, W. & Jianming, F. (2009). *Poly(1,3-butylene adipate) plasticized poly(lactic acid)/carbon black as electrical conductive polymer composites*, Polymer Composites, vol. 30(11), pp. 1576-1584.

EFFECTS OF HIGH-ENERGY BALL MILLING PARAMETERS ON STRUCTURE AND THERMAL BEHAVIOR OF TINCAL

Tuğba TUNÇ PARLAK*, Neşe GÜÇLÜ KALEİÇLİ, Kenan YILDIZ
Sakarya University, Metallurgy and Materials Engineering, Esentepe Campus, 54187, Sakarya-TURKEY
ttunc@sakarya.edu.tr

Abstract: Tincal is widely used mineral in ceramic and metallurgy industries and raw material of borax production. It contains clay minerals and crystal water in the structure. Tincal, named as sodium tetraborate decahydrate, that has same formulation with borax, as known as borax decahydrate is the member of sodium borates and its formulation is expressed as $Na_2B_4O_7.10H_2O$ or $Na_2(B_4O_5(OH)_4).8H_2O$. Extra weight of water in raw boron minerals may become problem in point of transportation, storage, energy cost for producing anhydrous borates and by-product. In this study, with the aim of removing structural water and creating structural alterations for the forward mineral processing with less cost. High-energy ball milling, as known as mechanical activation process, was applied by planetary mono mill with variable parameters such as revolution per minute-speed of main disc (100, 200, 300, 400, 500 and 600 rpm for 30 min at ball-to-mass ratio 20), ball-to-mass ratio (10, 20, 30 and 40 for 30 min at 600 rpm) and mechanical activation time (15, 30, 60, 90 and 120 min). Investigations of effects of activations parameters were done by using X-ray diffraction analysis, Fourier transform infrared spectroscopy and thermal analysis. It was concluded that structure of tincal was changed and loss of crystalline water was occurred during high-energy ball milling.
Keywords: Tincal, Amorphization, Stress energy, Mechanical activation

Introduction

Boron compounds are used in many sectors such as glass, glass fibre, ceramic, hygienic and cleaning products, flame retarder, metallurgy-materials area, health, cosmetic and energy. Among all chemical elements, boron has the highest volumetric heat of combustion (140 kJ/cm^3) and the third highest gravimetric heat of combustion (59 kJ/cm^3) after H_2 and Be (Liu et al., 2014).

Boron minerals can be grouped as sodium borates, calcium borates, calcium borosilicate, magnesium borates and sodium-calcium borates. West Turkey possesses the largest boron deposits with a worldwide share of 72% (851 Mtons) in terms of B_2O_3 content, and controlled by the national mining enterprise Eti Mine (Kavas et al., 2011). Eti Mine has four production facility position. Kırka boron plant mainly works on borax and tincal. Colemanite and boric acid are products of Emet. Colemanite ($2CaO.3B_2O_3.5H_2O$) and ulexite ($Na_2O.2CaO.5B_2O_3.16H_2O$) are obtained via open pit mining at Bigadiç. Bandırma boron plant has a wide variety of boron products.

Tincal that has clay minerals in the structure is raw material of borax production. Borax from tincal is produced via batch process. Tincal is fed to a stirred reactor containing water heated to 95-100°C. Colloidal clay in the water is coagulate with an anionic coagulant. After coagulating and precipitating of clay, clear solution is passed to filter-pressing and is then fed to a crystallizer (Boncukoğlu et al., 1999).

Tincal that has same formulation with borax as known as borax decahydrate is the member of sodium borates. Its formulation is expressed as $Na_2B_4O_7.10H_2O$ or $Na_2(B_4O_5(OH)_4).8H_2O$. In this structure two molecules of water are structurally incorporated in the borate ion ($B_4O_5(OH)_4^{2-}$) as hydroxyl groups whereas remaining water molecules are present at outside of the ionic structure (Koçakuşak et al., 1995). Same situation is expressed for borax pentahydrate ($Na_2B_4O_7.5H_2O$) and stated that 3 mol of water of crystallization could be eliminated easily by thermal treatment but remaining 2 mol of water are strongly attached to the structure and can be removed by molecular decomposition (Sahin and Bulutcu, 2002). In many point, water in the structure may become problem such as transportation, storage and by-product.

Mechanical activation process or high energy milling has been using in the powder preparation area with the aim of synthesis of amorphous alloy powders or synthesis of alloy powders with other meta stable phases, synthesis of nanocrystalline powders, nanopowders, metal-ceramic composites and nanocomposite powders (Zhang, 2004). The fundamental principle of size reduction is supplied energy from grinding media to the powder. Trapping powder between two colliding balls compressed into small pieces (Alves et al., 2013).

In this study, with the aim of removing structural water and creating structural alterations for the forward mineral processing with less cost. High-energy ball milling, as known as mechanical activation process, was applied by planetary mono mill with variable parameters.

Materials and Methods

Tincal was obtained from Eti Mine, Bandırma/Turkey. Because of the decomposition of tincal occurs above 50°C, obtained material was dried at room temperature for one day to eliminate the dehydration of the structure. After drying, ore was milled and sieved under 75 µm for standardization to mechanical activation process.

The ore was mechanically activated in Planetary Mono Mill, Fritsch Pulverisette 6. Milling process was carried out under dry condition in tungsten carbide bowl that has 250 ml capacity with same material ball with 8.15 g in weight and 10 mm in diameter. Initially revolution per minute was tried at 100, 200, 300, 400, 500 and 600 rpm for 30 min at ball-to-mass ratio 20. After determining the efficiency of revolution, ball-to mass ratio studies were carried out at 10, 20, 30 and 40 for 30 min at 600rpm. After confirmation of revolution and ball-to mass ratio, mechanical activation durations were tried for 15, 30, 60, 90 and 120 min.

Mechanically activated samples were analysed by X-ray diffractometer to observe the structural alterations and amorphization degrees (*A*) were calculated by using Equation 1 (Baláž, 2008),

$$A = \left(1 - \frac{I_X . B_0}{I_0 . B_X}\right) . 100 \quad (1)$$

where I_0 is the integral intensity of the diffraction peak for the non-activated tincal, B_0 is the background of the diffraction peak for the non-activated tincal, and I_x and B_x are the equivalent values for the activated tincal (Baláž, 2008).

Also stress energy that is generated by mechanical activation process on the powder samples was calculated according to Equation 2 (Erdemoğlu et al., 2009).

$$SE\ (J/kg) = \frac{m_B}{m_S} . a . n . t_m . D \quad (2)$$

where m_B, m_S, a, n, t_M and D refer to mass of grinding media (kg), mass of material charge (kg), theoretical acceleration in the centre of the bowl in the planetary mill (m/s^2), speed of revolution (1/s), grinding time (s) and mill diameter (m), respectively. Theoretical acceleration for this planetary ball mill is 26.41 m/s^2, as stated by the supplier.

Fourier transform infrared spectroscopy to understand which changes in progress for bonds and thermal analysis to determine the decomposition temperature changes in the activated tincal were carried out. X-ray diffraction analysis was performed using a Rigaku Ultima X-ray diffractometer and Cu Kα radiation. FT-IR was done by Shimadzu between 4000 cm^{-1}-500 cm^{-1}. DTA was performed using TA Instruments SDTQ 600 at heating rate of 5°C.min^{-1} under atmospheric conditions.

Result and Discussion

XRD analysis of the sample was given in Figure 1. Borax (JPDS card no 01-075-1078), dolomite (JPDS card no 01-075-1656) and borax pentahydrate known as tincalconite (JPDS card no 01-071-1536) phases were detected. Peak overlapping phenomenon observed mainly between borax and tincalconite.

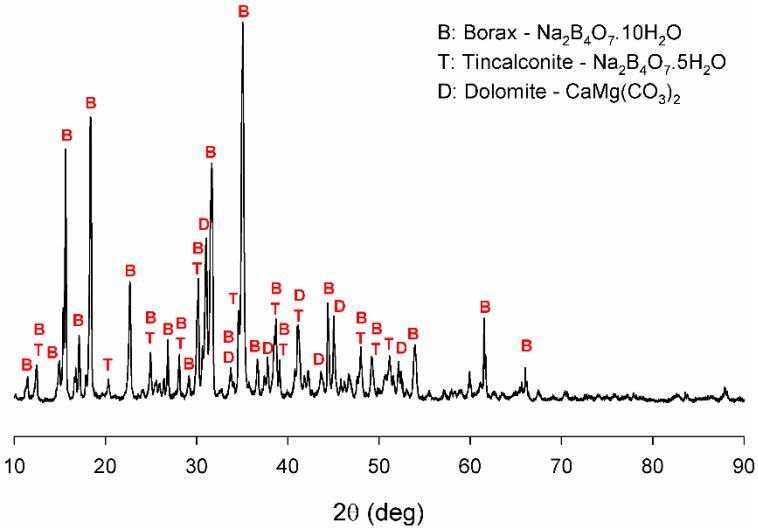

Figure 1. XRD analysis of the sample

Speed of main disc -revolution per minute- studies were carried out for 30 min and ball-to-mass ratio at 20. For observing changes at patterns, XRD was given at Figure 2 which was given between 10° - 40° to include most intensive peaks of the phases. At Figure 3, stress energy-I/I_0 (peak rate) and stress energy-amorphization degree (A%) dependence was given according to speed of main disc. As seen from the Figure 2, until 300 rpm no significant changes were obtained in terms of borax and dolomite. After 300 rpm, appearance of tincalconite was detected to accompaniment of intensity decrement of borax. By taking into consideration of crystallite size effect occurred as stretch and/or decrease in intensity of peak, peak rate (I/I_0) for borax presents at ~35° was considered where I_0 is the intensity of the non-activated sample and I is the intensity of activated one. As seen from the Figure 3, with increasing speed of main disc, stress energy increased. Peak rate decreased parallelly to amorphization degree increment. But these changes occurred drastically after 200 rpm in furtherance to XRD analysis. At higher speeds, due to temperature increase originated from ball-mass-bowl friction, borax phase underwent decomposition and in situ phase transformation to tincalconite occurred. When amorphization percentages were considered, speed of main disc was fixed at 600 rpm that borax patterns lost substantially.

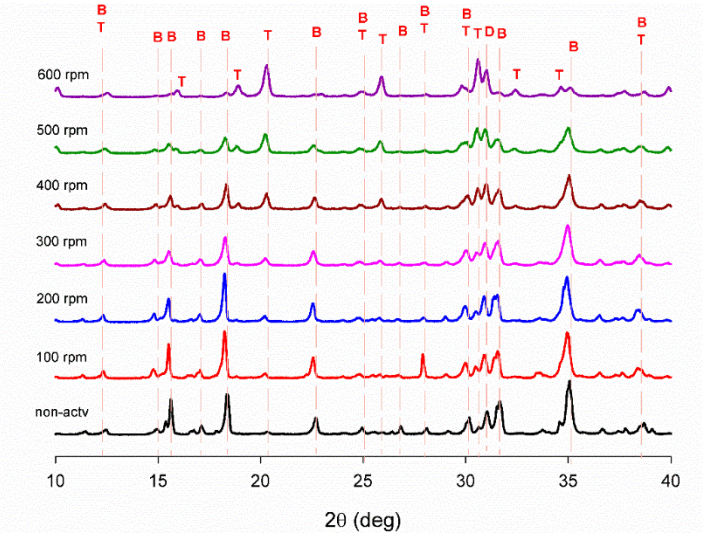

Figure 2. X-ray diffraction analysis of mechanically activated tincal sample at various speed

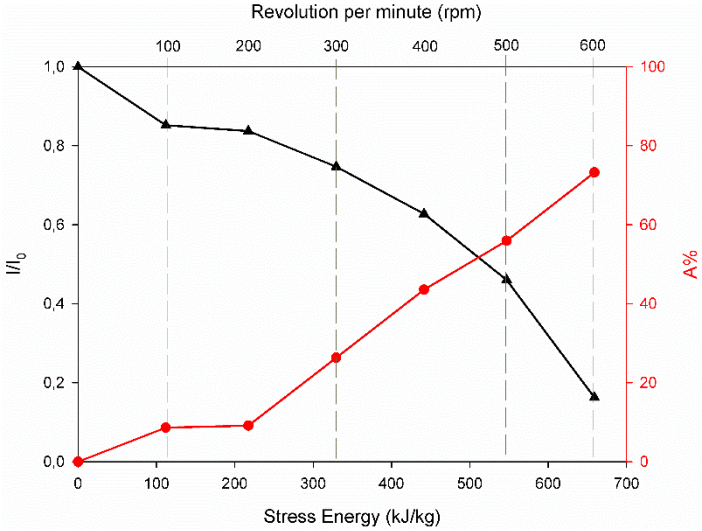

Figure 3. Stress Energy-I/I_0 and Stress Energy-%A dependance according to rpm

Effect of ball-to-mass ratio was given in Figure 4. Determination of ball-to-mass ratio was conducted at 600 rpm for 30 min. Tincalconite formation was observed for all parameter. At Figure 5, increased ball-to-mass ratio caused increment in stress energy and amorphization degree. Additionally, peak rate decrement occurred.

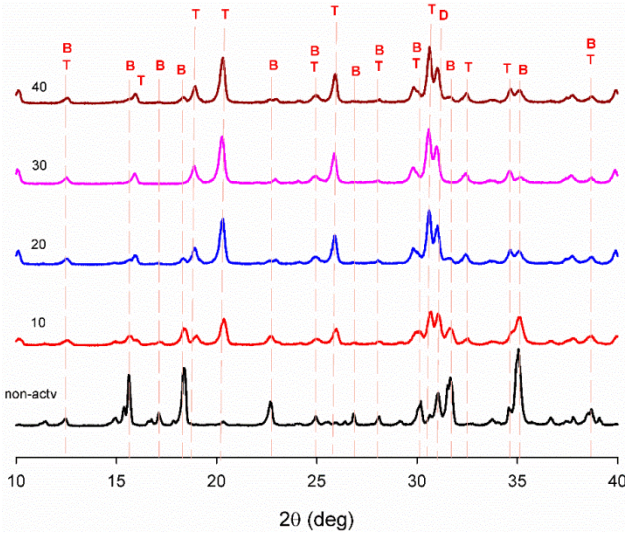

Figure 4. X-ray diffraction analysis of mechanically activated tincal at different ball-to-mass ratios.

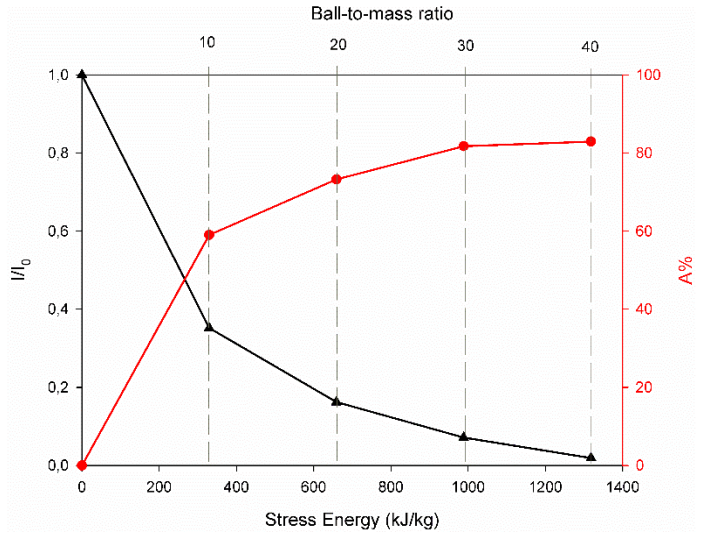

Figure 5. Stress Energy-I/I_0 and Stress Energy-%A dependance according to ball-to-mass ratio

When sample mass and amorphization degree considered together with regards to industrial application, higher ball-to-mass ratio like 30 and 40 not be logical for small variance in amorphization degree as shown in Figure 5 due to the less feed. Taking into consideration of this situation, ball-to-mass ratio was fixed at 20 for mechanical activation duration studies.

Role of mechanical activation duration was given in Figure 6. After 15 min, borax patterns lost substantially and tincalconite formation occurred. Prolonged mechanical activation time caused shifting and/or broadening of the peaks caused from mechanism of mechanical activation that base on motion of milling equipment and taken place impact on the particulate system. One of the effects of mechanical activation is released heat from the friction of the ball-sample-bowl at 600 rpm could be caused partial decomposition of tincalconite. It is stated that for a planetary mill, typical temperature is over 200°C and during milling two kinds of temperature are considered: local temperature pulses due to ball collisions and overall temperature in the vial (Baláž et al., 2013).

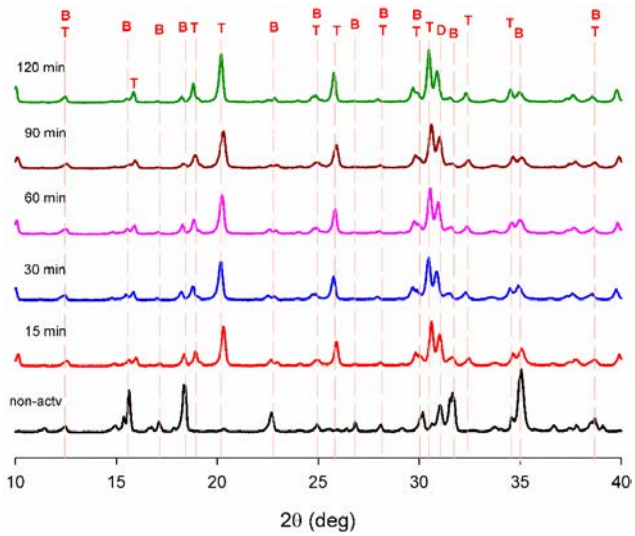

Figure 6. X-ray diffraction analysis of mechanically activated tincal for different durations.

Tromans and Meech (2001) stated that line broadening and disappearance of diffraction peaks that taken place on X-ray patterns after extended milling is a result of formation of meta-stable -amorphous phase- related with alteration of long-range lattice periodicity because of large number of dislocations and their related strain fields.

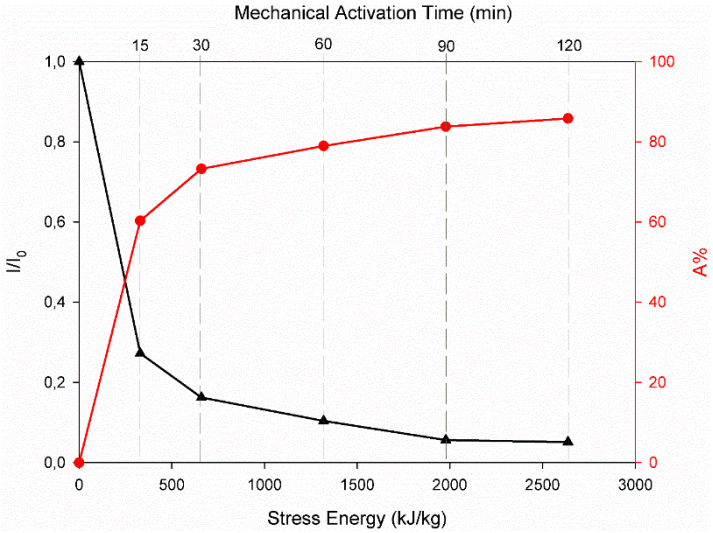

Figure 7. Stress Energy-I/I0 and Stress Energy-%A dependence according to ball-to-mass ratio

When Figure 7 was examined, it was understood that after 15 min mechanical activation duration, peak rate was drastically decreased with increased stress energy. More stress energy than provided stress energy about 360 kJ/kg by 15 min mechanical activation, formed little change in the intensity of the diffraction pattern and

amorphization degree. This phenomenon means that both crystal structure and crystal size didn't affect from increased mechanical activation time anymore after 15 min.

FT-IR analysis of non-activated and activated for 15 and 60 min samples are given in Figure 8. The region of 2700-3700 cm^{-1} is attributed as hydroxyl stretching region (Ruan et al., 2002). 3344 cm^{-1}, 3498 cm^{-1} and 3576 cm^{-1} band centres were determined in this region. But for mechanical activated samples band centres were determined at 3008 cm^{-1}, 3348 cm^{-1} and 3502 cm^{-1}. 3576 cm^{-1} was absent for these samples.

A shift of band centre to higher position means that strength of bonds is decreased. If the band shifts to a lower position it will result in tighter bonding. This region that indicates O-H stretching vibration is sensitive to dehydroxylation temperature. It was used for dehydroxylation of goethite by Ruan et al., (2002).

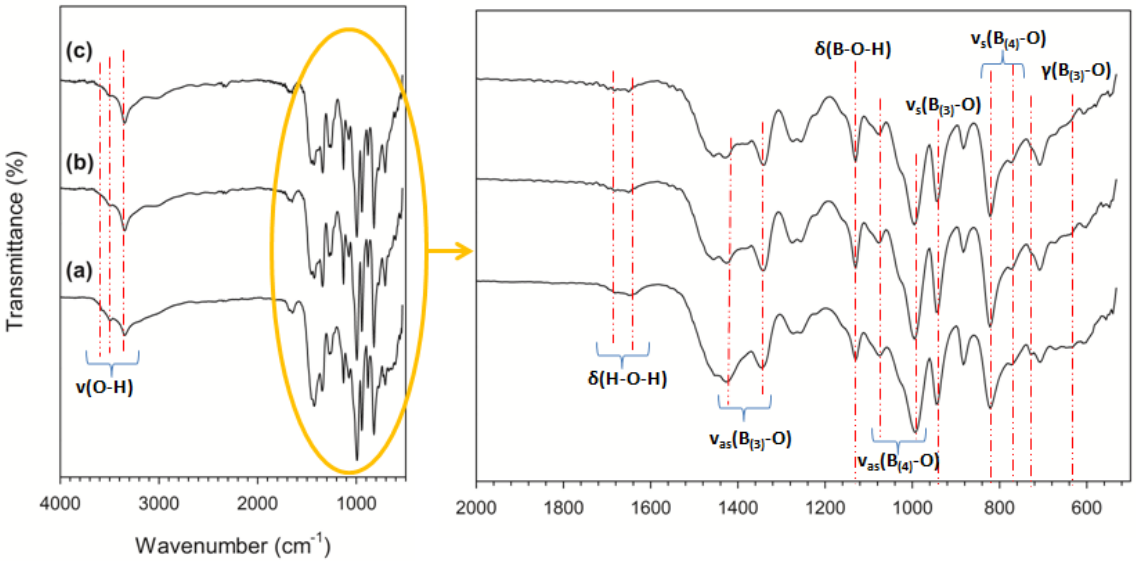

Figure 8. FT-IR analysis of a) non-activated and activated for b) 15 min and c) 60 min samples.

From these results, it can be said that with mechanical activation dehydroxylation was partially started but not completed because of existence of the characteristic band that differ in transmittance and broadness than the non-activated. The FT-IR analysis of ulexite that used for sodium borohydride production by Piskin (2009) had a band that found at 1625.84 cm^{-1} clarified as a free H_2O band. Yan et al. (2001) stated that sample at 70°C, the H-O-H bending mode exist at 1636 cm^{-1} and 1691 cm^{-1}. Like these studies, H-O-H bending mode was varied between 1578 cm^{-1} and 1691 cm^{-1} for different studies (Yan et al., 2001; Zhihong et al., 2003; Liu et al., 2006; Figen et al., 2010; Wang et al., 2010; Goel et al., 2013). Figen et al. (2010) and Wang et al. (2010) also stated that the H-O-H bending modes for their studies that found 1691-1649 cm^{-1} and 1662 cm^{-1} respectively, showed that the sample contains crystal water molecules. For tincal sample, this band was determined at 1647 cm^{-1} and 1681 cm^{-1}, and for activated sample they positioned at 1651 cm^{-1} and 1681 cm^{-1} that means mechanically activated samples still contain crystal water but not same strength of initial bond. In our FT-IR analysis wavenumber of the peaks are matching with data of Jun et al. (1995) for FT-IR of tetraborates. 730 cm^{-1} is clarified as in plane bending mode of CO_3 (Ji et al., 2009). As stated in the XRD results, tincal samples contain dolomite and this band confirms the presence of dolomite. But in mechanically activated samples this band couldn't determine.

DTA-TG analysis of the samples is given in Figure 9 and Figure 10 respectively. Tincal is an ore that starts losing its water at approximately 330K (Ekmekyapar et al., 1997). Non- activated and activated samples were compared in terms of physical water loss, peak temperatures of 70°C and 40°C were determined for non-activated and activated for 15 min samples. No related reaction at this temperature interval was determined for 60 min activated sample. Second and third endothermic reaction peak temperatures were determined at 115°C and 135°C for non-activated sample. This gradual decomposition trend turned into one step for 15 min mechanically activated sample at 140°C. 125°C and 135°C peak temperatures were determined for 60 min sample.

From the DTA analysis it was understood that for non-activated, activated for 15 and 60 min samples, tincalconite formation finished at 135°C. But the advantage of mechanical activation was confirmed as endothermic peaks area that is a describer of energy requirement of a reaction (Tunç et al., 2014).

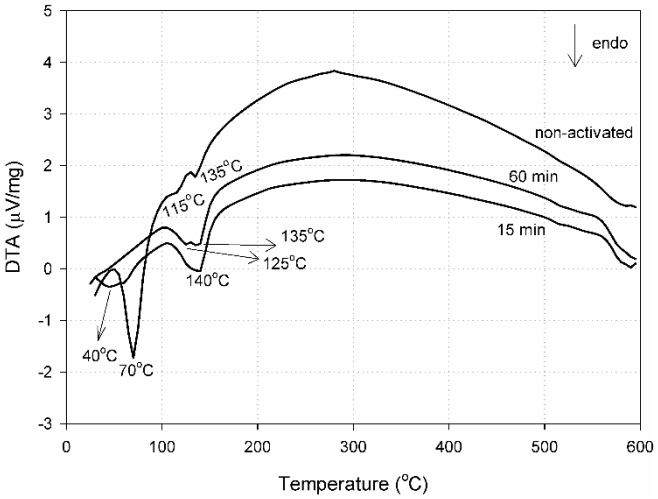

Figure 9. DTA analysis of non-activated and activated for 15 min and 60 min tincal.

When Figure 10 was examined it was understood that for non-activated sample, mass loss started as heating but for activated one, because of the physical water loss occurred during milling, decomposition started when reached at a certain temperature. When mass loss was investigated, this occurrent supported the heat occurrence during milling that cause elimination of water from the structure. Mass losses were calculated as 43%, %33 and %32 for non-activated, activated for 15 and 60 min activated samples. Form the XRD and DTA results it was understood that, decomposition of sample started in the milling process and TG results supported this phenomenon. Mass losses of the activated samples were less than the original one.

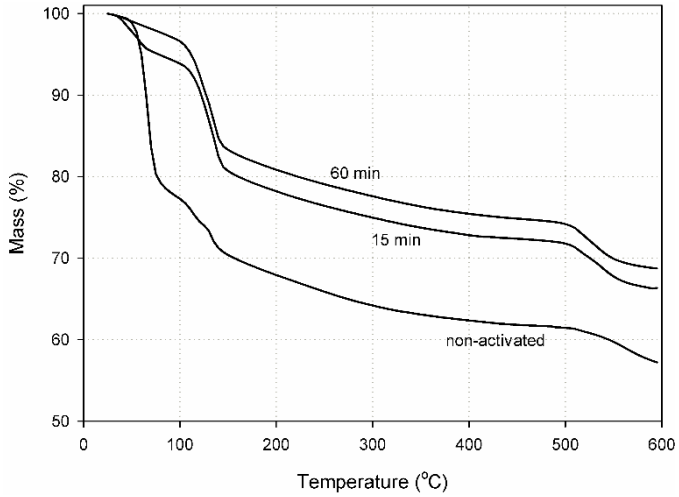

Figure 10. TG analysis of non-activated and activated for 15 min and 60 min tincal.

As determined from the XRD results, after 15 min mechanical activation, most of the diffraction peaks correspond to tincalconite and stress energy-I/I_0 graph showed that there was no need to excess energy input after 15 min to effect borax structure.

Conclusion

Tincal that is the raw material of the borax production was mechanically activated for observing structural alterations and structural water behaviour. Speed of main disc, ball-to-mass ratio and duration were chosen as parameters for mechanical activation process. In hydrated minerals, excess water molecules may be a problem during storage, transportation and production of other related boron products in the meaning of energy consumption.

XRD results shows that original tincal sample consist of borax and dolomite crystals.

By increasing the speed of main disc because of the friction thereby occurred heat energy, borax was decomposed and tincalconite formation occurred.
For industrial application, higher ball-to-mass ratio like 30 and 40 not be logical for little variance in amorphization degree due to the less feed. Taking into consideration of this situation, ball-to-mass ratio was fixed at 20 for mechanical activation duration studies.

Mechanical activation duration studies showed that after 15 min mechanical activation procedure, crystal structure changes about 75% by means of amorphization. Provided heat during mechanical activation via milling media motion, impact and friction cause in situ phase transformation of borax decahydrate to borax pentahydrate (tincalconite). More stress energy than provided stress energy about 360 kJ/kg by 15 min mechanical activation formed little change in the intensity of the diffraction pattern. This phenomenon means that both crystal structure and crystal size didn't affect from increased mechanical activation time anymore after 15 min and DTA-TG results supported this finding.

Borax decahydrate to borax pentahydrate (tincalconite) transformation was supported by FT-IR analysis. Because of the two molecules of water as hydroxyl unit in the borate ion, hydroxyl stretching vibrations were still present but not positioned at the same wavenumber that means amorphization by mechanical activation in force about alteration of the structure via changing the bond strength.

So, it can be said that, by mechanical activation tincal structure was changed and water lost was achieved without having to heat treatment.

References

Alves, A. K., Bergmann, C. P., Berutti, F. A. (2013). *Novel Synthesis and Characterization of Nanostructured Materials*, Verlag Berlin Heidelberg: Springer.

Baláž, P., Achimovičová, M., Baláž, M., Billik, P., Cherkezova-Zheleva, Z., Criado, J. M., Delogu, F., Dutková, E., Gaffet, E., Gotor, F. J., Kumar, R., Mitov, I., Rojac, T., Senna, M., Streletskii, A., Wieczorek-Ciurowa, K. (2013). Hallmarks of mechanochemistry: from nanoparticles to technology. *Chem. Soc. Rev.*, 42 (pp.7571-7637).

Baláž, P. (2008). *Mechanochemistry in Nanoscience and Minerals Engineering*, Berlin, Springer-Verlag.

Boncukcuoğlu, R., Kocakerim, M. M., Erşahan, H. (1999). Upgrading of the reactor waste obtained during borax production from tincal. *Minerals Engineering*, 12 (pp.1275-1280).

Ekmekyapar, A., Baysar, A., and Künkül, A. (1997). Dehydration kinetics of tincal and borax by thermal analysis. *Ind. Eng. Chem. Res.*, 36 (pp.3487-3490).

Erdemoğlu, M., Aydoğan, A., Gock, E. (2009). Effects of intensive grinding on the dissolution of celestite in acidic chloride medium. *Minerals Engineering*, 22 (14-24).

Figen, A. K., Yılmaz, M. S., Pişkin, S. (2010). Structural characterization and dehydration kinetics of Kırka inderite mineral: Application of non-isothermal models. *Materials Characterization*, 61 (pp.640-647).

Goel, N., Sinha, N., Kumar, B. (2013). Growth and properties of sodium tetraborate decahydrate single crystals. *Materials Research Bulletin* 48 (pp.1632–1636).

Ji, J., Ge, Y., Balsam, W., Damuth, J. E., Chen, J. (2009). Rapid identification of dolomite using a Fourier Transform Infrared Spectrophotometer (FTIR): A fast method for identifying Heinrich events in IODP Site U1308. *Marine Geology*, 258 (pp.60–68).

Jun, L., Shuping, X., Shiyang, G. (1995). FT-IR and Raman spectroscopic study of hydrated borates. *Spectrochimica Acta Part A: Molecular and Biomolecular Spectroscopy*, 51 (pp.519-532).

Kavas, T., Christogerou, A., Pontikes, Y., Angelopoulos, G.N. (2011). Valorisation of different types of boron-containing wastes for the production of lightweight aggregates. *Journal of Hazardous Materials*, 185 (pp.1381–1389).

Koçakuşak, S., Köroğlu, J. H., Ekinci, E., Tolun, R. (1995). Production of anhydrous borax using microwave heating. *Ind. Eng. Chem. Res.*, 34 (pp. 881-885).

Liu, Z., Li, P. and Zuo, C. (2006). Standard molar enthalpies of formation for the two hydrated calcium borates $xCaO.5B_2O_3.yH_2O$ (x = 2 and 4, y = 5 and 7). *J. Chem. Eng. Data*, 51 (pp. 272-275).

Liu, J., Xi, J., Yang, W., Hu, Y., Zhang, Y., Wang, Y., Zhou, J. (2014). Effect of magnesium on the burning characteristics of boron particles. *Acta Astronautica*, 96 (pp. 89-96).

Piskin, M. B. (2009). Investigation of sodium borohydride production process: Ulexite mineral as a boron source. *International Journal of Hydrogen Energy*, 34 (pp. 4773-4779).

Ruan, H. D., Frost, R. L., Kloprogge, J. T. and Duong, L. (2002). Infrared spectroscopy of goethite dehydroxylation. II. Effect of aluminium substitution on the behaviour of hydroxyl units. *Spectrochimica Acta Part A: Molecular and Biomolecular Spectroscopy*, 58 (pp. 479-491).

Sahin, O., Bulutcu, A. N. (2002). Production of high bulk density anhydrous borax in fluidized bed granulator. *Chemical Engineering and Processing: Process Intensification*, 41 (pp. 135–141).

Tromans, D., Meech, J. A. (2001). Enhanced dissolution of minerals: stored energy, amorphism and mechanical activation. *Minerals Engineering*, 14 (pp. 1359-1377).

Tunç, T., Apaydin, F., Yildiz, K. (2014). Structural alterations and thermal behaviour of mechanically activated alunite ore. *J Therm Anal Calorim.*, 118 (pp. 883-889).

Wang, Y., Pan, S., Hou, X., Liu, G., Wang, J., Jia, D. (2010). Non-centrosymmetric sodium borate: Crystal growth, characterization and properties on $Na_2B_4O_{12}H_{10}$. *Solid State Sciences*, 12 (pp. 1726-1730)

Yan, J., Yongzhong, J., Shiyang, G., Haidong, W., Shiying, Y. (2001). Thermal decomposition of $K_2O.CaO.4B_2O_3.12H_2O$. *Thermochimica Acta*, 374 (pp. 51-54).

Zhang, D.L. (2004). Processing of advanced materials using high-energy mechanical milling. *Progress in Materials Science*, 49 (pp. 537–560).

Zhihong, L., Bo, G., Mancheng, H., Shuni, L., Shuping, X. (2003). FT-IR and Raman spectroscopic analysis of hydrated cesium borates and their saturated aqueous solution. *Spectrochimica Acta Part A: Molecular and Biomolecular Spectroscopy*, 59 (pp. 2741-2745).

EPIDEMIOLOGY OF BRUCELLOSIS IN SHEEP AND GOATS IN THE IRAQI KURDISTAN REGION

Emad A. Aziz Alshwany[a], Ian D. Robertson[a,b]
[a] College of Veterinary Medicine, School of Veterinary and Life Sciences, Murdoch University, Australia
[b] China-Australia Joint Research and Training Center for Veterinary Epidemiology, Huazhong Agricultural University, Wuhan, China
Emada_sh@yahoo.com

Abstract:Brucellosis is an infectious zoonotic bacterial disease of worldwide importance. A cross-sectional serological study was undertaken in the Kurdistan Region to better understand the epidemiology of brucellosis in this region. A total of 694 sheep and 356 goats were sampled and tested with the Rose Bengal test. The seroprevalence in sheep (7.4%; 95% CI 5.5 - 9.6%) (OR 1.94; 95% CI 1.1 – 3.6) was significantly higher than that in goats (3.9%; 95% CI 2.2 - 6.5%). The highest seroprevalence among sheep (8.1%) was in Erbil province and the lowest in Dohuk province (4.9%). Among goats the highest seroprevalence (7.1%) was in Sulaymani province, and no seropositive goats were detected in Kirkuk and Dohuk provinces. The RBT seroprevalence in female sheep (6.5%; 95% CI 4.4 – 9.1%) was similar to that of males (9.3%; 95% CI 5.8 - 14.0%) (OR 0.67; 95% CI 0.38 – 1.21). The seroprevalence in female goats (4.7%; 95% CI 2.5 – 7.9%) was also similar to that of male goats (1.3%; 95% CI 0.0 – 6.9%) (OR 3.78; 95% CI 0.49 – 29.33).

Keywords: Epidemiology of Brucellosis, Sheep and Goats, Iraqi Kurdistan Region.

Introduction

Brucellosis is a zoonotic disease of livestock which is endemic in many countries of the world (Stites *et al*., 1987). The disease is caused by infection with bacteria belonging to the genus *Brucella* and has been recognized as a zoonotic disease since the discovery of *Brucella melitensis* in 1887 (Kaye and Petersdorf 1987). Transmission of *Brucella* occurs by contact with infected animals or their materials and disease in humans is always linked to disease in animals, predominantly livestock (Nicoletti, 1989). Brucellosis in animals results in significant economic losses because of abortions, reduced milk production, decreased reproduction rate and premature births (Pappas *et al*., 2006).

Although brucellosis has a worldwide geographical distribution, it particularly remains an important public health problem in the Mediterranean Region, North and East Africa, the Middle East, Southern and Central Asia, India, Central and South America (Faye *et al*., 2005). Infection of sheep with *B. melitensis* is endemic in the Mediterranean region, particularly along the eastern and northern shores. It is found through Central Asia, south to the Arabian Peninsula and as far as Mongolia and in India and Africa (European Commission, 2001). Although the main sources of infection are sheep, goats and their products, *B. melitensis* has emerged as an important problem in cattle in Saudi Arabia, Kuwait, some Southern European countries and Israel (First International Conferences on Emerging Zoonoses, 1997).

Materials and Methods

The Kurdistan Region is located in the north of Iraq and there are approximately 2.6 million sheep and 1.2 million goats in the Region (KRG, 2012), and these are mainly located in the villages, sub-districts and districts of the region. Field sampling was carried out from March 2015 to May 2015 throughout the Iraqi Kurdistan Region, and a two sampling plan was adopted. The first sampling plan was adopted in Sulaymani and Dohuk Provinces using a multi-stage sampling protocol. Six districts were randomly selected from Sulaymani Province and two from Dohuk Province for sampling. Within each selected district one sub-district was randomly selected. Two villages were then randomly selected from each selected sub-district and within each village five farmers were randomly selected from those available. Finally five animals (sheep and/or goats) were randomly selected from the selected farmers. Therefore in total 300 blood samples (216 sheep and 84 goats) were randomly collected (6 districts × 1 sub-district × 2 villages × 5 farmers × 5 animals = 300 samples) from Sulaymani Province and 100 blood samples (82 sheep and 18 goats) were randomly collected from Dohuk Province (2 districts × 1 sub-district × 2 villages ×

5 farmers × 5 animals = 100 samples). The number of sheep and goats sampled in the provinces was in proportion to the number of animals in that province. In Erbil and Kirkuk Provinces, blood samples were collected from sheep and goats by cooperating with the Veterinary Medical Centers (VMC) in these provinces. In Erbil Province there are 27 VMC, and 18 of these randomly collected 25 blood samples (sheep and goats) from each VMC (total 450 blood samples - 236 sheep and 214 goats). In Kirkuk Province 8 VMC collected 25 samples each for a total of 200 blood samples (160 sheep and 40 goats).

Overall a total of 694 blood samples were collected from sheep and 356 samples from goats in the four sampled provinces (Erbil, Sulaymani, Kirkuk and Dohuk). Five ml of blood was collected from the jugular vein directly into vacutainer tubes from each of the selected animals. Samples were then transported to the laboratories in the four provinces (Erbil, Sulaymani, Kirkuk and Dohuk) where they were centrifuged at 4000 rpm for 5 minutes and the sera separated and stored in Eppendorf Tubes prior to testing. All samples were tested within 24 hours of collection with the Rose Bengal Test (RBT) at room temperature as per the manufacturer's recommendations.

Using average values from the research of Blasco *et al*. (1994), EFSA-Q, (2006) and Rahman *et al*., (2013) the sensitivity and specificity of the RBT was estimated at 87.9 and 99.8%, respectively. These values were used to work out the real prevalence from the test prevalence.

Results

Of the 1050 animals sampled the overall seroprevalence was 6.2% (95% CI 4.8% - 7.8%). The seroprevalence in sheep based on the RBT (7.4%; 95% CI 5.5 - 9.6%) was significantly higher than that in goats (3.9%; 95% CI 2.2 - 6.5%) (OR 1.94; 95% CI 1.1 – 3.6). The overall real prevalence was estimated at (6.8%; 95% CI 4.8 – 7.8%) (Table 1).

Table 1: Seroprevalence to brucellosis based on the Rose Bengal Test in sheep and goats.

Species	Total number tested	Number positive on RBT	Seroprevalence (95% CI)	Real Prevalence (95% CI)	Odds ratio (95% CI)
Sheep	694	51	7.4% (5.5 - 9.6)	8.2% (6.3 – 10.5)	1.94 (1.1 – 3.6)
Goats	356	14	3.9% (2.2 - 6.5)	4.2% (2.4 – 6.8)	1.0
Total	1050	65	6.2% (4.8 - 7.8)	6.8% (4.8 – 7.8)	-

There was no significant difference in the seroprevalence in sheep between provinces based on the RBT. Similar observations were found for goats (Table 2). The seroprevalence was highest in sheep from Erbil (8.1%) and lowest in Dohuk (4.9%). In contrast for goats the seroprevalence was highest in Sulaymani (7.1%), and no seropositive goats were detected in both Kirkuk and Dohuk.

Table 2: Seroprevalence of brucellosis in sheep and goats originating from different provinces sampled in Kurdistan based on the RBT.

Species	Province	Total number of samples	Number RBT +ve	Prevalence (95% CI)	Odds ratio (95% CI)
Sheep	**Sulaymani**	216	17	7.9% (4.7 - 12.3)	0.98 (0.49 – 1.93)
	Kirkuk	160	11	6.9% (3.5 - 12.0)	0.84 (0.39 – 1.82)
	Dohuk	82	4	4.9% (1.4 - 12.1)	0.59 (0.19 – 1.78)
	Erbil	236	19	8.1% (5.0 - 12.3)	1.00

Goats	**Sulaymani**	84	6	7.1% (2.7 - 14.9)	1.98 (0.67 – 5.89)
	Kirkuk	40	0	0.00% (0.0 - 8.8)	-
	Dohuk	18	0	0.00% (0.0 - 18.5)	-
	Erbil	214	8	3.7% (1.6 - 7.2)	1.00

Table 3: Seroprevalence of brucellosis based on the RBT in male and female in sheep and goats.

Species	**Sex**	**Total**	**RBT +ve**	**Serorevalence (95% CI)**	**Odds ratio (95% CI)**
Sheep	**Female**	479	31	6.5% (4.4 – 9.1)	0.67 (0.38 – 1.21)
	Male	215	20	9.3% (5.8 – 14.0)	1.0
Goats	**Female**	278	13	4.7% (2.5 - 7.9)	3.78 (0.49 – 29.33)
	Male	78	1	1.3% (0.0 - 6.9)	1.0
Total	**Female**	757	44	5.8% (4.2 - 7.7)	0.8 (0.47 – 1.37)
	Male	293	21	7.2% (4.5 - 10.8)	1.0

The seroprevalence in female sheep (6.5%; 95% CI 4.4 – 9.1) was similar to that of males (9.3%; 95% CI 5.8 - 14.0%) (OR 0.67; 95% CI 0.38 – 1.21), also the seroprevalence in female goats (4.7%; 95% CI 2.5 – 7.9) was similar to that of male goats (1.3%; 95% CI 0.0 – 6.9) (OR 3.78; 95% CI 0.49 – 29.33) (Table 3).

Discussion

In this study overall 6.2% of animals were classified as seropositive. This was lower than that previously reported (14.5%) in Sulaymani (Jabary and Al-Samarraee, 2015) in unvaccinated herds and that reported by Al-Naqshabendy *et al.*, (2014) (39.1%) in non-vaccinated ewes in Dohuk. The differences in these two surveys may be the result of ongoing control programs through mass vaccination in the surveyed regions (Ministry of Agriculture and Water Resources, 2017). In the current study the seroprevalence in sheep (7.4%) was significantly higher than that in goats (3.9%). This difference is unexpected given the similar traditional husbandry practices of handling both species. Others have reported a higher seroprevalence in sheep than goats (Arslan *et al.*, 2011, Shareef, 2006) (23.6 and 10.6%, respectively).

Although recently other studies have been conducted on brucellosis in the same area as the current study, those studies included only a few districts and, similar to the current study, did report a significant difference in the seroprevalence between sheep and goats (Jabary and Al-Samarraee, 2015). In this study there was no significant difference in the animal-level seroprevalence between provinces. This was not surprising as the management and husbandry systems adopted are similar between provinces. Surprisingly no seropositive goats were found in Kirkuk and Dohuk Provinces. This could be due to the sample size, as the number of sheep and goats sampled in Erbil and Sulaymani provinces was larger than that for Kirkuk and Dohuk (overall the probability of detecting at least one seropositive goat was one positive to 25 goats sampled).

The seroprevalence in males and females (for both sheep and goats) was also similar in the current study. This finding was also expected because of the similar management practices males and females are subjected to. These findings concur with those previously obtained by Jabary and Al-Samarraee, (2015) who reported a prevalence of 14.3 and 15.1% in females and males, respectively and the study of Al-Hankawe and Rhaymah (2012) who reported a prevalence of 16.1 and 15.2% in females and males, respectively. Differences in seroprevalences between studies can arise from: the sample size; the tests used and the method of interpreting seropositivity ie in series or in parallel; the study location and the associated management and husbandry practices adopted within these locations; and the control methods, such as biosecurity measures and vaccination, adopted.

There are numerous reasons why brucellosis remains endemic in Iraq and Kurdistan Region. These include the uncontrolled movements of livestock flocks and herds particularly given the endemic status of brucellosis in surrounding countries, limited veterinary support services, the geopolitical situation, political instability, and husbandry practices which favor the spread of infection.

An efficient surveillance system is key to any successful control program, and should include regional and national surveillance, vaccination to increase the proportion of protective population, and strong collaboration between the veterinary and public health sectors. Critical to disease control is good management and husbandry practices, particularly associated with the introduction of animals, isolation/quarantine of animals which abort and the presence of wildlife which can act as reservoirs for the disease. Control or elimination of these factors will reduce the potential for disease transmission in an area. It is recommended that a vaccination program against brucellosis be implemented in Kurdistan and educational activities be implemented to improve awareness of the disease by livestock owners in the region.

Conclusions

Although brucellosis is close to being or has been eradicated from a number of developed countries, it continues to be a major animal and public health problem in many regions and countries of the world. From the results of this study it can be concluded that brucellosis is endemic in Iraqi Kurdistan Region and poses an important zoonotic risk to the human community.

References

Al-Hankawe, O. K. H., and M. S. Rhaymah. (2012). "*Comparison between ELISA and other serological tests for diagnosis of brucellosis in sheep in Ninevah province*." Iraqi J Vet Sci no. 26:97-103.

Al-Naqshabendy, A., A. Aveen, A. Ibrahiem, and O. H. Azeez. (2014). "*Effect of Brucella Melitensis on the Serum Lipids Profiles in Ewes*."

Arslan, SH, NA Al-Hussary, QT Al-Obaidi, and MM Hassan. (2011). "*Changes in some biochemical parameters accompanied with Brucellosis in native goats."* Iraqi Journal of Veterinary Sciences no. 25 (1).

Blasco, J.M., Garin-Bastuji, B., Marín, C., Gerbier, G., Fanlo, J., Jiménez De Bagués, M., Cau, C., (1994). *Efficacy of different Rose Bengal and Complement Fixation antigens for the diagnosis of Brucella melitensis in sheep and goats.* Vet. Rec. 134, 415–420.

EFSA-Q-2006. The EFSA Journal (2006) 432, 1–44 Scientific Opinion on *"Performance of Brucellosis Diagnostic Methods for Bovines, Sheep, and Goats"*, pp. 110–111.

European Commission. (2001). *Brucellosis in Sheep and Goats (Brucella melitensis).* Scientific committee on animal health and animal welfare.

Faye B, Castel V, Lesnoff M, Rutabinda D, Dhalwa J (2005). *Tubercullosis and Brucellosis prevalence on dairy cattle in Mbarara milk basin (Uganda).* Preventive Veterinary Medicine 67: 267-281.

First International Conference on Emerging Zoonoses. (1997). *Brucellosis: an overview. Emerg. Infect.* Dis. 3: 213-221.

Jabary, Osman M, and Ikram A Al-Samarraee. (2015) "*Detection of Brucella antibodies of sheep and goats by using two serological tests in Al-Sulaimanya governorate*."

KRG, Ministry of Planing. (2017). *Building the Kurdistan Region of Iraq.* Kurdistan Regional Government - Iraq 2012 [cited 21 Feb 2017 2017].

Kaye, D. and Petersdorf, R.G (1987). *Brucellosis. Harrison ś principles of internal medicine.* Vo.1.

Ministry of Agriculture. (2017). *General Directorate of Animal Wealth and Veterinary*. Ministry of Agriculture and Water Resource KRG 20152017].

Nicoletti Paul, L. (1989). *Relationship between Animal and Human Disease*. 41 - 52. In: Young Edward J, Corbel Michael J Brucellosis: Clinical and Laboratory Aspects1989. CRC Press, Inc., Boca Raton, Florida.

Pappas G, Papadimitriou P, Akritidis N, Christou L, Tsianos E. V. (2006). *The new global map of human brucellosis. Lancet Infect Dis*.; 6:91–9.

Rahman A.K.M. Anisur, Claude Saegerman, Dirk Berkvens, David Fretin, M.d. Osman Gani, M.d. Ershaduzzaman, Muzahed Uddin Ahmed, Abatih Emmanuel. (2013). *Bayesian estimation of true prevalence, sensitivity and specificity of indirect ELISA, Rose Bengal Test and Slow Agglutination Test for the diagnosis of brucellosis in sheep and goats in Bangladesh.* Preventive Veterinary Medicine 110/ 242–252.

Shareef, J.M. (2006). "*A review of serological investigations of brucellosis among farm animals and humans in northern provinces of Iraq (1974–2004).*" Journal of Veterinary Medicine, Series B no. 53 (s1):38-40.

Stites, D. P.; Stobo, J. D.; and Vivian wella, J. (1987). *Basic and clinical Immunology*. 6th ed. Appleton and Lange, London, P: 567.

EVALUATING USER SATISFACTION IN STUDENT APARTMENTS BASED ON COMFORT CONDITIONS: BURSA / GORUKLE EXAMPLE

Filiz ŞENKAL SEZER
Uludag University Department of Architecture
filizss@gmail.com

Secil BALLI HEPTASKIN
secilheptaskin@gmail.com

Abstract: Without doubt one of the most important problems for students that start their university education in a city different than the city of their families is "residence". Many students that enroll in universities in Turkey prefer to live in state dormitories, private dormitories or student apartments. Apartments are places that continuously provide residences to students. The goal of this study is to determine the important apartment criteria for students and to provide suggestions that may provide solutions to ensure that these types of buildings provide the necessary performance conditions. It is also aimed to determine dissatisfaction based on user views and based on these views to create design criteria for buildings to be constructed. A hypothesis, which states that increasing structural comfort conditions in apartments will increase the productivity of students, is also put forward. In the scope of this study a survey was made in four student apartments located in the Gorukle District, which is near the exit of the Uludag University Gorukle Campus in Bursa, the 4th largest city in Turkey. The stages of this study are literature research on the subject of this analysis, evaluation of information on indoor comfort conditions, determining comfort conditions and preparing a survey to receive feedback on the experience of users in the designed environment, and evaluating the survey results to understand users' current satisfaction levels and comfort needs. Based on these data, transportation and security, ergonomics, thermal comfort, audial comfort, natural and artificial lighting, indoor air quality were used as evaluation criteria as a means to ensure optimum comfort conditions are met in buildings.
Keywords: Comfort conditions, student apartments, thermal comfort, audial comfort

Introduction

Quality of life is considered as a person's view towards his/her own life, and is used synonymously with terms such as satisfaction from life, well-being, living conditions, and happiness (Cella, 1996). According to World Health Organization, physical functions of people, their psychological status, social relations in and outside the families, their interaction with the environment and their beliefs are also in the scope of the quality of life. Satisfaction from life is an indicator of general well-being and quality of life and includes the decision of a person regarding his/her quality of life and well-being based on the qualities that person has selected (Sahin, 1997). Satisfaction from life in general involves the whole life and various dimensions of life of a person and is influenced from many factors such as age, gender, health, professional life, economic status, educational level, religion, marriage, social support and environmental conditions (Matheny & Curlette & Aysan, & Harrington, 2002).Satisfaction from life is important for university students similar to all age groups. In Turkey most of the students enroll to a university in a city different than the city they used to live with their families. In general, the first and one of the most important problems in university life experienced by students is related to accommodation (Ersoy & Arpacı 2003).

Accommodation is one of the most important necessities for providing and sustaining the feeling of security. In Turkey accommodation, in addition to student dormitories within universities or private dormitories, is provided via student apartments that are close to campuses. When the needs and arrangements of these buildings are considered it can be seen that privacy conditions should be considered with a higher priority. When these buildings fail to adequately provide the needs of students, student apartment turn to become places where students only go for sleeping. The inability to fully satisfy the individual and social needs of students reduces students' satisfaction levels and reduces their quality of life. This also reduces students' motivation for success. Institutions of higher education are places where knowledge is generated and shared. The ability to carry out high quality research and provision of a comprehensive education does not only rely on the academic environment but also the environment created by the physical and social surroundings. When it is evaluated from such a viewpoint, the environment of the accommodation facilities for higher education students that enable

necessary climatic, acoustic and visual comfort conditions for studying and that provide the infrastructure for social interaction will support the creation of a higher quality education environment.

In this regard, student apartments inside the Gorukle district of the city of Bursa (Turkey), which is where Bursa Uludag University Gorukle Campus is located, were selected as the study field. The research method is composed of the following stages:

- Carrying out research on literature related to the subject area to be analyzed and review of relevant information and knowledge related to indoor comfort requirements,
- Determining comfort conditions and preparing a survey to receive feedback from user experience in the designed environment,
- Evaluation of the survey results to understand comfort needs and the current level of satisfaction of users.

The evaluation criteria were examined under the following headings to ensure that the buildings met the optimum comfort conditions: ● Transportation and safety ● Ergonomics ● Thermal comfort ● Auditory comfort ● Natural and artificial lighting ● Indoor air quality

Determining the level of actual user satisfaction is a widely used method to increase the efficiency of current building and to provide directions for future building designs. Accordingly, the reference "Post-Occupancy Indoor Environmental Quality Evaluation of Student Housing Facilities" states the benefits of Post Occupancy Evaluation (POE) as follows;

- To rapidly understand problems and solutions in buildings,
- To increase feedback related to building performance and space usage,
- Creating important cost savings during construction and building lifecycle
- Creating long term improvements in building performance
- Creating a knowledge resource for improving databases, standards and criteria (Hassanain, M. A. 2007).

In order to evaluate the experiences of users related to their living space usage, a "user satisfaction survey" was prepared and the results were analyzed.

Field Study

The area selected for the field study is Gorukle district, which is 18 kilometers from Bursa city center, the 4th largest city in Turkey, and near the Uludag University Gorukle Campus (Image 1). Students in the campus can reach this district on foot and they are also able to use private cars, public and private busses. Student apartments in average have rooms that can accommodate 1, 2, 3, and 4 persons, are usually furnished and have kitchen and bathrooms. There are also apartments that have services such as laundry, private security, breakfast, dinner, social areas, cafés etc. Apartments are usually close to the university campus.

Image 1. Uludag University Campus and Gorukle (Google Earth, 2017)

The apartments selected for this study are defined below.

Apartment A: This apartment was completed and has a total of 62 beds. The building is 1 block and has a ground floor and 4 storeys. There are 3 apartments in the ground floor and 8 apartments each in upper floors, which makes a total of 35 apartments. All the apartments have one living room and one bedroom. A section of the ground floor is allocated to commercial units, kitchen for personnel and a pressing room (Image 2).

***Image 2**. Apartment A, view from inside and outside*

Apartment B: This 1 block building was constructed in 2006 and has a ground floor and 3 storeys. There are a total of 30 apartments in the building. 12 of those apartments face the front façade, 12 face the rear façade and 6 face the side façade. All the apartments have one living room and one bedroom and the total bed count is 50. There is a kitchen for personnel and a pressing room (Image 3).

***Image 3.** Apartment B, view from inside and outside*

Apartment C: This 3 block building was constructed in 2007 and has a ground floor and 4 storeys. The apartments are situated around a corridor which is illuminated with an atrium. The building blocks have a total of 149 apartments. 103 of those apartments have one living room and a bedroom and 46 of them have two living rooms and a bedroom (Image 4).

***Image 4.** Apartment C, view from inside and outside*

Apartment D: These buildings were constructed in 1998. There are four blocks, two for females and two for males. All blocks have a ground floor and 4 storeys. There are a total of 108 apartments. 21 of them have a bedroom and two rooms and 87 of them have one bedroom and one room. There are a total of 129 beds in these apartments (Image 5).

Image 5. *Apartment D, view from inside and outside*

The survey was conducted in October 2016 in daytime between 12.00 and 16.00. Within the literature analysis first key concepts to measure physical environment quality were defined and then 17 questions were asked to the building inhabitants. The closed ended questions were evaluated with a three point Likert Scale. The survey was carried out with a total of 120 students (30 students in each building) and were presented proportionally (%) to ensure they could be understood and evaluated easily.

Research Findings

Table 1 shows the demographics of inhabitants of each building that participated to the survey. The demographic findings based on the survey shows that 66% of the participating students were female and 34% of the participants were male. It was seen that %55 of the participants of the survey were aged 21-25, 24% were 18-20, 21% were 25 and over. 88% of the participants of the survey were students and 12% were employees.

Table 1. Demographics

Demographics (%)		Apartment A	Apartment B	Apartment C	Apartment D
Gender	Female	100	67	42	53
	Male	0	33	58	47
Age	18-20	5	33	24	35
	21-25	57	40	62	61
	25 and over	38	27	14	4
Status	Student	100	71	82	100
	Employee	0	29	18	0

67% of the apartments are 1+1, 31% are 2+1 and 2% are 3+1. 51% of the inhabitants live alone in the apartments, whereas 34% have 2, 11% have 3 and 4% have 4 inhabitants. Specifications of the apartments where the survey was conducted are given in Table 2.

Table 2. Specifications of apartment where surveys were conducted

Features of the Apartment (%)		Apartment A	Apartment B	Apartment C	Apartment D
Apartment type	1+1	100	79	26	62
	2+1	0	21	74	28
	3+1	0	0	0	10
Number of inhabitants in the apartment	1 person	100	41	39	24
	2 people	0	45	53	39
	3 people	0	14	8	23
	4 people	0	0	0	14

In the survey, access to the building and safety concepts were taken into consideration as "Accessibility" criteria (Figure 1). Storey height inside the apartments and the size of windows are considered as “Ergonomics" criteria (Figure 2).

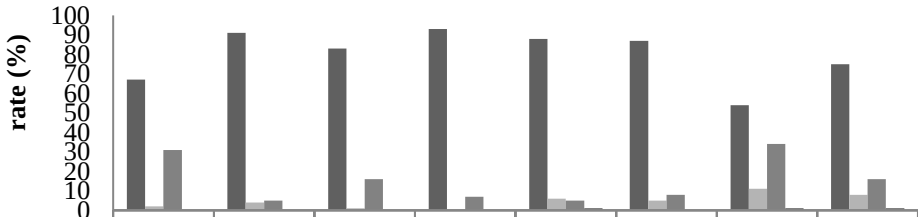

	Apart A	Apart B	Apart C	Apart D	Apart A	Apart B	Apart C	Apart D
	transportation				safety			
satisfied	67	91	83	93	88	87	54	75
neither satisfied nor dissatisfied	2	4	1	0	6	5	11	8
dissatisfied	31	5	16	7	5	8	34	16
can't choose	0	0	0	0	1	0	1	1

Figure 1. User opinions related to accessibility

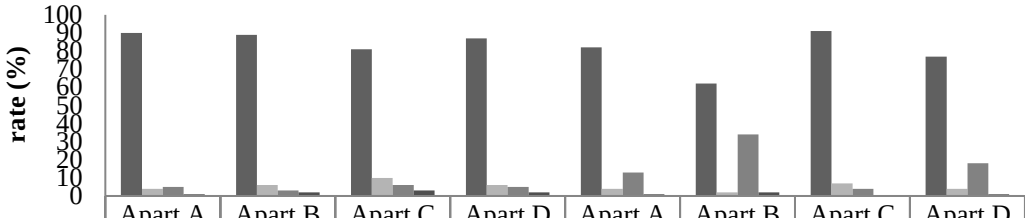

	Apart A	Apart B	Apart C	Apart D	Apart A	Apart B	Apart C	Apart D
	indoor storey height				window size			
memnun	90	89	81	87	82	62	91	77
ne memnun ne değil	4	6	10	6	4	2	7	4
memnun değil	5	3	6	5	13	34	4	18
fikri yok	1	2	3	2	1	2	0	1

Figure 2. User opinions related to size

For the physical environmental control and "Thermal Comfort" aspects, opinions were gathered related to indoor temperature both in winter and summer (Figure 3). Thermal comfort is defined by The American Society of Heating, Refrigerating and Air-conditioning Engineers (ASHRAE) Standard 55 as satisfaction from the thermal conditions. Optimum thermal environments are defined as environments in which 80% or more of their users agree that the environment is acceptable.

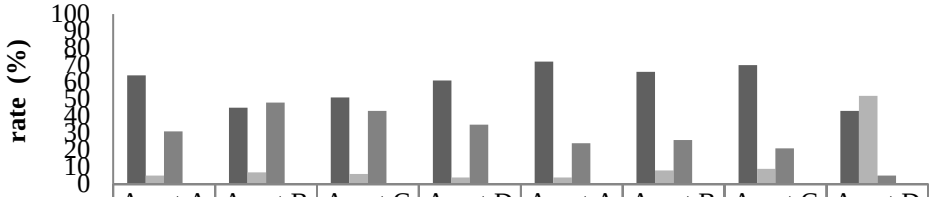

	Apart A	Apart B	Apart C	Apart D	Apart A	Apart B	Apart C	Apart D
	summer-indoor temperature				winter-indoor temperture			
satisfied	64	45	51	61	72	66	70	43
neither satisfied nor dissatisfied	5	7	6	4	4	8	9	52
dissatisfied	31	48	43	35	24	26	21	5
can't choose	0	0	0	0	0	0	0	0

Figure 3. User opinions related to thermal comfort

In the study sound transfer between rooms and storeys and noise coming from outside were taken into consideration as “Acoustic Comfort” (Figure 4). Navai and Veitch define acoustic comfort as «a state of contentment with acoustic conditions». Acoustic comfort does not only involve "creating a good acoustic environment" but also defining all factors that "prevent acoustic comfort".

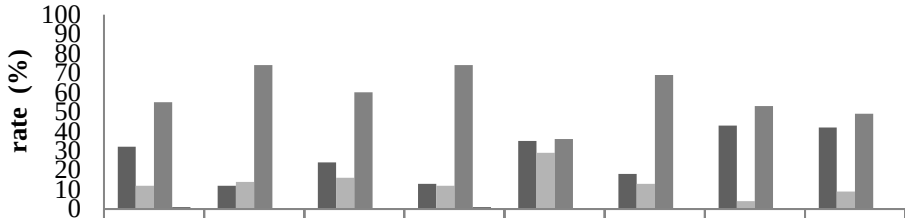

	Apart A	Apart B	Apart C	Apart D	Apart A	Apart B	Apart C	Apart D
	sound transfer between living spaces				noise from outside			
satisfied	32	12	24	13	35	18	43	42
neither satisfied nor dissatisfied	12	14	16	12	29	13	4	9
dissatisfied	55	74	60	74	36	69	53	49
can't choose	1	0	0	1	0	0	0	0

Figure 4. User opinions related to acoustic comfort

As the criteria for “Visual Comfort” the adequacy of natural light and the condition of artificial lighting were examined (Figure 5). Visual comfort is defined as a “subjective condition stimulated by the visual surroundings”. This definition takes into consideration the psychologic dimension of comfort and includes physical features that effect visual comfort. Visual comfort parameters are amount of natural light, distribution of brightness, amount of glare, color of light, amount of flickering light and the level of luminousness. Visual comfort quality is defined as the quality and quantity of the light source and how it brightens its close surroundings.

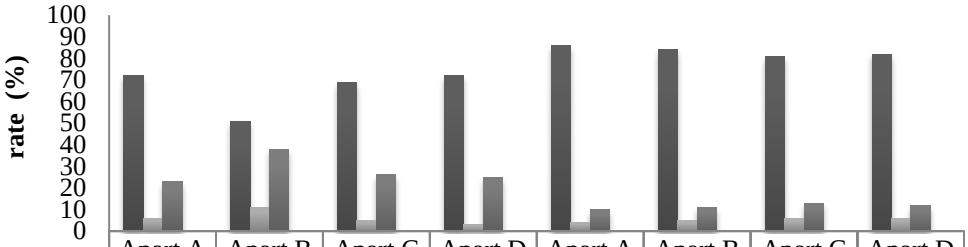

	Apart A	Apart B	Apart C	Apart D	Apart A	Apart B	Apart C	Apart D
	natural lighting				artificial lighting			
satisfied	72	51	69	72	86	84	81	82
neither satisfied nor dissatisfied	6	11	5	3	4	5	6	6
dissatisfied	23	38	26	25	10	11	13	12
can't choose	0	0	0	0	0	0	0	0

Figure 5. User opinions related to visual comfort

Related to “Indoor Air Quality”, the conditions of natural ventilation, satisfaction from indoor air quality were taken into consideration (Figure 6). Indoor air quality is defined based on the dissatisfaction (odor, sensual discomfort) of inhabitants. According to ASHRAE Standard 1999-62 indoor air quality is achieved when there are no harmful air pollutant concentrations and most of the users (80%) feel satisfied from an environment.

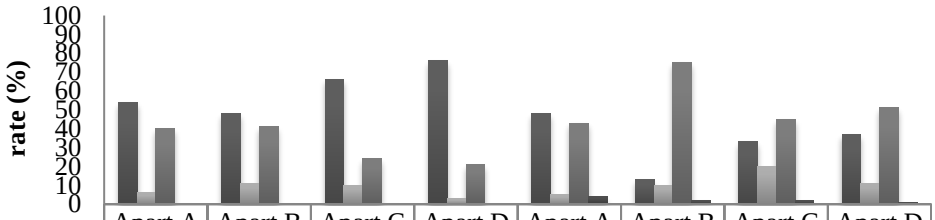

	Apart A	Apart B	Apart C	Apart D	Apart A	Apart B	Apart C	Apart D
	natural ventilation				indoor air quality			
satisfied	54	48	66	76	48	13	33	37
neither satisfied nor dissatisfied	6	11	10	3	5	10	20	11
dissatisfied	40	41	24	21	43	75	45	51
can't choose	0	0	0	0	4	2	2	1

Figure 6. User opinions related to indoor air quality

Results

In the scope of the study, it is very important to define the issues that users are dissatisfied to establish design criteria for future buildings and to establish main goals for future designs. In this regard, the results of the study are summarized in the table below (Table 3).

Table 3. Comparative satisfaction levels of users

Satisfaction Criteria		Apartment A		Apartment B		Apartment C		Apartment D	
		Satisfied	Not Satisfied	Satisfied	Not Satisfied	Satisfied	Not Satisfied	Satisfied	Not Satisfied
Accessibility	Transportation	36		86		67		86	
	Safety	83		79		20		59	
Ergonomics	Indoor storey height	85		86		75		82	
	Windows size	69		28		87		59	
Thermal comfort	Summer-indoor temperature	33			**-3**	8		26	
	Winter-indoor temperature	48		40		49		38	
Acoustic comfort	Sound transfer between living spaces		**-23**		**-62**		**-36**		**-61**
	Noise from outside		**-1**		**-51**		**-10**		**-7**
Visual comfort	Natural lighting	49		13		43		47	
	Artificial lighting	76		73		68		70	
Indoor air quality	Natural ventilation	14		7		42		55	
	Indoor air quality	5			**-62**		**-12**		**-14**

● **Accessibility:** In the accessibility indicator related to the apartment that the users inhabited only 15% and 16% have indicated dissatisfaction with transportation and safety respectively. In general, it has been understood that inhabitants were very content with transportation and safety.

● **Ergonomics:** the performance criterion in this category was whether stores height and window size were sufficient. 5% of the users expressed discontent with inadequate storey height and 17% of the users expressed that they did not believe window sizes were ergonomic. In general, the satisfaction levels of this category were very high.

● **Thermal comfort:** Users participated in the survey expresses discontent with the indoor air temperature during summers (39%) and during winters (19%). In general users were satisfied with thermal conditions.

● **Acoustic comfort:** 66% of the users indicated dissatisfaction because of the high level of sound transfer between living spaces and 52% of the users indicated that they felt discontent because of outside noise reaching inside. These views indicate that users were dissatisfied from the acoustic comfort aspect.

● **Visual comfort:** In the survey, which has taken adequacy of daylight and comfortable usage of artificial lighting inside the apartments as a performance criterion, only 28% of the users indicated that they found natural lighting insufficient and 12% of the users indicated that they found artificial lighting insufficient. In general users were satisfied with visual comfort conditions.

● **Indoor air quality:** the performance criterion under this category was related to the conditions of natural ventilation and indoor air quality. Only 32% of the users indicated that natural ventilation was inadequate; the dissatisfaction from indoor air quality was 54%. Even though there wasn't dissatisfaction with natural ventilation, the users were dissatisfied with the indoor air quality.

When the students were asked to present general positive features of the apartment, they answered with "a good design example", "meets climatic, visual and acoustic comfort conditions". "I like its location in the city", and "transportation is easy". When negative aspects were asked, the participants provided the following answers "I believe the structural quality is subpar", "I believe relations with neighbors are inadequate", "I believe there are many shortcomings of the architectural design", "I am dissatisfied with the noise", "I cannot heat the building enough", "I gets very hot in summers", and "I feel the living space in the apartment is inadequate".

When open ended questions on which architectural changes were needed to create optimum comfort conditions were asked the following answers were provided: heat insulation should be installed for thermal comfort; special joineries should be used in window and door frames and cases that provide sound insulation; providing high quality artificial lighting and lighting systems that do not strain eyes when students work at their desks; installing sunshades at the south façade of the building both for thermal and visual comfort; and installing air conditioning systems to provide optimum air quality.

When the students were asked to comment on the apartments from a social viewpoint they indicated that the amount of space per person in the sports hall, mess hall, guest house and social areas, and landscaping were inadequate. Also, the students were discontent with circulation areas and the lack of fire escape. However, being close to other friends was expressed as a positive aspect.

The data collected in this study will provide new dimensions to future buildings to be designed and will help those who will make architectural adjustments to current buildings.

References

ASHRAE, Standard 55 (2013). Thermal Environmental Conditions for Human Occupancy

ASHRAE, Standard 62-1999 (2000). Ventilation for Acceptable Indoor Air Quality

Cella, D. F. (1996). Quality of life: concepts and definition. Journal of Pain-Symptom Management, 9(3): 186 - 192, file:///C:/Users/user/ AppData/Local/Microsoft/ Windows/INet Cache/IE/9S5WTO65/543.pdf

Ersoy, A. F., Arpacı, F. (2003). Universite Öğrencilerinin Konut Kosullarının ve Konutta Yasamayı Tercih Etme Nedenlerinin İncelenmesi, Milli Eğitim Dergisi, 158.

Hassanain, M. A. (2007). Post-Occupancy Indoor Environmental Quality Evaluation of Student Housing Facilities. Architectural Engineering And Design Management. 3, 249–256.

Matheny, K. B., Curlette W. L., Aysan, F., Harrington, A. (2002). Coping resources, perceived stres and life satisfaction among Turkish and American university students. Int J Stress Management 9: 81-97.

Navai, M, Veitch, J. A. (2003). Acoustic satisfaction in open-plan offices: review and recommendations. Research Report RR-151. Ottawa, Canada: Institute for Research in Construction. National Research Council Canada.

Sahin, H. (1997). Eski Bir Kavram Yeni Bir Ölçüt: Yaşam Kalitesi. Toplum ve Hekim;12: 40-6.

EVALUATION OF POLYETHYLENE BASED INSULATION MATERIAL IN TEXTILE DYEING MACHINES

Betül Özer*, Behçet Güven
Kırklareli University, Department of Energy Systems Engineering, Kırklareli-TURKEY
*email: betulozer@klu.edu.tr
Tel:+90.542 722 48 39

Abstract: Energy efficiency efforts are getting more importance in accordance with the better understood of the sustainable development in all over the world. Accordingly improvements in the energy efficiency, reducing energy intensity both sectoral and macro-level are primary components of Turkish national energy policy. Textile sector has a significant share in the production and export industry of Turkey. A significant percentage of heat energy is being lost in the dyeing processes through wastewater, equipment surfaces, and exhaust gasses. These energy losses can be reduced via an efficient isolation of the machinery. The subject of this study is to evaluate the energy-saving efficiency of a highly cross-linked polyethylene foam insulation material in textile dyeing machines. Dyeing machines are heated to 130^{O}C and cooled again during the process. 27% heat saving was achieved after 48 tons of dyed fabric in 20 days of trial period.
Keywords: textile finishing sector, energy saving, heat loss, isolation

Introduction

Energy is one of the main factors of economic and social development and indispensable input of the production. Accordingly, energy demand is continuing to increase in all over the world due to the factors such as population growth, improving technology and trends for rising life qualities. Projection studies indicate that in case of the continuation of current energy policies, global energy demand will reach about 1.5 times of 2014 value in 2040 by 1.4% annual increase ratio (from 13.68 Mtoe to 19.64 Mtoe) (EUAŞ, 2014, IEA, 2016). On the other hand, the largest contribution of fossil fuels to the energy supply, corresponding climate change problem, the increase in the energy costs and the depletion risks of the fossil fuels make necessary the efficient use and saving of energy.

Energy efficiency is defined as the mitigation of the energy consumption per unit or product amount without leading to the decrease of the quality and the quantity of production, economic development and obstructing the social welfare (Url-1). It is a growing policy priority for the most of the countries around the world and widely presumed as the most cost-effective and readily available. That is addressing the energy supply security, the economic and social impacts of high energy prices, and concerns about climate change (Url-2). The policies on the energy efficiency are "required to be sensitively discussed because of its direct relation to the economic and social development objectives' sustainability and its key role played in reducing the total greenhouse gas emissions". Reducing energy intensity both sectoral and macro-level is significant and primary components of Turkish national energy policy. Turkey's 2023 national strategic objectives and energy policies include providing energy supply safety, reducing the external dependency, the sustainability of the energy costs, protecting the environment and increasing the efficiency of the struggle against the climate change, those all fulfil the national strategic targets of Turkish energy policy (Url-1). Consequently, energy efficiency should be improved in all stages from energy production to the consumption at the end users. Through the energy efficiency studies, energy intensity that is energy consumption per national income of Turkey is aimed to be reduced (energy consumed per national income) as 20% until 2023 compared to 2011 (Official Gazette, 2012).

Textile sector has a significant share in the production and export industry of Turkey. The number of the enterprises and the employees correspond to about a quarter of the manufacturing sector whereas value added has 16% share as given in Table 1 (MoDev, 2014). Besides it has been mentioned as the 3rd most energy-intensive sector after iron-steel and cement industries in Turkey (Alkaya and Demirer 2014, Ozturk, 2005).

Table 1: The shares of textile and ready to wear sectors in Turkish production industry, % (MoDev, 2014)

Number of enterprises	23,3
Number of employees	26,3
Production values	14,9
Value-added	15,5

Energy cost corresponds to 8-12% of the total production cost in the sector (Gümüşderelioğlu, 2009, Koç University, 2012, Palamutçu, 2010). On the other hand, the most demanded energy type that is more than 80% of the total demand is the heat energy in the textile industry. Approximately 50% of this energy is lost through wastewater, the surface of the machines and exhaust gases those indicate the most energy saving potential (Moser and Schnitzer, 1985, Yamankaradeniz. et. al, 2007, Url-3). Besides, in a globalizing world, the increasingly difficult competitive conditions necessitate a reduction of the production costs.

The aim of this study is to evaluate the energy-saving efficiency of a highly cross-linked polyethylene (PE) foam insulation material used on the dyeing machines in a textile finishing sector. This is one of the initial studies on prevention of heat losses for dyeing machines including also cooling processes. In this study, the cost and the energy saving potential of glass wool and polyethylene based insulation materials are compared for reducing heat losses in dyeing machines.

Materials and Methods

The finishing processes in the factory include dyeing with machines those are heated to 130ºC and cooled again. The most of the energy cost comes from heating processes in textile finishing sector. Stainless steel made machines are used and during the whole process, significant heat is lost mainly at the surfaces. A typical dyeing machine is given in Figure 1.

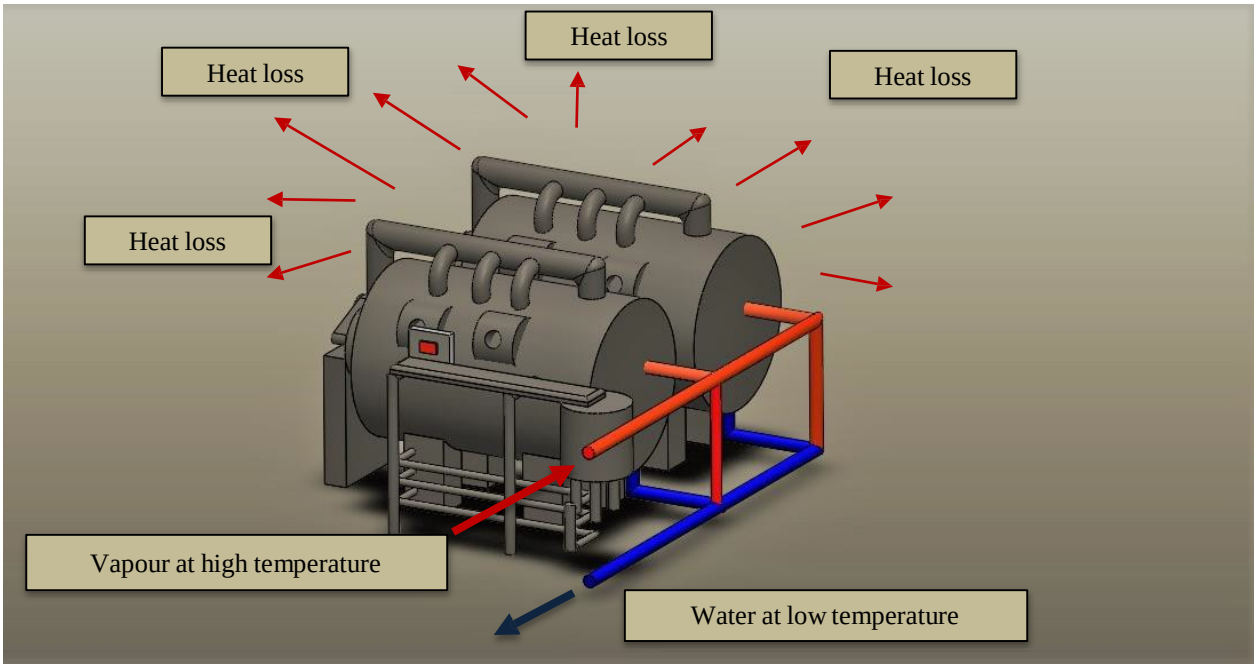

Figure 1. Typical dyeing machine

In the dyeing processes corrosive chemicals are used with water. Therefore, the use of chemical resistant isolation materials is essential. Currently, 26% of heat saving is achievable with some of the machines those are isolated with silicone coated glass fiber and glass wool blended material in the factory. Due to no adhesive property, this material can only be applied via roping or snap fasteners to the machinery. Therefore, it cannot be applied to the small joints of the machines, on the surfaces where the shapes are changing, and recess ledges of the machines, where all cause the most energy losses. Furthermore, the insulation material is susceptible to water and especially to the chemicals used in the processes consequently, deformations began to occur at the end of the first year and it needed to be totally changed at the end of the second year. Therefore, more corrosive resistant isolation materials are needed to be used.

In this study highly cross-linked polyethylene foam material is used as an alternative to the silicone coated glass fiber and glass wool blended material for the isolation of dyeing machines. The material has adhesive property thus whole machine surfaces even recess ledges and small joints of the machines can be isolated. Applying is quite simple that it can be attached on the machines by steam or hot water and efficiently block the heat transmission. Due to the high thermal insulating property, heat and a great chemical resistance much energy saving and long lasting isolation are expected. Moreover, it can be cleaned easily.

Three types of dying machines having same technical properties with 900 kg capacities were used in the trials. These are:

1. without isolation; as the reference case
2. isolated with silicone coated glass fiber and glass wool blended material
3. isolated with highly cross-linked PE foam material. (Fig.2-4).

The same process conditions were set for all the machines and the saved energy was compared to both insulation materials in order to determine the material that is more long lasting and can provide energy saving more. Energy saving was evaluated basing on the steam and cooling water consumption of the machines. Measurements were made 20 working days for all the shifts (3 shifts in a day). Cotton-polyester dyeing and cotton dyeing processes were tested. The outer surfaces of the dyeing machines and machinery temperatures were measured with thermal cameras to see the heat losses. The results are given in Fig. 5. hot surfaces indicate the places of the energy losses. The values have also been verified with the actual temperatures on the machines.

Figure 2. Dyeing machines without isolation

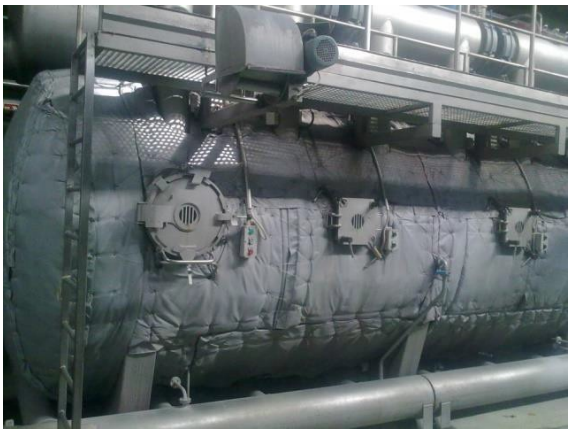

Figure 3. Dyeing machines isolated with silicone coated glass fiber and glass wool blended material

Figure 4. Dyeing machines isolated with highly cross-linked polyethylene foam manufactured insulation material

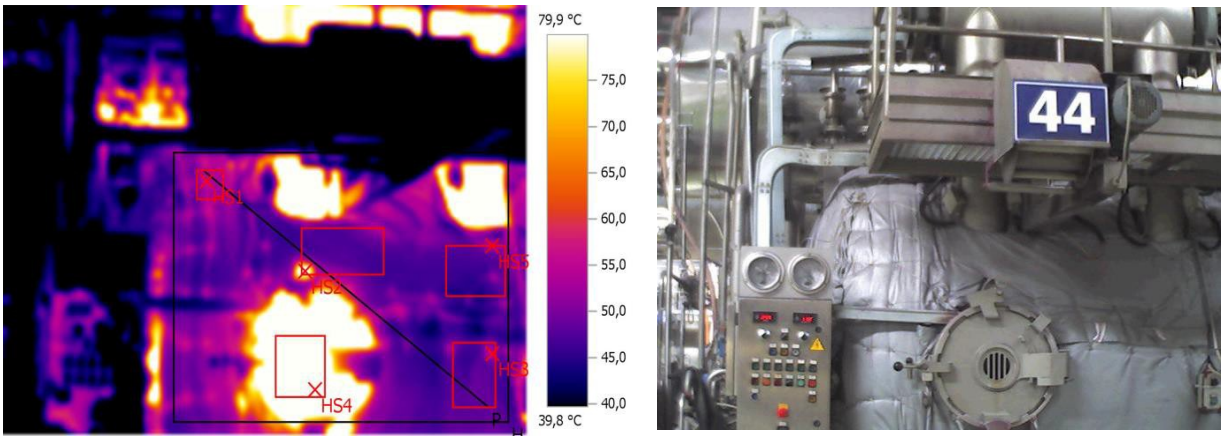

Figure 5. Thermal camera views of the machines

Due to the cooling times of the machines changes, process recipes are also checked if any adjustments are needed for the evaluation of the isolation material.

Results and Discussion

At the end of the 20 working days, approximately 48 tons of fabric was dyed through 60 trials. The unit steam consumptions that is kg steam needed per kg fabric, were compared for the same garment dyeing processes in the tested machine types and the results are given with Figures 6-7.

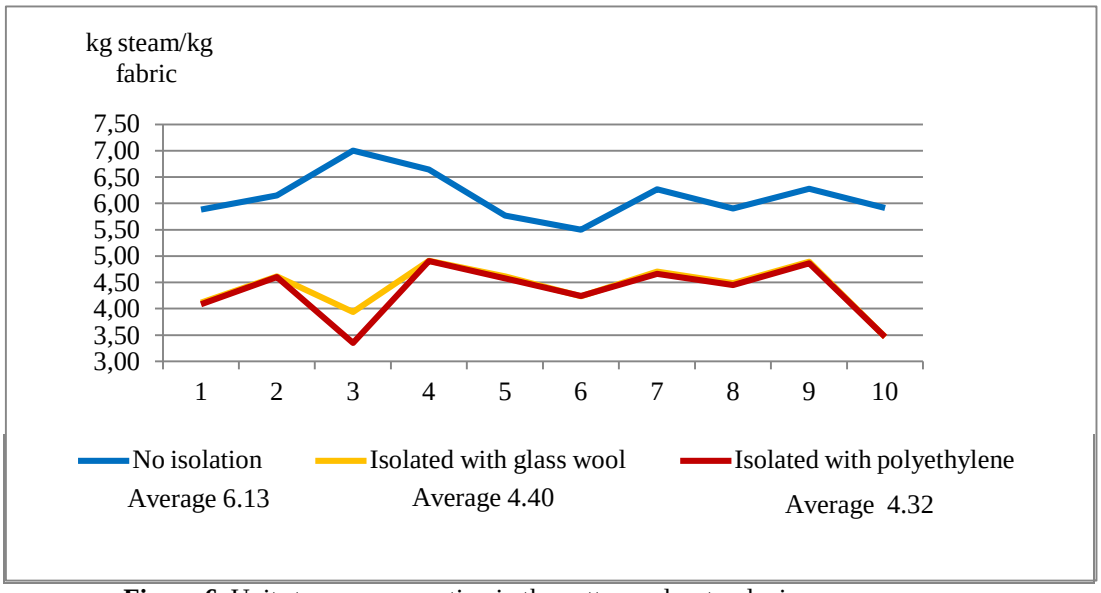

Figure 6. Unit steam consumption in the cotton-polyester dyeing process

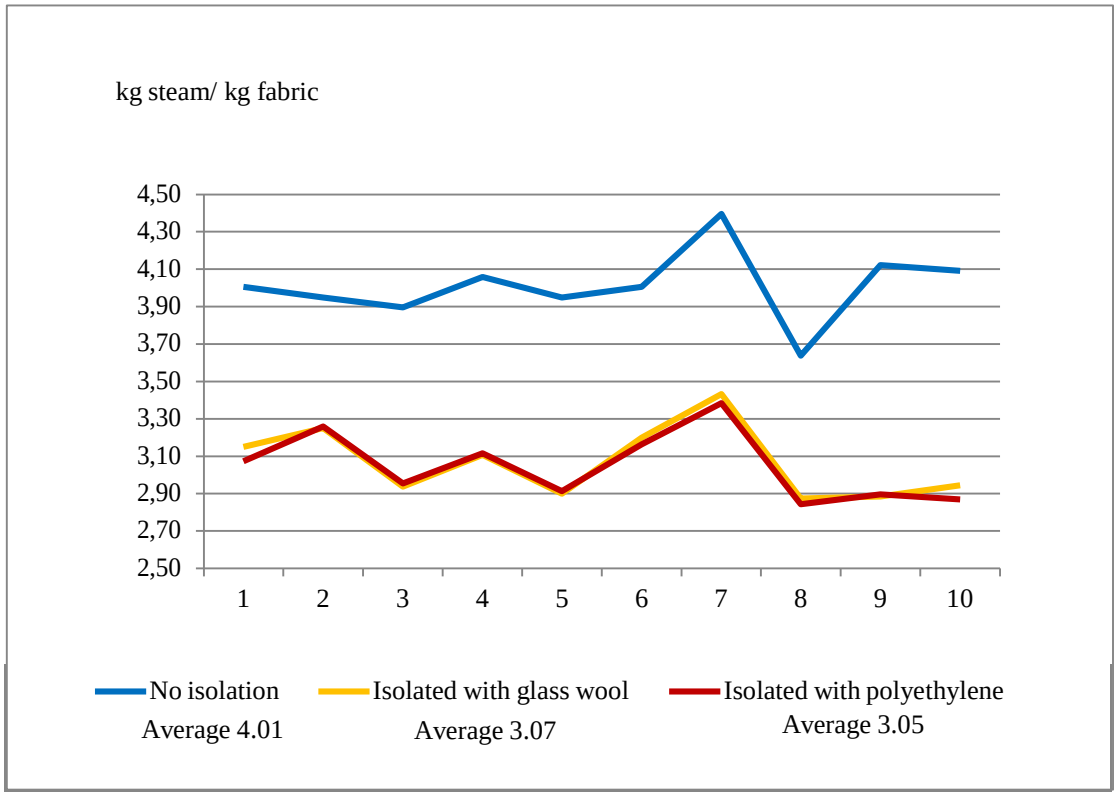

Figure 7. Unit steam consumption in the cotton dyeing process

The results indicate the energy saving with:

- the silicone coated glass fiber and glass wool blended material is: 25.76%,
- highly cross-linked polyethylene (PE) foam insulation material is: 26.6%

in the tested machines. The energy saving potential seems similar for both materials. 62,416 tons of steam is consumed in 2015 in the machine isolated with the silicone coated glass fiber and glass wool blended material, whereas 16,072 tons of steam was saved which corresponds to the approximately steam consumption of 3 months in the factory. PE material was used 18 months in the factory, and no deformation was observed. This also indicates the long-lasting property of PE based insulation material. On the other hand, the unit steam generation costs are 11.4 USD/ton steam generation via domestic coal and 22.73 USD/ton steam generation via natural gas. The annual cost savings for the steam generations are approximately 183 thousand USD if domestic coal with 4000 kCal/kg calorific value is used for the steam generation, whereas it is approximately 365 thousand USD if natural gas is used. The results also indicate that there was no change for cooling time and the amount of cooling water in the tested machines; there were all about 302 thousand liters and no recipe changes were needed that would affect the chemical consumption.

Conclusion

In this study, silicone coated glass fiber and glass wool blended and highly cross-linked polyethylene foam manufactured insulation materials are compared for reducing the heat losses in textile dyeing machines in the context of the cost and energy saving potentials. The factory has used the silicone coated glass fiber and glass wool blended material on some of the dyeing machines and 26% of heat saving can be achieved. Totally 48 tons of fabric was dyed during 60 trials in the same process conditions of two types of isolation systems and a reference case of no isolated machine. The results indicate the energy saving potential seems similar for both isolation materials; however, for reducing the energy losses polyethylene foam material was determined as more long-lasting since after 18 months no deformation was observed, whereas glass fiber and glass wool blended material deformed after 12 months. Furthermore, PE material can be cleaned easily and the application is quite simple due to its adhesive property. Since the cooling time of the processes did not change, recipe changes were not needed. Correspondingly chemical consumption stayed same causing no cost increase. Energy costs can be reduced at least 15% annually after isolation which corresponds to 183 thousand and 365 thousand USD compared to coal and natural gas use, respectively.

The results of this study may contribute to mitigate the energy losses at dyeing machines used in the textile sector which is mentioned as the 3rd most energy-intensive sector with 16% of value added in Turkish production industry

(Alkaya and Demirer 2014, Ozturk, 2005, MoDev, 2014). Accordingly, the energy which is the main cost component of the manufacture can be reduced.

Since this is one of the initial studies on saving heat energy at dyeing machines also including cooling processes an important know-how is gained for the sector. These applications are intended to be representative to the similar factories. The results may also spread to the dye-houses in Turkey ensuring serious energy savings and may guide to the dyeing machine producers for the new design of the machines.

Acknowledgements

The authors are grateful for the supports provided by Kırklareli University with the project no. KLUBAP-132 and
the textile factory Özen Mensucat A.Ş.

References

Alkaya, E, Demirer G. N. 2014. Sustainable textile production: a case study from a woven fabric manufacturing mill in Turkey, Journal of Cleaner Production 65 (2014) 595-603. EUAŞ, 2014. Electricity Production Sectoral Report, Ankara, Turkey, 2016.

Gümüşderelioğlu, S. 2009. Energy Efficiency Studies on Turkish Industry, Increasing of Energy Efficiency in Industry and SME Project Preparatory Work, in Turkish, General Directorate of Electricity Survey and Development Administration, Ankara, Turkey, 11 June 2009.

IEA (International Energy Agency), 2016, "World Energy Outlook 2016".

Koç University, 2012. Energy Efficiency Map of Turkey and Targets Project Report, in Turkish, 2012.

MoDev 2014. The Republic of Turkey, The Ministry of Development, 10th Development Plan 2014-2018, Textile, Leather, Confection Working Group Report, Ankara, Turkey, 2014.

Moser, F., Schnitzer, H.,1985. Heat pump in industry, Elsevier, New York.

Official Gazette, 2012. No: 28215, Energy Efficiency Strategy Paper, 2012- 2023, 25.02.2012.

Ozturk, H.K., 2005. Energy usage and cost in the textile industry: a case study for Turkey. Energy 30, pp.2424-2446.

Palamutçu, S. 2010. Electric energy consumption in the cotton textile processing stages, Energy, Vol: 35 7 pp.2945-2952.

Url-1 http://www.enerji.gov.tr/en-US/Pages/Energy-Efficiency, accessed on: 23.09.2017.

Url-2 http://www.iea.org/publications/freepublications/publication/energy-efficiency-indicators- essentials-for-policy-making.html, accessed on 01.09.2017.

Url-3 (http://www.tttsd.org.tr/images/enerji.pdf, Yalçın, E. Efficient use of energy in textile finishing sector, in Turkish, Electricity Survey and Development Administration, accessed on: 22.06.2015.

Yamankaradeniz. N., Coşkun, S., Can, M.,2007. Comparing of the classical system and heat pump for energy saving using waste heat in textile industry, Uludağ University The Journal of Engineering and Architecture Faculty, Vol. 12, (1).pp. 115-124.

EXTRACTION OF CUSTOMER DEMOGRAPHIC CHARACTERISTICS IN SUPERMARKETS BASED ON IMAGE PROCESSING TECHNIQUES

Selay ILGAZ SÜMER
Baskent University, Department of Management, Ankara - Turkey
silgaz@baskent.edu.tr

Görkem ÖZGÜRBÜZ
Baskent University, Department of Computer Engineering, Ankara - Turkey
gorkemozgurbuz@gmail.com

Emre SÜMER
Baskent University, Department of Computer Engineering, Ankara - Turkey
esumer@baskent.edu.tr

Abstract: Analysis of video data in a retail environment provides valuable information for business operators. Customer gender identification and age interval estimation are commonly used to better plan resources and marketing strategies. In this study, some demographic characteristics (gender and age interval) of hypothetical customers are extracted from video images. To extract gender information, geometric facial features are used. On the other hand, age intervals are estimated by measuring the size and proportions of the human face, and edge analysis as well. Besides, the trajectories of the customers are determined by image processing techniques. The preliminary experimental results show that promising clues are extracted to be used in the retail video analytics. In the future, we believe that these characteristics can be associated with heatmaps of customer walk-through patterns, which allows for optimal product placement and efficient floor setup.
Keywords: Retail Video Analytics, Customer Demographic Characteristics, Consumer Buying Behavior, Image Processing

Introduction

In recent years businesses are focused on satisfying the customer's needs and expectations in an efficient way than their competitors. Although the expectations of consumer markets are different from industrial markets, for both of the markets, the best way of meeting wants are based on identifying the consumers' needs and organizing the marketing activities according to them. At this point, the concept of consumer behavior becomes more important in the value creation process. Consumer behavior "is the study of the processes involved when individuals or groups select, purchase, use, or dispose of products, services, ideas, or experiences to satisfy needs and desires (Solomon, 2006: 7).''

In the literature, various studies are conducted to explore the impact of demographic factors on consumer behavior. Kumar (2014) expressed that demographic factors such as sex, age, marital status, ethnic, income, education, occupation and family size are the important factors which effect buying decisions. Hence, firms have to examine the demographic characteristics of the consumers carefully to plan their marketing activities efficiently. Therefore actually, customer demographic characteristics are important inputs for the businesses.

In the study, in order to understand the consumer behavior partly; image processing techniques are taken into consideration. By using image processing techniques, it is aimed to determine and understand the behavior of the consumers in a store. Briefly, there are two aims of the study. First one is to extract the customer demographic information in a hypothetical store, second is to determine the instore customer trajectories through image processing techniques. In this study, customer demographic characteristics are limited to gender and age. In this context, first consumer buying behavior is introduced. Next, extraction of customer demographic characteristics such as gender and age interval estimation is explained. Further, customer trajectory determination is discussed. Finally; results, discussion and conclusion are expressed.

Consumer Buying Behavior

From past to present, consumer buying behavior is the main research topic of marketers. Although many studies are focused on consumer buying behavior, still the reasons of the buying behavior of consumers cannot be discovered exactly. Moreover, for this reason, consumer's mind is like a black box. Hence, it is not so easy to answer the questions such as "when they buy?", "why they buy?", "what they buy?" etc. It is the truth that the success of the businesses is depending on understanding the expectations of the customers and planning all their

activities according to them. Product designs, pricing the goods and services, shelf designs etc. are among these activities. Herein, considering and studying the factors that affect consumers to behave in a certain manner are important (Khaniwale, 2015: 281).

According to Kotler and Armstrong (2012: 159), major factors that affect the buying behavior of consumers are classified as:

- Cultural factors
  Culture, subculture, social class
- Social factors
  Reference groups, family, roles and status
- Personal factors
  Age, life cycle stage, occupation, economic situation, lifestyle, personality and self-concept
- Psychological factors
  Motivation, perception, learning, beliefs and attitudes

Khaniwale (2015) classified the factors which influence consumer buying behavior as external and internal. External factors consist of cultural and social factors. On the other hand, internal factors are composed of personal and psychological factors.

Extraction of Customer Demographic Characteristics

In the context of video analysis, some demographic characteristics of hypothetical customers are extracted. These characteristics are determined as gender and age in the present study. Furthermore, the instore customer trajectories are detected through image processing functions.

Gender Estimation

Gender estimation is carried out using a portrait photo taken before entering the store. As a first step, the detection of face region is performed. To do that, Matlab's vision.CascadeObjectDetector function is used (https://www.mathworks.com/help/vision/ref/vision.cascadeobjectdetector-class.html, 07.08.2017). This function uses the Viola-Jones algorithm and detects people's faces, noses, eyes, mouth, or upper body (Viola and Jones, 2001). Then, the eye, nose and lip regions are cropped from the face. A sample detected face and the corresponding regions cropped from the face are shown in Figure 1.

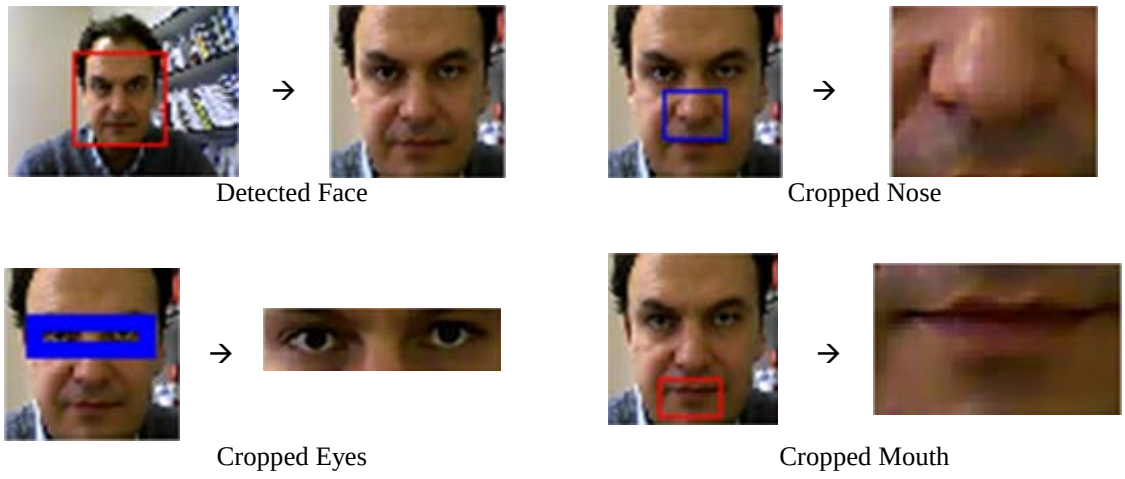

Figure 1. Results of face detection and face region cropping

After that four different ratios are computed using the geometric facial distances (Ramesha *et al.* 2010). The distances are illustrated in Figure 2, and the ratios are given in the following equations 1 to 4.

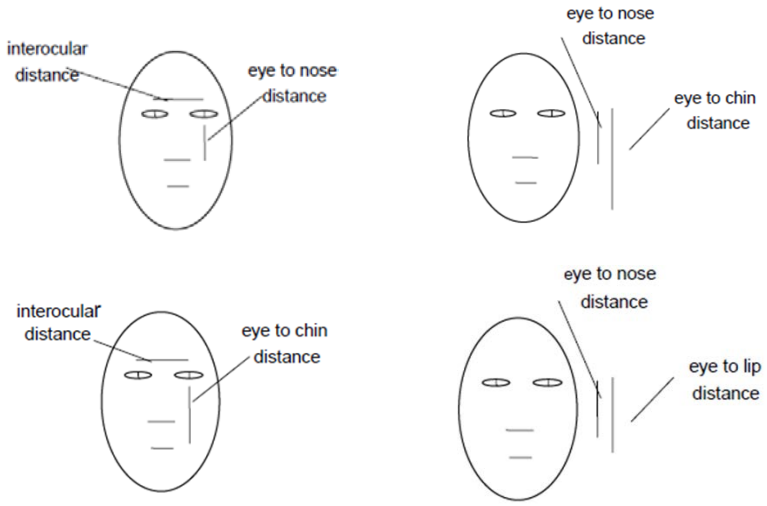

Figure 2. The distances used in gender detection (adapted from Ramesha *et al.* 2010)

$$Ratio1 = \frac{interocular\_distance}{eye\_to\_nose\_distance} \quad (1)$$

$$Ratio2 = \frac{eye\_to\_nose\_distance}{eye\_to\_chin\_distance} \quad (2)$$

$$Ratio3 = \frac{interocular\_distance}{eye\_to\_chin\_distance} \quad (3)$$

$$Ratio4 = \frac{eye\_to\_nose\_distance}{eye\_to\_lip\_distance} \quad (4)$$

The interocular distance is defined as the distance between the right and left eyes in the cropped face image. On the other hand, eye to nose, eye to chin and eye to lip distances are assumed as the distances between the line joining the eyes and nose tip (midpoint of cropped nose), lip (mid line of cropped mouth) and chin (bottom line of cropped mouth), respectively. After performing several experiments, optimum threshold values that differentiate male from female are determined for each ratio.

Age Interval Estimation

The age interval is estimated by the analysis of wrinkles. In the present study, three age intervals are considered which are (i) young, (ii) middle age and (iii) old. The regions labeled as "1" and "2" are used in the wrinkle map (Figure 3). These regions are automatically located for each face by generating buffer zones above and below the eye regions.

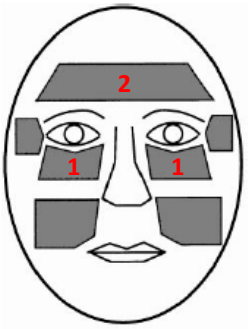

Figure 3. The regions of wrinkle map (adapted from Kwon and Lobo 1999)

To reveal the wrinkles, Canny edge detection operator is used (Canny, 1986). This operator uses a multi-stage algorithm to detect edges in images. It also provides low error rate, good localization and minimal detector

response per edge. The detected wrinkles (edges) on the cropped face image are shown in Figure 4. After obtaining all wrinkles, the edges fall within the predefined regions given in Figure 3 are counted. According to the number of lines counted, the age interval is determined. After performing numerous experiments, optimum separation values that differentiate three age intervals are determined.

Figure 4. Detected wrinkles on a sample image

Customer Trajectory Determination

In the final step, the instore trajectories of customers are determined by object segmentation techniques. In a video data taken from an oblique angle, the initial (empty) image frame is accepted as the background frame. The following frames are subtracted from the initial frame to reveal the moving objects. The moving objects are considered as customers in our hypothetical scenario. Sample moving objects segmented by background subtraction technique are illustrated in Figure 5.

Figure 5. The original image frames (left) and their segmented counterparts in binary form (right).

To determine the walking paths of the customers, segmented blobs are analyzed according to their Center of Mass (CoM) positions. To do that, for each image frame, the centroid points are computed for each isolated blob. These points found in each frame are marked on a still image cumulatively. Different colors are used for each customer to provide a better discrimination. In an example given in Figure 6, three different instore trajectories are obtained colored by yellow, green and blue.

Figure 6. Computed instore trajectories of three different customers.

Results and Discussion

The preliminary experimental results show that promising clues are extracted to be used in the retail video analytics. The tests are conducted on Chicago Face Database, which is developed at the University of Chicago (Ma *et al*., 2015). The database provides high quality, standardized face images of females and males between the ages 17-65. Of 50 female images chosen from the database, 32 were found to be correct (64% accuracy) in terms of gender and age interval. On the other hand, the accuracy of male images was computed to be 70% by predicting 35 images out of 50, correctly. The overall accuracy of the proposed approach is found to be 69%.

Although the proposed approach produces promising outcomes, some limitations are still apparent. First, instead of using real shopping videos with real customers, an indoor environment video with hypothetical customers is utilized due to difficulty in getting legal permissions. Second, the age interval is limited to three categories as young, middle age and old. More sophisticated prediction algorithms are needed to extend the age intervals.

Conclusion

Understanding the behavior of consumers is very important in the success of the businesses. On the other hand, it is the truth that understanding each of them is not so easy. In this situation, the best way is to make collaboration with other disciplines such as computer science and informatics.

As a matter of fact, consumer's behaviors are tried to be analyzed with image processing techniques. In this study, a preliminary video data analysis is performed in a retail environment, which provides valuable information for business operators. To do that, customer gender identification and age interval estimation are carried out, which are commonly used to better plan resources and marketing strategies. Besides, the instore customer trajectories are revealed by image processing algorithms. The overall accuracy of gender identification and age interval estimation is found to be 69%. The preliminary experimental results show that promising clues are extracted to be used in the retail video analytics.

As a future work, the demographic characteristics can be associated with heat maps of customer walk-through patterns, which allows for optimal product placement and efficient floor setup.

References

Canny, J. (1986). A computational approach to edge detection. *IEEE Transactions on Pattern Analysis and Machine Intelligence*. 6, (pp.679-698).

https://www.mathworks.com/help/vision/ref/vision.cascadeobjectdetector-class.html

Khaniwale, M. (2015). Consumer Buying Behavior. *International Journal of Innovation and Scientific Research*, 14(2), (pp.278-286).

Kotler, P. & Armstrong, G. (2012). *Principles of Marketing*. U.S.A.: Pearson.

Kumar, R. (2014). Impact of Demographic Factors on Consumer Behaviour – A Consumer Behaviour Survey in Himachal Pradesh. *Global Journal of Enterprise Information System*, 6(2), (pp.35-47).

Kwon, H.Y. & Lobo N.D.V. (1999). Age classification from facial images. *Journal of Computer Vision and Image Understanding*, 74(1), (pp.1-21).

Ma, D.S., Correll, J. & Wittenbrink, B. (2015). The Chicago Face Database: A Free Stimulus Set of Faces and Norming Data. *Behavior Research Methods*, 47, (pp.1122-1135).

Ramesha, K., Raja, K.B., Venugopal, K.R. & Patnaik, L.M. (2010). Feature extraction based face recognition, gender and age classification. *International Journal of Computer Science and Engineering*, 2(1),

(pp.14-23).
Solomon, M.R. (2006). *Consumer Behavior: Buying, Having and Being*. U.S.A.: Prentice Hall.
Viola, P. & Jones, M.J. (2001). Rapid Object Detection using a Boosted Cascade of Simple Features. *IEEE Computer Society Conference on Computer Vision and Pattern Recognition*, 08-14 December, (pp.511-518).

IDENTIFYING PREDICTIVE GENES FOR SEQUENCE CLASSIFICATION USING ARTIFICIAL IMMUNE RECOGNITION SYSTEM

Canan BATUR
Yıldız Technical University, Department of Computer Engineering, Istanbul- TURKEY
canan@ce.yildiz.edu.tr

Banu DİRİ
Yıldız Technical University, Department of Computer Engineering, Istanbul- TURKEY
banu@ce.yildiz.edu.tr

Abstract: The small sample data in the high-dimensional data space are encountered in biological applications such as in gene expression microarrays and proteomics mass spectrometry. Due to the fact that such data have characteristics such as high-dimensionality and small sample dimension, their classification becomes hard. Many feature selection algorithms were developed for the purpose of reducing the dimensionality of this kind of data and improving the accuracy of classifiers. In the realization of area discoveries through feature sets, the selected feature subsets skip important information in unnecessary feature sets. This problem comes into prominence with the feature, in the process of performing the discovery of information from the high-dimensional data space. This paper evaluates the proposed ensemble gene selection method based on a local feature selection to Artificial Immune Recognition algorithms in order to find the optimal biological sequences. The unique feature of this study is developing the different type of associated feature groups defined using high-dimensional data in order to find important tumor-related genes. The comparative tests were performed on the training set and test set separately with using support vector machines and k-NN classifiers.
Keywords: Group Based Learning, Gene Selection, Sequence Classification, Machine Learning

Introduction

The discovery of biomarkers from high-dimensional data is an important research topic in the biomedical field. Selecting the most distinctive or critical features for classification is a feature selection problem. Many feature selection algorithms were developed for the purpose of reducing the dimensionality of this kind of data and improving the accuracy performance of the classifiers. A gene selection framework must be established in order to select the most discriminating genes in order to identify biomarkers.

Feature selection is a problem of minimum subset selection from the original feature set for the best accuracy estimation. Generally high dimensional feature selection methods can be classified into two categories: Filters and Wrappers. For filter methods, evaluation of the feature discriminability depends on only the inherent features of the microarray data and subclass information, such as density, correlation, Chi-square statistics, and relief. Wrapper methods search for an optimal feature subset by the evaluation function of a learning algorithm for assessing the goodness of a feature subset. Filters sometimes used as a pre-processing step for other approaches and usually fast.

The idea of the ensemble gene selection framework is converging to original feature groups by creating a set of feature groups is based on the principles of group-based learning method. Ensemble gene selection method depends on feature group formation and feature selection procedures in order to improve the model. In feature grouping stage, different samplings of the original data are generated to create different subset groups. Identifying different type of feature groups relying on data-driven or knowledge-driven group formation method. The data-driven group formation method, exploits the characteristics of target data and the knowledge-driven group formation method is to find group of associated genes or proteins that have coherent expression pattern in the same pathway (He, Yu, 2010). Within the scope of this work, data-driven feature group formation used to pre-select the different type associated gene subset groups. Each type of associative feature group is improved by being optimized with Artificial Immune Recognition Systems and learning is performed at the group level. Within the scope of this study, in the feature selection framework the feature groups were taken as a basis. An attempt to develop the associated feature groups defined using high-dimensional data based on a local feature selection to Artificial Immune Recognition System (LFSAIRS1, LFSAIRS2, Parallel-LFSAIRS1, Parallel -LFSAIRS2).

Creating different type associated feature groups from high-dimensional data is mentioned as a associative feature groups in the second part of the paper, the Artificial immune recognition systems with proposed ensemble gene selection framework is mentioned in the third part, the data set is mentioned in the fourth part, and the comparative performance measurements of the optimal biological sequences are mentioned in the fifth part.

Associative Feature Groups

The idea of converging to original feature groups by creating a set of feature groups is based on the principles of group-based learning method. Relational features have a very high correlation in high-dimensional data sets makes it possible to use feature groups by being taken as a basis.

In this paper, the first type of the associative feature groups was obtained by the DGF (Dense Group Finder) algorithm. The main part of the DGF is the kernel density estimation and iterative mean shift procedure for all features. Density-based feature groups were obtained using the kernel density estimation designated in equation (1). The *h* parameter used for the kernel bandwidth refers to the number of nearest neighbors, *p* refers to the total number of features in the data set, *fi* refers to any feature, and *K* refers to the kernel function. (C_j+1) was calculated to determine the order of sequential locations of the kernel function. (C_j+1) positions the average by shifting it to a denser peak point using the other features in the local region determined with *h* parameter starting from the average of a certain *fi* feature (Loscalzo et al., 2009).

$$\mathrm{Cj}+1=\frac{\sum_{i=1}^{p}\mathrm{fi}\ \mathrm{K}\ \left(\frac{\mathrm{Cj}-\mathrm{fi}}{h}\right)}{\sum_{i=1}^{p}\ \mathrm{K}\ \left(\frac{\mathrm{Cj}-\mathrm{fi}}{h}\right)},\ \mathrm{j}=1,2,\ldots \qquad (1)$$

The second type of the associative feature groups was obtained by the CFG (Correlation-Based Feature Group) algorithm. The CFG is a filter-based feature selection method that sorts the feature subset by the correlation-based intuitive function. The CFG algorithm examines the usefulness of subset of attributes based on a heuristic evaluation function. In choosing a correlation-based feature, each attribute is taken into account in the correlation between the attributes, as well as the predictive predicting of the class label. The value of the heuristic evaluation function used in the evaluation of the attributes is determined by equation 2. The intuitive usability of a subset of *S* attributes with *k* attributes is represented by $meritS$, the mean attribute-class correlation is presented by *rcf* for ($f \epsilon S$), and the correlation between the mean attributes is presented by *rff* parameters.

$$meritS=\frac{\mathrm{k}*\mathrm{rcf}}{\sqrt{\mathrm{k}+(\mathrm{k}-1)*\mathrm{rff}}} \qquad (2)$$

The third type of the associative feature groups was obtained by the IGFG (Information Gain-Based Feature Group) algorithm. This method selects attributes with entropy based scores. The Entropy criterion makes a choice with the help of knowledge in the feature. For this reason, the feature is treated as a distribution and its entropy is found. The entropy of the f_t attribute with *M* data can be found by equation 3.

$$E=\ -\sum_{i=1}^{M}(ft(i)\log(ft(i)) \qquad (3)$$

Within the scope of this study, an attempt to create feature group sets was made by the DGF, CFG and IGFG algorithms. These feature groups obtained based on the ensemble feature selection framework using data perturbation. These feature group sets were developed with the meta-dynamics of the Artificial Immune Recognition Systems like a single cell in order to find the optimal biological sequences.

Artificial Immune Recognition System

Artificial Immune Systems are a class of adaptive computer algorithm based on metaphor of the mammalian immune system. Application areas of the Artificial Immune Systems are pattern recognition, fault and anomaly detection, data mining, classification, robotics, optimization and anomaly detection. Artificial immune recognition algorithm is one version of the Artificial Immune System which is specifically designed for the classification problems.

Artificial Immune Recognition Systems (AIRS) consist of the stages of initialization, memory cell recognition, resource competition and the selection of memory cells. In this approach, an antigen represents a single data instance and allocated to the closest matching ARB (antibody) in the pool of ARBs. At the initialization stage, the data set is normalized to the range of [0,1]. After normalization, the affinity threshold is calculated by equation (4). At the next stage, antigens are presented to the storage pool with antigen training. At the memory cell

recognition stage, a stimulation value is assigned to these cells by stimulating the recognition cells in the memory pool. Affinity is calculated by equation (5), the stimulation values are calculated by equation (6) and (7).

The recognition cell with the highest stimulation value is calculated by equation (8) then M_{cmatch} cell is cloned and mutated. The number of clones is calculated by equation (9),

$$affinity\ \ threshold = \sum_{i=1}^{n} \sum_{j=j+1}^{n} \left(\frac{affinity(\text{agi,agj})}{n(n+1)/_2} \right) \quad (4)$$

$$affinity(\text{agi}, \text{agj}) = 1 - \text{Euclidean}\ \ \text{distance}(\text{agi}, \text{agj}) \quad (5)$$

$$stimulation = 1 - \text{affinity} \quad (6)$$

$$stimulation(\text{mc}, \text{ag}) = \begin{cases} \text{affinity}(\text{mc}, \text{ag}) & \text{if}\ \ \text{mc.class} = \text{ag.class} \\ 1 - \text{affinity} & \text{otherwise} \end{cases} \quad (7)$$

$$\boldsymbol{Mcmatch} = \mathbf{argmax}(\mathbf{stimulation}(\mathbf{mc}, \mathbf{ag})) \quad (8)$$

$$\boldsymbol{numClones} = \mathbf{stimulation} * \mathbf{clonalRate} \quad (9)$$

At the resource competition stage, when mutated clones are added to the ARB (artificial recognition spheres, antibody) pool, competition begins for the time source. According to the stimulation value, limited resource assignment to the ARB pool is made according to the stimulation value. ARBs without enough resources are removed from the system. When the stop criterion is achieved, the process ends, and the ARB with the highest stimulation value is selected as the candidate memory cell. At the selection of memory cells stage dynamically and evolving developed Memory cell pool in the algorithm is used for the classification process (Brownlee, 2005).

The basic steps of the AIRS1 algorithm, the first version of artificial immune recognition systems, and the AIRS2 algorithm, the second version, are same. The main difference between them is that the ARB pool is used as a permanent resource in the AIRS1 algorithm; it is used as a temporary resource in the AIRS2 algorithm. In the case of being used as a permanent resource, ARBs remaining from previous steps cause the algorithm to spend more time by being involved in the competition for limited resources. Therefore, the complexity of the AIRS2 algorithm is less. While AIRS1 uses the mutation parameter that can be defined by the user, AIRS2 uses the concept of somatic hyper mutation where the mutation ratio of a clone is proportional to the affinity (Wang, Chen, Adrian, 2014). While the classes of clones may change after the mutation process in the AIRS1 algorithm, classes are not allowed to change in the AIRS2 algorithm. Parallel AIRS is work into exploiting the parallelism, which caused some loss in the data reduction benefits of artificial immune recognition system. The versions of the Parallel AIRS are Parallel AIRS 1 and Parallel AIRS2. Which are modeled based on the distributed nature and parallel processing feature of the mammalian immune system (Brownlee, 2005). At first, each part of the training data set is assigned to np number of processes. Thus, it is ensured that np number of the memory pool is created by running the AIRS algorithm on each process. As a result, the memory pools obtained are merged.

A. The proposed ensemble gene selection Framework

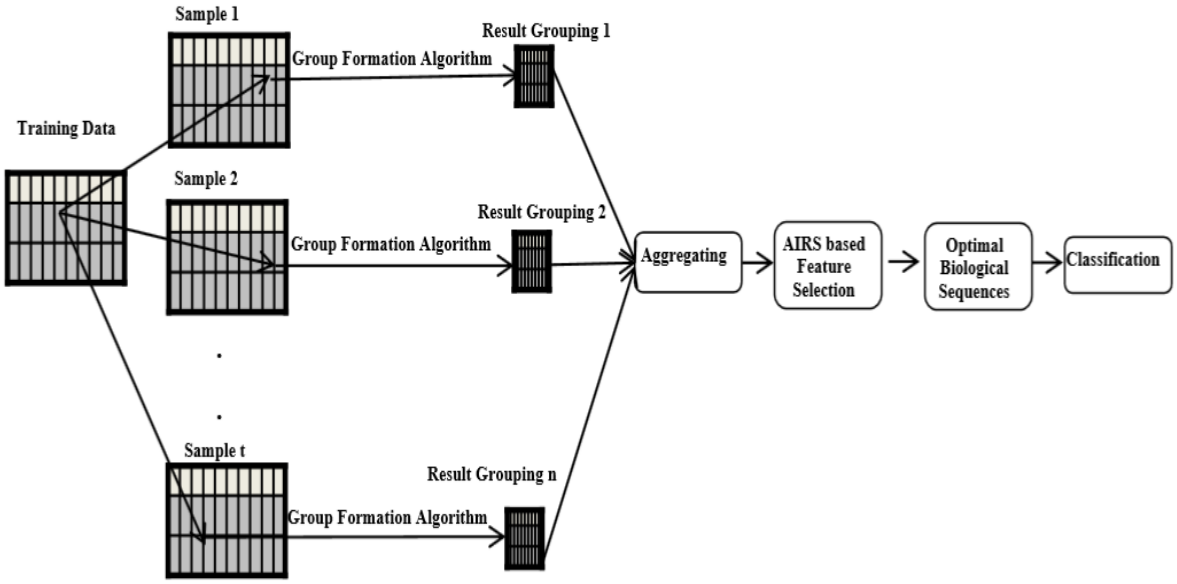

Figure 1. Proposed ensemble gene selection framework

B. Standard Artificial Immune Recognition Systems:

Input: InputPatterns, clone rate, mutationrate, stimthresh, resourcemax, affinitythresh
Output: cell memor ←eInitializeMemoryPool(InputPatterns)
For (InputPatterni ∈ InputPatterns)
Stimulate (cellsmemory, InputPatterns)
cellbest esGetMostStimulatedby1NN (InputPatterni, cellsmemory)
If cellclass,best ≠eInputPatternclass,i
Then cellmemory moCreateNewMemoryCell (InputPatterni)
Else clonenum ← cellsstim, best x clonerate x mutationrate
cellsclones ←lcellsbest
For (i to clonenum)
cellsclone ←lCloneAndMutate (cellsbest)
End
While (AverageStimulation (cellsclones) ≤, stimthresh
For (celli ∈ cellsclones)
cellsclones loCloneAndMutate (cellsi)
End
Stimulate (cellsclones, InputPatterns)
ReducePoolToMaximumResources (cellsclones, resourcemax)
End
cellsc elGetMostStimulated (InputPatterni, cellsclones)
If (cellsstim , c > cellsstim , best)
Then
cellsmemory ←ecellsc
If (Affinity(cellsc , cell best) ≤ affinitythresh
Then DeleteCell (cellsbest , cell memory)
End
End
End
End
Return (cell memory)

The Pseudo code of the standard AIRS is represented (Wang et al, 2014).

C. *Local Feature Selection to Artificial Immune Recognition Systems: LFSAIRS*

1. The initial set of feature group sets are created based on associative group formation algorithm.
2. Do for each Antigen (Ag) until training process is completed:
    2.1. Calculating fitness value of the each feature set is calculated by taking into account only best matching cell
    2.2. Until termination do :
    2.3. The highest fitness value of the feature set is selected as a best feature set
    2.4. Generation of l clones of the best feature set
    2.5. Mutation of the each clone
    2.6. Calculating fitness of the each clone by taking into account only best candidate cell
    2.7. Set the highest fitness value of the feature set as a candidate optimum feature subset
    2.8. If best candidate cell is sufficient calculate the optimum subset then go step 3. else go 2.3
3. After memory cell replacement stage, set the optimum subset of attributes as the subset of the new attribute. If training process is completed go to Step 4, else go to step 2.
4. Selection of the best optimized feature set
5. Classification of the best optimized feature sets based on test set

Data Sets

The most common six microarray data sets were used in this study. Table 1 includes information on the genes, samples and class numbers contained in the data sets used in this study (Loscalzo et al, 2008).

Table 1: Microarray Data set

Dataset	Gene	Sample	Class
Colon	2000	62	2
Lungstd	5000	181	2
Prostate	6034	102	2
SRBCT	2308	63	4
Lymphoma	4026	62	3
Leukemia	7129	72	2

The goal of this work is identifying predictive genes for sequence classification at the group level using Artifical Immune Recognition Systems. Experimentally obtained performance values were achieved by dividing the data sets as 70% training and 30% test set. The proposed ensemble gene selection framework is applied only on training set. The goal of the designed framework is to select optimal biological sequences only on the training set in order to avoid over-fitting and selection bias problems. Therefore, the test set independent of the gene selection process. Within the scope of this work, *t* is the number of bootstraps. Bootstrap was applied on the training data set in order to ensure the resistance of training samples against variations. Then *n* is a number of the selected feature groups, which are created by DFG, CFG and IGFG algorithms. These group feature selection algorithms are separately running on the each of the bootstrap data sets. We set the *t* and *n* parameters respectively to 10 and 10 for all algorithms within the scope this paper. The number of features contained in the feature groups obtained at the end of the each group feature selection algorithm varies to for each data set. Learning was performed at the group level by improving the feature groups presented to the LFSAIRS1, LFSAIRS2, Parallel-LFSAIRS1 and Parallel-LFSAIRS2 like a single cell. Selecting an informative gene subset obtained by classification ability of a gene subset. The fitness function of each candidate solution was calculated according to the KNN classifier accuracy performance. WEKA was used to obtain classifying accuracies. For all algorithms, the classifying accuracy of the optimal candidate solution obtained at the end of each run with using the test data set with 10 cross-fold validations. The performance values added to the results were calculated by taking the average of the number of runs. Moreover, to assessment of the discrimination of more important genes is measured by its occurrence frequency of gen subset formation.

Each of the feature groups represents a candidate solution and the presence of the related feature in a feature group was encoded with 1 while the absence of it was encoded with 0. In this study, the affinity threshold value, clonal ratio, mutation ratio, np, total source, stimulating value, hypermutation ratio, run number and iteration number parameters of the Artificial Immune Recognition Systems took the values of 0.1, 10, 0.15,2, 150, 0.9, 2.0, 30 and 50, respectively.

Performance Results and Discussions

Within the scope of this study, it was focused on the problem of identifying predictive genes for sequence classification in order to find important tumor-related genes.

Table 2: Representative gene subsets obtained by LFSAIRS1 and LFSPAIRS1 based on Associative feature groups

			LFSAIRS1	SVM		KNN		LFS PAIRS1	SVM		KNN	
Data Set	Group Type	No	Optimal Gene Subsets	10 CV % on		10 CV % on		Optimal Gene Subsets	10 CV % on		10 CV % on	
				Train Set	Test Set	Train Set	Test Set		Train Set	Test Set	Train Set	Test Set
Colon	DFG	1	**{T63133,T57630}**	63.2	69.2	**73.4**	**92.3**	{T47377,H55759,D15057, H77536}	67.3	69.2	73.4	61.5
		2	{T53889,M22632,R83349,U10117,X14830}	61.2	69.2	73.4	61.5	{M83751, M27903}	63.2	69.2	59.1	53.8
	CFG	1	{L35545,H79349}	63.2	61.5	57.1	69.2	{U25265,T47584,X02750}	63.2	69.2	63.2	64.6
		2	{T52003,L35249,L11370}	63.2	61.5	63.2	61.5	**{H22579,X59871}**	**73.4**	**76.9**	**79.1**	**77.9**
	IGFG	1	{H55759,M83254,D15057}	63.2	69.2	69.1	76.9	{R38513,H29293,T67905, U18934}	63.2	69.2	65.3	61.5
		2	{T55558,R41561, M87434}	71.4	69.2	65.3	69.2	{R60217, J00277}	63.2	69.2	67.8	84.6
Lungstd	DFG	1	{32952_AT, 32980_F_AT}	86.8	88.8	95.2	88.2	**{35052_R_AT, 35053_AT, 35064_AT}**	**98.6**	**92.2**	**96.5**	**97.2**
		2	**{33052_AT, 33078_AT, 33087_S_AT}**	**95.8**	**88.8**	**96.5**	**92.8**	{35922_AT, 35932_AT, 36232_AT}	97.2	91.6	96.5	88.8
	CFG	1	{33270_I_AT, 33306_AT}	82	86.1	74.4	77.7	{32704_AT, 33270_I_AT, 33306_AT}	82	86.1	78.6	86.1
		2	{40401_AT, 40686_AT, 40700_AT}	82	88.8	80	91.6	{36370_AT, 36411_S_AT}	82	86.1	80.6	88.8
	IGFG	1	{33301_G_AT, 33307_AT, 33304_AT}	82	86.1	78.6	91.6	{AFFX-THRX-5_AT, 31439_F_AT, 31447_AT, 31477_AT}	84.8	86.1	82	88.8
		2	{32702_AT, 32711_G_AT, 32716_AT}	82	86.1	78.6	92.4	{36720_AT, 36806_AT}	82	86.1	76.5	77.7
Prostate	DFG	1	{32950_AT, 33469_R_AT}	80.2	71.4	71.6	71.4	{33973_AT, 34020_AT}	74	57.6	69.1	57.1
	CFG	1	{32376_AT, 32884_AT}	51.8	66.6	53.0	61.9	{41012_R_AT, 41017_AT, 41023_AT}	56.7	55	59.5	52.8
	IGFG	1	{38933_AT, 38953_AT}	49.3	47.6	76.5	71.4	{33958_AT, 33959_AT}	61.7	57.6	59.2	52.3
		2	{34930_AT, 34931_AT, 34934_AT}	42.8	46.9	60.4	71.4	{34930_AT, 34932_AT, 34934_AT 37469_AT, 37470_AT, 37471_AT}	70.3	57.4	59.2	52.3
SRBCT	DFG	1	**{GENE2125, GENE2142, GENE2144, GENE2190, GENE2197}**	**66**	**63.8**	**68**	**84.6**	{GENE1802, GENE1820}	68	63.8	66	69.2
	CFG	1	{GENE1113, GENE1114, GENE1115, GENE1679, GENE1680}	60	63.8	38	69.2	**{GENE971, GENE990, GENE1709, GENE1711}**	**69**	**68.4**	**68**	**69.2**
	IGFG	1	{GENE1007, GENE1008, GENE1009, GENE2305, GENE2306}	62	68.4	68	56.1	{GENE773, GENE774, GENE842, GENE843, GENE844}	64	38.4	56	61.5
Lymphoma	DFG	1	**{GENE654X, GENE627X, GENE659X}**	**81.6**	**76.9**	**93.8**	**84.6**	{GENE3142X, GENE3096X}	65.5	76.9	77.5	84.6
		2	{GENE579X, GENE585X}	81.6	76.9	93.8	61.5	**{GENE770X, GENE761X, GENE507X}**	**83.6**	**84.6**	**81.6**	**92.3**
	CFG	1	{GENE2559X, GENE1194X}	65.3	76.9	67.3	61.5	{GENE58X, GENE1094X, GENE40X}	65.3	76.9	57.1	69.2
	IGFG	1	{GENE2740X, GENE2741X}	65.3	76.9	59.1	69.2	{GENE3145X, GENE3105X}	65.3	76.9	57.1	61.5

Leukemia	**DFG**	1	**{M24748_CDS2_S_AT, M31211_S_AT}**	**85.9**	**86.6**	**78.9**	**86.6**	{M32639_AT, M34192_AT}	61.4	86.6	66.6	73.3
		2	**{M96740_AT, S46622_AT, S69232_AT}**	**85.9**	**86.6**	**73.6**	**86.6**	**{X04391_AT, X04707_AT}**	**70.1**	**86.6**	**73.6**	**80**
	CFG	1	{M19722_AT, M19961_AT}	59.6	86.6	63.1	86.6	{AFFX-PHEX-M_AT, AFFX-HUMGAPDH/M33197_3_AT}	59.6	86.6	63.1	73.3
		2	**{U40622_AT, U40714_AT}**	**77.8**	**86.6**	**66.6**	**86.6**	{X04327_AT, X07948_AT, X12433_AT}	61.4	86.6	56.1	73.3
	IGFG	1	{D87002_CDS2_AT,HG2846-HT2983_AT}	59.6	86.6	54.3	73.3	{U61263_AT, U62531_AT, U63717_AT}	63.1	86.6	57.8	80

Table 3: Representative gene subsets obtained by LFSAIRS2 and LFSPAIRS2 based on Associative feature groups

			LFSAIRS2	**SVM**		**KNN**		**LFSPAIRS2**	**SVM**		**KNN**	
Data Set	**Group Type**	**No**	**Optimal Gene Subsets**	**10 CV % on**		**10 CV % on**		**Optimal Gene Subsets**	**10 CV % on**		**10 CV % on**	
				Train Set	**Test Set**	**Train Set**	**Test Set**		**Train Set**	**Test Set**	**Train Set**	**Test Set**
Colon	**DFG**	1	{T99498, X15183}	69.3	69.2	67.3	53.8	{U37673,H51015,R54422, R46502}	69.3	61.5	73.6	61.5
		2	{T63539,T93284,U29607}	69.3	69.2	65.3	69.2	{L08069, R93337, T89175}	67.3	61.5	65.3	69.2
	CFG	1	{U25265, T47584, R39130}	63.2	69.2	48.9	61.5	{R21901, R39531, T92736, X14830}	63.2	69.2	59.1	46.1
		2	{M37510, L13738}	63.2	69.2	65.3	46.1	{V00523, T72889}	63.2	69.2	48.9	84.6
	IGFG	1	{D00763,X66839}	63.2	69.2	57.1	69.2	{R09479, M73481,H79349, T41207, T54364, R56052}	63.2	69.2	59.1	69.2
Lungstd	**DFG**	1	**{34171_AT}**	**91.7**	**86.1**	**86.3**	**91.6**	{33969_AT, 34028_AT}	89.6	83.3	87.5	83.3
	CFG	1	{39640_AT,41037_AT, 2047_AT}	82	86.1	84.8	91.6	**{31806_AT, 31840_AT}**	**90.3**	**86.1**	**91**	**86.1**
	IGFG	1	{33324_S_AT,33334_AT}	82	86.1	81.3	80.5	{31980_AT, 32010_AT, 32383_AT, 32396_F_AT}	82.7	86.1	80	83.3
		2	{33336_AT, 33337_AT, 33698_AT}	83.4	86.1	88.9	86.1	{40719_AT, 40721_G_AT}	82	88.8	83.4	91.6
Prostate	**DFG**	1	{34718_AT,35172_AT}	76.5	61.9	62.9	47.6	**{37822_AT, 37823_AT, 38156_AT, 38170_AT}**	**90**	**72.3**	**86.4**	**71.4**
		2	{41405_AT, 41439_AT, 41616_AT}	66.6	67.2	61.7	47.6	**{40727_AT, 41016_AT, 41032_AT}**	**88.8**	**76.1**	**83.9**	**71.4**
	CFG	1	{33714_AT, 33809_AT, 34764_AT}	65.4	42.8	58	47.6	{32663_AT, 32735_AT}	53	52.3	66.6	66.6
	IGFG	1	{36768_AT, 36769_AT, 36770_AT}	61.7	57.1	62.9	57.1	{36763_AT, 36764_AT, 36766_AT, 37051_AT, 37054_AT, 37056_AT}	60.4	52.3	60.4	66.6
SRBCT	**DFG**	1	**{GENE403, GENE415, GENE2048, GENE2081}**	**58**	**61.5**	**72**	**61.5**	{GENE234, GENE253, GENE274}	54	53.8	64	69.2
	CFG	1	{GENE1709, GENE1711}	62	58.4	62	66.1	**{GENE1639, GENE1676, GENE1680}**	**61.3**	**58.9**	**63.2**	**72.4**
	IGFG	1	{GENE767, GENE768, GENE769}	62	58.4	62	63	{GENE864, GENE865}	62	54.6	61.3	60.2
Lymphoma	**DFG**	1	**{GENE1764X, GENE3594X}**	**77.5**	**76.9**	**77.5**	**84.6**	**{GENE2226X, GENE2902X}**	**81.6**	**76.9**	**77.5**	**92.3**
		2	**{GENE2368X, GENE2369X, GENE2370X, GENE2109X, GENE2108X}**	**93.8**	**76.9**	**89.7**	**76.9**	**{GENE2774X,GENE704X, GENE699X}**	**83.6**	**76.9**	**81.6**	**76.9**
	CFG	1	{GENE1910X, GENE2060X, GENE330X, GENE235X}	65.3	76.9	63.2	53.8	{GENE1241X, GENE891X}	65.3	76.9	55.1	61.5
		2	{GENE1269X, GENE1194X}	63.2	76.9	69.2	53.8	{GENE2598X,GENE2616X, GENE2010X}	65.3	76.9	61.2	69.2
	IGFG	1	{GENE2648X,GENE2647X, GENE2684X}	65.3	76.9	55.1	61.5	**{GENE526X, GENE527X}**	**71.4**	**76.0**	**85.7**	**84.6**
Leukemia	**DFG**	1	**{M32639_AT, M34192_AT, U40282_AT, U41387_AT}**	**82.4**	**86.6**	**73.3**	**77.1**	**{M72885_RNA1_S_AT, X58528_S_AT}**	**82.4**	**86.6**	**77.1**	**86.6**
	CFG	1	**{M22382_AT, M23533_AT, X17620_AT, X56465_AT}**	**76.6**	**86.6**	**71.9**	**86.6**	**{D50855_S_AT, Y10807_S_AT}**	**74.9**	**86.6**	**76.6**	**86.6**
	IGFG	1	{U83117_AT, X16546_AT, X78712_AT}	59.6	86.6	61.4	73.3	{M17446_S_AT, U50327_S_AT}	61.4	86.6	59.6	73.3

The average classifier accuracy on the training set and test set separately with using support vector machines and k-NN classifier shown in Table 2 and 3. For Colon data set, 2-gene subsets {T63133, T57630} with 73.4% training accuracy has 92.3% prediction accuracy with KNN classifier based DFG for LFSAIRS1. 2-gene subsets {H22579, X59871} with 73.4% training accuracy has 76.9% prediction accuracy with SVM classifier and 79.1% training accuracy has 77.9% prediction accuracy with KNN classifier based CFG for LFSPAIRS1. For Lungstd data set, 3-gene subsets {33052_at, 33078_at, 33087_s_at} with 95.8% training accuracy has 88.8% prediction accuracy with SVM classifier and 96.5% training accuracy has 92.8% prediction accuracy with KNN classifier based DFG for LFSAIRS1. 3-gene subsets {35052_r_at, 35053_at, 35064_at} with 98.6% training accuracy has 92.2% prediction accuracy with SVM classifier and 96.5% training accuracy has 97.2% prediction accuracy with KNN classifier based DFG for LFSPAIRS1. 1-gene subset {34171_at} with 91.7% training accuracy has 86.1% prediction accuracy with SVM classifier and 86.3% training accuracy has 91.6% prediction accuracy with KNN classifier based DFG for LFSAIRS2. 2-gene subset {31806_at, 31840_at} with 90.3% training accuracy has 86.1% prediction accuracy with SVM classifier and 91% training accuracy has 86.1% prediction accuracy with KNN classifier based CFG for LFSPAIRS2. For Prostate data set, 4-gene subsets {37822_at, 37823_at, 38156_at, 38170_at} with 90% training accuracy has 72.3% prediction accuracy with SVM classifier and 86.4% training accuracy has 71.4% prediction accuracy with KNN classifier based DFG for LFSPAIRS2. 3-gene subsets {40727_at, 41016_at, 41032_at} with 88.8% training accuracy has 76.1% prediction accuracy with SVM classifier and 83.9% training accuracy has 71.4% prediction accuracy with KNN classifier based DFG for LFSPAIRS2. For SRBCT data set, 5-gene subsets {GENE2125, GENE2142, GENE2144, GENE2190, GENE2197} with 66% training accuracy has 63.8% prediction accuracy with SVM classifier and 68% training accuracy has 84.6% prediction accuracy with KNN classifier based DFG for LFSAIRS1. 4-gene subsets {GENE971, GENE990, GENE1709, GENE1711} with 69% training accuracy has 68.4% prediction accuracy with SVM classifier and 68% training accuracy has 69.2% prediction accuracy with KNN classifier based CFG for LFSPAIRS1. 4-gene subsets {GENE403, GENE415, GENE2048, GENE2081} with 58% training accuracy has 61.5% prediction accuracy with SVM classifier and 72% training accuracy has %61.5 prediction accuracy with KNN classifier based DFG for LFSAIRS2. 3-gene subsets {GENE1639, GENE1676, GENE1680} with 61.3% training accuracy has 58.9% prediction accuracy with SVM classifier and 63.2% training accuracy has 72.4% prediction accuracy with KNN classifier based CFG for LFSPAIRS2. For Lymphoma data set, 3-gene subsets {GENE654X, GENE627X, GENE659X} with 81.6% training accuracy has 76.9% prediction accuracy with SVM classifier and 93.8% training accuracy has 84.6% prediction accuracy with KNN classifier based DFG for LFSAIRS1. 3-gene subsets {GENE770X, GENE761X, GENE507X} with 83.6% training accuracy has 84.6% prediction accuracy with SVM classifier and 81.6% training accuracy has 92.3% prediction accuracy with KNN classifier based DFG for LFSPAIRS1. 2-gene subsets {GENE1764X, GENE3594X} with 77.5% training accuracy has 76.9% prediction accuracy with SVM classifier and 77.5% training accuracy has 84.6% prediction accuracy with KNN classifier based DFG for LFSAIRS2. 5-gene subsets {GENE2368X, GENE2369X, GENE2370X, GENE2109X, GENE2108X} with 93.8% training accuracy has 76.9% prediction accuracy with SVM classifier and 89.7% training accuracy has 76.9% prediction accuracy with KNN classifier based DFG for LFSAIRS2. 2-gene subsets {GENE2226X, GENE2902X} with 81.6% training accuracy has 76.9% prediction accuracy with SVM classifier and 77.5% training accuracy has 92.3% prediction accuracy with KNN classifier based DFG for LFSPAIRS2. 3-gene subsets {GENE2774X,GENE704X, GENE699X}with 83.6% training accuracy has 76.9% prediction accuracy with SVM classifier and 81.6% training accuracy has 76.9% prediction accuracy with KNN classifier based DFG for LFSPAIRS2. 2-gene subsets {GENE526X, GENE527X} with 71.4% training accuracy has 76% prediction accuracy with SVM classifier and 85.7% training accuracy has 84.6% prediction accuracy with KNN classifier based IGFG for LFSPAIRS2. For Leukemia data set, 2-gene subsets {M24748_cds2_s_at, M31211_s_at} with 85.9% training accuracy has 86.6% prediction accuracy with SVM classifier and 78.9% training accuracy has 86.6%prediction accuracy with KNN classifier based DFG for LFSAIRS1. 3-gene subsets {M96740_at, S46622_at, S69232_at} with 85.9% training accuracy has 86.6% prediction accuracy with SVM classifier and 73.6% training accuracy has 86.6% prediction accuracy with KNN classifier based DFG for LFSAIRS1. 2-gene subsets {U40622_at, U40714_at} with 77.8% training accuracy has 86.6% prediction accuracy with SVM classifier and 66.6% training accuracy has 86.6% prediction accuracy with KNN classifier based CFG for LFSAIRS1. 2-gene subsets {X04391_at, X04707_at} with 70.1% training accuracy has 86.6% prediction accuracy with SVM classifier and 73.6% training accuracy has 80% prediction accuracy with KNN classifier based DFG for LFSPAIRS1. 4-gene subsets {M32639_at, M34192_at, U40282_at, U41387_at} with 82.4% training accuracy has 86.6% prediction accuracy with SVM classifier and 73.3% training accuracy has 77.1% prediction accuracy with KNN classifier based DFG for LFSAIRS2. 4-gene subsets {M22382_at, M23533_at, X17620_at, X56465_at} with 76.6% training accuracy has 86.6% prediction accuracy with SVM classifier and 71.9% training accuracy has 86.6% prediction accuracy with KNN classifier based CFG for LFSAIRS2. 2-gene subsets {M72885_rna1_s_at, X58528_s_at} with 82.4% training accuracy has 86.6% prediction accuracy with SVM classifier and 77.1% training accuracy has 86.6% prediction accuracy with KNN

classifier based DFG for LFSPAIRS2. 2-gene subsets {D50855_s_at, Y10807_s_at} with 74.9% training accuracy has 86.6% prediction accuracy with SVM classifier and 76.6% training accuracy has 86.6% prediction accuracy with KNN classifier based CFG for LFSPAIRS2.

Conclusion

Conclusion

In this paper, we proposed an ensemble gene selection framework to select informative gene subsets. The informative gene subsets obtained from the different type of the associative feature groups mine many tumor-related genes. Based on the obtained optimal gene subsets, we aim to find reliable accuracy on the training set and test set separately. The significance of a gene subset is measured by its frequency occurrence. Each type of the associative feature groups obtained by group-based learning was presented as a candidate solution to Artificial Immune Recognition Systems in order to improve with its meta-dynamics. The presented framework makes it possible to obtain more robust tumor-related genes. The prediction accuracies obtained by SVM and KNN classifiers. The classifier results obtained were compared with six commonly used microarray data sets.

References

He Z., Yu W., (2010), *Stable feature selection for biomarker discovery*. Pubmed.

Loscalzo S , YU L., Ding C. (2009), *Consensus group stable feature selection*, June28–July1, Paris,France.

Brownlee J. (2005). *Artificial immune recognition system (airs): A review and analysis*, Technical Report.

Wang K., Chen K.,Adrian A., (2014), *An improved artificial immune recognition system with the opposite sign test for feature selection* , Knowledge-Based Systems ,Taiwan.

Loscalzo S , YU L., Ding C. (2008), *Stable feature selection via feature groups*, August 24–27, Las Vegas, Nevada, USA.

http://www.cs.waikato.ac.nz/ml/weka/

Y.Saeys, I.Inza, and P. Larranaga, (2008). *A review of feature selection techniques in bioinformatics*, Bioinformatics,vol. 23, no. 19, pp. 392-403.

T. Abeel, T.Helleputte, Y.V. de Peer, P. Dubont, and Y. Saeys, *Robust biomarker identification for cancer diagnosis with ensemble feature selection methods*, Bioinformatics, in press.

I. Guyon, J. Weston, S. Barnhill, and V. Vapnik, (2002). *Gene selection for cancer classification using support vector machines*, Machine learning, vol. 46, no. 1, pp. 389-422.

J. Dutkowski and A. Gambin, (2007). *On consensus biomarker selection*, BMC Bioinformatics, vol.8, no. Suppl 5, pp. S5,

S. Ma, J. Huang, (2008), *Penalized feature selection and classification in bioinformatics*, Brief. Bioinform. Vol.9 no. 5, pp. 392-403.

Q. Song, J. Ni, G. Wang, (2013). *A fast clustering-based feature subset selection algorithm for high dimensional data*, IEEE Trans. Knowl. Data Eng. Vol. 25 no.1, pp. 1-4.

Oh S. , Lee J.S., Moon B.R. (2004). *Hybrid genetic algorithms for feature selection* .Vol. 26, No.11, November.

Timmis J. and Neal J.,(2000), *Investigating the evolution and stability of a resource limited artificial immune system*, Special Workshop on Artificial Immune Systems, Genetic and Evolutionary Computation Conference (GECCO) 2000, Las Vegas, Nevada, U.S.A., pp. 40-41.

Mark A. Hall, Lloyd A. Smith., (1998) *Practical feature subset selection for machine learning*, In C. Mcdonald (ed.), Computer Science '98 Proceedings of the 21st Australian Computer Science Conference ACSC'98, Perth, 4-6 February, 1998 (pp. 181-191), Berlin: Springer.

Carter J.H., (2000), *The immune system as a model for classification and pattern recognition*, Journal of the American Informatics Association, vol.7.

Watkins A. and Timmis J.,(2002), *Artificial immune recognition system (airs): Revisions and refinements*, 1st International Conference on Artificial Immune Systems (ICARIS2002), University of Kent at Canterbury, pp. 173-181.

Mini-Review : THE CLASSIFICATION STUDIES DONE FOR EARLY DIAGNOSIS OF THE STOMACH CANCER

Furkan ESMERAY*, İbrahim Hanifi ÖZERCAN
*Electric and Energy Department, Munzur University, Tunceli, Turkey
Pathology Department, Fırat University, Elazığ, Turkey
furkanesmeray@munzur.edu.tr ozercanih@yahoo.com

Abstract: Cancer is a heterogeneous disease. Cancer is a heterogeneous disease Cancer is composed of many different subtypes. The early diagnosis and diagnosis of gastric cancer has become imperative in cancer research because it may facilitate the subsequent clinical treatment of patients. Separation of gastric cancer patients into normal, low and high groups has become important in bioinformatics and biomedical fields. This has led to an increase in the practice of machine learning (ML) methods for early cancer diagnosis in the literature. Machine learning methods have been used to model the progression and treatment of stomach cancer. ML methods have been used to detect complex cell characteristics in cancer images. (ANN), Bayesian Networks (BNS), Random Forest (RF), Support Vector Machines (SVM), Decision Trees (DT), Linear Discriminant Analysis (LDA), Sammon mapping, Stochastic Neighbor New algorithms have been proposed using various machine learning techniques such as Embedding (SNE), Isomap, Classical multidimensional scaling (MDS), and Local Linear Embedding (LLE). Although machine learning techniques for gastric cancer have been widely applied and ultimately yielded high classification performances, an appropriate level of validation is required to take these methods into account in daily clinical treatment and practice. In this study, the methods used in algorithms for early diagnosis of stomach cancer and the classification ratios are described. In the advanced algorithms, various different features and image data are used. As a result, in this article, ML methods for gastric cancer research are increasing. For this reason, published articles have been presented to model the risk of stomach cancer.
Keywords: Stomach Cancer, Machine Learning Techniques, Classification

Introduction

Stomach cancer is a rapidly developing and spreading type of cancer (Tannapfel, 2001). It usually starts in the form of ulcer complaints. Stomach cancer can affect the organs and lymph glands (Tolbert, 1999). It can be spread by direct neighbors, lymphatic, blood and intraabdominal (Siddiqi, 2008). The stomach tumor may grow through the outer layer of the miter and extend into the surrounding organs, such as the pancreas, esophagus or intestine (Mikami, 2004). Stomach cancer cells can spread by blood metastases to the liver, lungs, and other organs (Ahmad, 2007). Cancer cells can also spread to all the lymph glands in the body through the lymphatic system (Fenoglio, 2000). Cancer first starts at the center of the cells that make up the tissues, and at the same time, these tissues bring the organs of the body to the bloom (Cappell, 2002). For a normal individual, the cells grow, develop, and the body is divided to create cells that are new in need. Cells are sufficiently digested and digested by the cell when they are old and are killed and replaced by new ones. But sometimes this process is in the wrong direction. So much so that, despite the fact that the body does not need much, new cells form and the old cells that should die do not die. These excess cells can eventually turn into tumor masses called tumors. Tumors may be benign or malignant.Stomach cancer that occurs from stomach wall and stomach tissue is a type of cancer. According to studies conducted by the Ministry of Health in our country, stomach cancer was identified as the second most common type of cancer. Endoscopy is the most important factor in the early diagnosis of this disease. Endoscopic examination of the midge and biopsy specimens are used to diagnose pathological examinations. It is observed that half of the people who have this disease are late in the diagnosis and doctors can not apply any treatment (Lambert, 2002). The most common sites of this disease in the world are far-east countries such as Japan and China. In Japan, people who get stomach cancer account for about 30% of other cancer diseases. In the United States, the number of people with stomach cancer is increasing every year (Internet, 2015), (Internet: Cancer Facts and Statictics, 2015). According to research conducted worldwide, 26% of males and 11% of females had gastric cancer. Stomach cancer is located in the third after the lungs and breast cancer in women and second place after the lung cancer in men. According to the statistics done in our country, it is estimated that the number of new gastric cancer patients is about 30 thousand per year (Fujioka, 2004). Stomach cancer is a type of cancer which spreads rapidly and also leads to death when the patient is diagnosed late (Tannapfel, 2001). Stomach cancer usually begins with ulcer and gastritis complaints. Cancer can affect lymph nodes and other peripheral organs (Tolbert, 1999). Machine learning techniques are widely used in computer assisted analysis of histopathological stomach cancer images. In the literature, machine learning techniques such as Bayesian Networks (BN), Decision

Trees (DT), Artificial Neural Networks (YSN), and Support Vector Machines (SVM) have been extensively applied in cancer surveys for the development of predictive models with effective outcomes (Kourou, 2015) An important cause of gastric cancer is H. pylori infection. There are many studies on machine learning techniques on other types of cancer besides stomach cancer in the literature (Korkmaz, 2015), (Korkmaz and Poyraz, 2014), (Korkmaz, S. A., Korkmaz, M. F., and Poyraz, 2016), (Korkmaz, S. A and Korkmaz, M. F. 2015), (Korkmaz, S. A. and Eren, H. 2013), (Korkmaz, 2016), (Korkmaz, 2015), (Korkmaz, 2018). Machine learning techniques have also been used to classify more diverse data analyzes (KORKMAZ, 2017), (Korkmaz and Poyraz 2016). But, we will examine computer-aided studies of stomach cancer in this article. In Literature, there are computer assisted studies in machine learning techniques in stomach cancer diagnosis.

Related Work

In this article, 13 studies in the literature on stomach cancer were reviewed. The first study (Korkmaz and Binol, 2017) proposed a computer-aided study to help diagnose stomach cancer early and reduce mortality rates. For this purpose, stomach cancer microscope images were taken from Pathology laboratory of Fırat University Medical Faculty. These images feature the Local Binary Patterns (LBP) and Histogram of Oriented Gradients (HOG). The dimensions of these computed features are Sammon mapping, Stochastic Neighbor Embedding (SNE), Isomap, Classical multidimensional scaling (MDS), Local Linear Embedding (LLE), Linear Discriminant Analysis (LDA), t- Distributed Stochastic Neighbor Embedding and Laplacian Eigenmaps are reduced by size reduction techniques. Artificial neural networks (ANN) and random forest (RF) classifiers were applied to these features which were reduced in size. It has been suggested that the best classification performances are found with the LBP_MDS_ANN and LBP_LLE_ANN methods.

In the second study (Korkmaz, S. A., Bínol, H., Akçiçek, A., and Korkmaz, M. F. 2017), a study for the early diagnosis of gastric cancer was proposed. For this, a total of 180 stomach image cells, normal, benign and malignant, were obtained. Of the 60 normal, 60 benign and 60 malignant stomach images, 90 were used for educational purposes and 90 were used for educational purposes. The histograms of oriented gradients (HOG) properties of these images were calculated. High-dimensional HOG features were reduced to lower dimensions by Linear Discriminant Analysis (LDA). After applying the LDA method, Artificial Neural Network (ANN) classifier was used. The images were found as 88.9% with ANN classifier. This result has been compared with some studies in the literature. It has been stated that the result obtained provides higher performance. It has also been suggested that this result in a shorter time.

In the third study (Korkmaz, S. A., Akçiçek, A., Bínol, H., and Korkmaz, M. F., 2017), histograms of oriented gradients (HOG) were used for early detection of gastric cancer. These HOG properties are found by the curve of the HOG properties. Bins and h histogram values were subtracted from the histogram plot. Bandwidth ranges were obtained by using h and bins values of normal, benign and malign images. The h values of normal and benign stomach images obtained were higher than malign gastric images. In one, it was suggested that the h values of the normal stomach image are higher than the benign stomach image.

In the fourth study (Korkmaz, 2018), Local Binary Pattern (LBP) features of images for early detection of gastric cancer were found. These properties were reduced to lower dimensions by the Locality Preserving Projections (LPP) method. The property values obtained after this process are classified by Random Forest (RF), Naive Bayes (NB), and Artificial Neural Networks (ANN) classifiers. It is stated that the highest classification performance is 96.29% with ANN classifier and the lowest classification performance is 70% with NB classifier. Moreover, it is stated that the feature size used when finding the highest performance with ANN is lower than the feature size used with other classifiers.

In the fifth study (Korkmaz, S. A. and Esmeray, F. 2018), Maximally Stable Extremal Regions (MSER) properties of stomach images for early diagnosis of gastric cancer were calculated. Discrete Fourier Transform (DFT), Local Tangent Space Alignment (LTSA) and Neighborhood Preserving Embedding methods have been applied to reduce the size to the calculated high dimensional MSER properties. The Random Forest (RF) classifier was applied to these low dimensional feature values. It has been stated that a higher classification result is obtained compared to other classifiers in the literature.

In the Sixth Study (Sasaki, 2010), S. Yoshihiro and colleagues studied a computerized system to predict risk factors for stomach cancer. Digital endoscopy images of patients with H. pylori bacteremia were studied in the system. Three parameters have been used to classify the gastric mucosa.The data obtained from this class is processed by

Bayes theorem and output is obtained. This study sheds light on the identification of patients at high risk for endoscopies.

In the seventh study (Ahmadzadeh, 2013), D. Ahmadzadeh and colleagues developed a stomach cancer diagnosis system using the local pattern algorithm and the DSM (Decision Supporting Machine) method. In the advanced system, a system is obtained that corrects early cancer after noise reduction, feature extraction, feature identification, classification steps.55 volunteer patients were randomly selected. The diagnostic accuracy rate was 91.8%. The authors suggested that it is a system that helps experts save time and money.

In the eighth study (Garcia, 2017), Garcia and colleagues used Deep Convolutional Neural Networks to suggest an approach for automated tumor-infiltrating lymphocytes on immunohistochemical images of gastric cancer. The accuracy rate of this study was 96.88%.

In the ninth study (Zhang, 2017), authors used a concurrent model called the Gastric Precancerous Disease Network (GPDNet) to distinguish between erosion, ulcer and polyp classes using convolutional neural networks (CNN). The classification rate with GPDNet was 88.90%.

The tenth article (Shichijo, 2017), established the convulsion nerve network (CNN) and assessed its ability to diagnose Helicobacter pylori gastritis infection. The first deep CNN has 22 layers. A total of 32,208 images, positive or negative, were used for the education of H. Pylori. Another CNN was trained using images classified according to 8 anatomic regions. For the test, 11,481 histopathological stomach images were used. Sensitivity, specificity, accuracy and diagnostic time for the first CNN were 81.9%, 83.4%, 83.1% and 198 s respectively. For secondary CNN, 88.9%, 87.4%, 87.7% and 194 s respectively are obtained. A higher accuracy result was obtained with the secondary CNN. For 23 endoscopists, these values were 79.0%, 83.2%, 82.4% and 230 ± 65 minutes respectively.According to endoscopists, H. pylori gastritis can be diagnosed more precisely and in a shorter time using CNN.

In the eleventh study (Bollschweiler, 2004), artificial neural networks (ANN) were used to estimate 4302 patients with lymph node metastases with gastric cancer. And, a marine computer program (MCP) was developed. ANN was compared with MCP. The authors suggest that the predictive value for lymph node metastasis varies in each of the lymph node metastases. This variation is between 42% and 70% for MCP and between 64% and 64% for ANN. The classification rate of YSA was found to be 93%.

In the twelfth study (Cosatto, 2013), haematoxylin and eosin stained gastric tissue samples were examined. And in these cases, a machine-learning based computer system that can detect cancer is recommended. In the computer system, high-level medically relevant features such as nuclei and glands are used. The Multilevel Learning Framework (MIL) classifier is used to classify the data set. The system has been trained and tested with a large-scale dataset of 26K textures. 1'196 positive tissue and 8'558 patients from 16'692 negative tissue. A test data consisting of 4,168 patients was obtained from 582 positive tissues and 8125 negative tissues. The accuracy performance of the system was 96% with AUC.

In the thirteenth study Akbari and colleagues (Akbari, 2011) developed a stomach cancer diagnosis system using infrared ultra-spectral imaging. This study was conducted by selecting patients with gastric cancer. The spectral features were extracted from cancerous and normal tissues, and the comparison was made and the detection of the cancerous regions was performed by using the KDM method with the spectral diagram.

Conclusions

Stomach cancer is a rapidly developing and spreading type of cancer (Tannapfel, 2001). It usually starts in the form of ulcer complaints. Stomach cancer can affect the organs and lymph glands (Tolbert, 1999). It can be spread by direct neighbors, lymphatic, blood and intraabdominal (Siddiqi, 2008). The stomach tumor may grow through the outer layer of the miter and extend into the surrounding organs, such as the pancreas, esophagus or intestine (Mikami, 2004).
Stomach cancer cells can spread by blood metastases to the liver, lungs, and other organs (Ahmad, 2007). Cancer cells can also spread to all the lymph glands in the body through the lymphatic system (Fenoglio, 2000). Cancer first starts at the center of the cells that make up the tissues, and at the same time, these tissues bring the organs of the body to the bloom (Cappell, 2002). For a normal individual, the cells grow, develop, and the body is divided to create cells that are new in need. Cells are sufficiently digested and digested by the cell when they are old and

are killed and replaced by new ones. But sometimes this process is in the wrong direction. So much so that, despite the fact that the body does not need much, new cells form and the old cells that should die do not die. These excess cells can eventually turn into tumor masses called tumors. Tumors may be benign or malignant. For this reason, the early diagnosis and diagnosis of gastric cancer has become imperative in cancer research because it may facilitate the subsequent clinical treatment of patients. Separation of gastric cancer patients into normal, low and high groups has become important in bioinformatics and biomedical fields. This has led to an increase in the practice of machine learning (ML) methods for early cancer diagnosis in the literature. Machine learning methods have been used to model the progression and treatment of stomach cancer. ML methods have been used to detect complex cell characteristics in cancer images. Artificial Neural Networks (ANN) ,Bayesian Networks (BNS), Random Forest (RF), Support Vector Machines (SVM), Decision Trees (DT), Linear Discriminant Analysis (LDA), Sammon mapping, Stochastic Neighbor new algorithms have been proposed using various machine learning techniques such as Embedding (SNE), Isomap, Classical multidimensional scaling (MDS), and Local Linear Embedding (LLE), which is used to diagnose stomach cancer early. Although machine learning techniques for gastric cancer have been widely applied and ultimately yielded high classification performances, an appropriate level of validation is required to take these methods into account in daily clinical treatment and practice. In this study, the methods used in algorithms for early diagnosis of stomach cancer and the classification ratios are described. In the advanced algorithms, various different features and image data are used. As a result, in this article, ML methods for gastric cancer research are increasing. For this reason, published articles have been presented to model the risk of stomach cancer.

References

Tannapfel, A., Schmelzer, S., Benicke, M. et al. (2001). Expression of the p53 homologues p63 and p73 in multiple simultaneous gastric cancer. The Journal of Pathology, 195, 163–170. 18.

Tolbert, D., Fenoglio-Preiser, C., Noffsinger, A. et al. (1999). The relation of p53 gene mutations to gastric cancer subsite and phenotype. Cancer Causes and Control, 10, 227–231. 19.

Siddiqi, A. M., Li, H., Faruque, F. et al. (2008). Use of hyperspectral imaging to distinguish normal, precancerous, and cancerous cells. Cancer Cytopathology, 114(1), 13–21. 20.

Mikami, T., Sasaki, Y., Fukuda, S., Hada, R., Munakata, A. (2004). Computer-aided diagnosis of superficial type early oesophageal cancer by image processing on ordinary endoscopic pictures. Gastrointestinal Endoscopy, 59, 258. 21.

Ahmad, Z., Idrees, R., Sahar, A. N., Ahmed, R., Ahsan, A., Asghar, N. (2007). Gastric carcinoma: typing, staging, lymph node and resection margin status on gastrectomy specimens. Journal of the College of the Physicians and Surgeons Pakistan, 17(9), 539. 22.

Fenoglio-Preiser, C., Carneiro, F., Correa, P. (2000). Tumours of the stomach, Pathology and Genetics of Tumors of the Digestive System. International Agency for Research on Cancer, 37–52. 23.

Cappell, M. S., Friedel, D. (2002). The role of esophagogastroduodenoscopy in the diagnosis and management of upper gastrointestinal disorders. Medical Clinics of North America, 86, 1165–216.

Lambert, R., Guilloux, A., Oshima, A., Pompe-Kirn, V., Bray, F., Parkin, M., Ajiki, W., Tsukuma, H. (2002). Incidence and mortality from stomach cancer in Japan, Slovenia and the USA. International Journal Of Cancer, 97, 811–818.

İnternet: Cancer Facts and Figures. (2015). American Cancer Society. URL: http://www.webcitation.org/query?url=http%3A%2F%2Fwhyquit.+com%2Fstudies%2F2003_acs_cancer_facts.+pdf&date=2016-02-11. Son Erişim Tarihi : 11.02.2016.

İnternet: Cancer Facts and Statictics. (2015). American Cancer Society. URL:http://www.webcitation.org/query?url=http%3A%2F%2Fwww.+cancer.+org%2Fresearch%2Fcancerfactsstatistics%2Fcancerfactsfigures2015%2F&date=2016-02-11. Son Erişim Tarihi : 11.02.2016 .

Fujioka, N., Morimoto, Y., Arai, T., Kikuchi, M. (2004). Discrimination between normal and malignant human gastric tissues by Fourier transform infrared spectroscopy. Cancer Detection and Prevention, 28(1), 32–36.

Tannapfel, A., Schmelzer, S., Benicke, M. et al. (2001). Expression of the p53 homologues p63 and p73 in multiple simultaneous gastric cancer. The Journal of Pathology, 195, 163–170.

Tolbert, D., Fenoglio-Preiser, C., Noffsinger, A. et al. (1999). The relation of p53 gene mutations to gastric cancer subsite and phenotype. Cancer Causes and Control, 10, 227–231.

Kourou, K., Exarchos, T. P., Exarchos, K. P., Karamouzis, M. V., & Fotiadis, D. I. (2015). Machine learning applications in cancer prognosis and prediction. Computational and structural biotechnology journal, 13, 8-17.

Korkmaz, S. A., & Poyraz, M. (2015). Least square support vector machine and minumum redundacy maximum relavance for diagnosis of breast cancer from breast microscopic images. Procedia-Social and Behavioral Sciences, 174, 4026-4031.

Korkmaz, S. A., & Poyraz, M. (2014). A New Method Based for Diagnosis of Breast Cancer Cells from Microscopic Images: DWEE—JHT. Journal of medical systems, 38(9), 92.

Korkmaz, S. A., Korkmaz, M. F., & Poyraz, M. (2016). Diagnosis of breast cancer in light microscopic and mammographic images textures using relative entropy via kernel estimation. Medical & biological engineering & computing, 54(4), 561-573.

Korkmaz, S. A., & Korkmaz, M. F. (2015). A new method based cancer detection in mammogram textures by finding feature weights and using Kullback–Leibler measure with kernel estimation. Optik-International Journal for Light and Electron Optics, 126(20), 2576-2583.

Korkmaz, S. A., & Eren, H. (2013, December). Cancer detection in mammograms estimating feature weights via Kullback-Leibler measure. In Image and Signal Processing (CISP), 2013 6th International Congress on (Vol. 2, pp. 1035-1040). IEEE.
Korkmaz, S. A., Korkmaz, M. F., Poyraz, M., & Yakuphanoglu, F. (2016). Diagnosis of breast cancer nano-biomechanics images taken from atomic force microscope. *Journal of Nanoelectronics and Optoelectronics*, *11*(4), 551-559.
Korkmaz, S. A., Poyraz, M., Bal, A., Binol, H., Özercan, I. H., Korkmaz, M. F., & Aydin, A. M. (2015). New methods based on mRMR LSSVM and mRMR KNN for diagnosis of breast cancer from microscopic and mammography images of some patients. *International Journal of Biomedical Engineering and Technology*, *19*(2), 105-117.
Korkmaz, S. A. (2018). DETECTING CELLS USING IMAGE SEGMENTATION OF THE CERVICAL CANCER IMAGES TAKEN FROM SCANNING ELECTRON MICROSCOPE. The Online Journal of Science and Technology-January, 8(1).
KORKMAZ, S. A. (2017). VARIATION OF DRIVING CONCENTRATION WITH DRIVER PERCEPTION THROUGH IN-CAR VIEW ROAD SCENE AS VISUAL STIMULANT. The Online Journal of Science and Technology-July, 7(3).
Korkmaz, S. A., & Poyraz, M. (2016, October). Path planning for rescue vehicles via segmented satellite disaster images and GPS road map. In Image and Signal Processing, BioMedical Engineering and Informatics (CISP-BMEI), International Congress on (pp. 145-150). IEEE.
Korkmaz, S. A., & Binol, H. (2017). Analysis of Molecular Structure Images by using ANN, RF, LBP, HOG, and Size Reduction Methods for early Stomach Cancer Detection. Journal of Molecular Structure.
Korkmaz, S. A., Bínol, H., Akçiçek, A., & Korkmaz, M. F. (2017, September). A expert system for stomach cancer images with artificial neural network by using HOG features and linear discriminant analysis: HOG_LDA_ANN. In Intelligent Systems and Informatics (SISY), 2017 IEEE 15th International Symposium on (pp. 000327-000332). IEEE.
Korkmaz, S. A., Akçiçek, A., Bínol, H., & Korkmaz, M. F. (2017, September). Recognition of the stomach cancer images with probabilistic HOG feature vector histograms by using HOG features. In *Intelligent Systems and Informatics (SISY), 2017 IEEE 15th International Symposium on* (pp. 000339-000342). IEEE.
Korkmaz, S. A. (2018). LBP Özelliklerine Dayanan Lokasyon Koruyan Projeksiyon (LPP) Boyut Azaltma Metodunun Farklı Sınıflandırıcılar Üzerindeki Performanslarının Karşılaştırılması. Sakarya University Journal of Science, 22(4), 1-1.
Korkmaz, S. A., Esmeray, F. (2018). "Classification with Random Forest Based on Local Tangent Space Alignment and Neighborhood Preserving Embedding for MSER features: MSER_DFT_LTSA-NPE_RF." *International Journal of Modern Research in Engineering and Technology*, 3.2:31-37.
Sasaki, Y., Hada, R., Yoshimura, T., Hanabata, N., Mikami, T., & Fukuda, S. (2010, September). Computer-aided estimation for the risk of development of gastric cancer by image processing. In IFIP International Conference on Artificial Intelligence in Theory and Practice (pp. 197-204). Springer, Berlin, Heidelberg.
Ahmadzadeh, D., Fiuzy, M., & Haddadnia, J. (2013). Stomach Cancer Diagnosis by Using a Combination of Image Processing Algorithms, Local Binary Pattern Algorithm and Support Vector Machine. Journal of Basic and Applied Scientific Research www. textroad. com.
Garcia, E., Hermoza, R., Castanon, C. B., Cano, L., Castillo, M., & Castanñeda, C. (2017, June). Automatic Lymphocyte Detection on Gastric Cancer IHC Images Using Deep Learning. In Computer-Based Medical Systems (CBMS), 2017 IEEE 30th International Symposium on (pp. 200-204). IEEE.
Zhang, X., Hu, W., Chen, F., Liu, J., Yang, Y., Wang, L., ... & Si, J. (2017). Gastric precancerous diseases classification using CNN with a concise model. PloS one, 12(9), e0185508.
Shichijo, S., Nomura, S., Aoyama, K., Nishikawa, Y., Miura, M., Shinagawa, T., ... & Tada, T. (2017). Application of Convolutional Neural Networks in the Diagnosis of Helicobacter pylori Infection Based on Endoscopic Images. EBioMedicine, 25, 106-111.
Bollschweiler EH, Monig SP, Hensler K, et al. (2004). Artificial neural network for prediction of lymph node metastases in gastric cancer: a phase II diagnostic study. Ann Surg Oncol, 11:506-11.
Cosatto, E., Laquerre, P. F., Malon, C., Graf, H. P., Saito, A., Kiyuna, T., ... & Kamijo, K. I. (2013, March). Automated gastric cancer diagnosis on h&e-stained sections; ltraining a classifier on a large scale with multiple instance machine learning. In Medical Imaging 2013: Digital Pathology (Vol. 8676, p. 867605). International Society for Optics and Photonics.
Akbari, H., Uto, K., Kosugi, Y., Kojima, K., Tanaka, N. (2011). Cancer detection using infrared hyperspectral imaging. The Official Journal of The Japanese Cancer Association, 102(4), 852-857.

NUMERICAL INVESTIGATION OF MACHINING CHARACTERISTICS OF HASTELLOY-X

Mehmet Alper Sofuoğlu[1*], Fatih Hayati Çakır[2], Selim Gürgen[2], Sezan Orak[1], Melih Cemal Kuşhan[1]

[1]Eskişehir Osmangazi University, Mechanical Engineering Department, 26480, Eskişehir, Turkey
[2]Vocational School of Transportation, Anadolu University, 26470, Eskişehir, Turkey
Corresponding author:*asofuoglu@ogu.edu.tr

Abstract: Nickel-based alloys provide high corrosion resistance and high-temperature strength but these alloys possess poor machinability. Hastelloy-X is one of the nickel-based alloys. There are many studies about finite element modeling of nickel-based alloys but studies of Hastelloy- X are limited. In the present work, machining characteristics of Hastelloy-X were investigated and a numerical model was developed for the turning operation of Hastelloy-X. Cutting speed of 40 m/min and feed rate 0.1 mm/rev were taken into consideration in the operations and the results were evaluated considering process outputs such as cutting forces, cutting temperature and effective stresses The proposed model is applicable for the turning operation of Hastelloy-X.
Keywords: Hastelloy-X, turning operation, DEFORM-2D

Introduction

Modern product designs and manufacturing technologies are changing day by day. In this context, there are many innovative methods used in manufacturing and many methods applied in improving manufacturing processes. Some of the developed methods (3d printing, etc.) work differently according to the traditional manufacturing methods. The use of nickel alloys is important with the development of aviation and the energy sector. For this reason, it's machining needs to be investigated thoroughly.

Nickel-based alloys are extensively used because of their advantages in the spacecraft engines and gas turbine components These alloys have some important benefits: being heat-resistant, retaining their high mechanical and chemical properties at elevated temperatures, having high melting temperatures, enhanced corrosion resistance as well as resistance to thermal fatigue, thermal shock, creep, and erosion (Akıncıoğlu et al., 2016; Ulutan and Özel, 2010). However, these alloys have some problems in machining because they have an austenitic matrix and similar with stainless steels, work hardening is rapidly seen during machining. Also, increase in tool flank wear, cratering and notching are observed at elevated temperatures. (Choudhury and El-Baradie, 1998).

According to literature studies, machining of Hastelloy was not sufficiently investigated. Furthermore, previous studies focus on the statistical models based on experimental results. Hastelloy is a candidate material to be investigated through numerical studies in order to improve the machining operations and reduce the experimental expenses. In the present work, a numerical model was developed for the turning operation of Hastelloy-X. The verification of the numerical model was performed comparing the maximum insert cutting temperatures with the experimental results. In addition to these outputs, effective stresses and cutting forces were discussed.

Materials and Methods

In this work, 2D finite element model for orthogonal cutting is developed in DEFORM-2D program. In this context, Langrange finite element formulation is used by continuous and adaptive meshing method. Dry cutting conditions are used in the tests. 2-dimensional simulation studies in machining are preferred because of their simplicity and solution time comparing to 3D simulation studies. Hastelloy-X is used as material. The workpiece is assumed as plastic. The tool is assumed rigid in developed model. In the simulations, ultrasonic vibration is applied at 20 kHz and 20 microns in the cutting direction. The feed rate is taken as 0.1 mm/rev. Cutting speed is selected as 40 m / min. Mesh convergence is obtained. 2500 elements for Hastelloy-X and 1500 elements for tungsten carbide tool are determined and results are not changed above the number of these elements. With the remeshing operation, the number of mesh is increased in the cutting region at the time of machining, thereby facilitating the convergence of the solution. In the simulations, X is the cutting direction and Y is the feed direction (Figure 1).

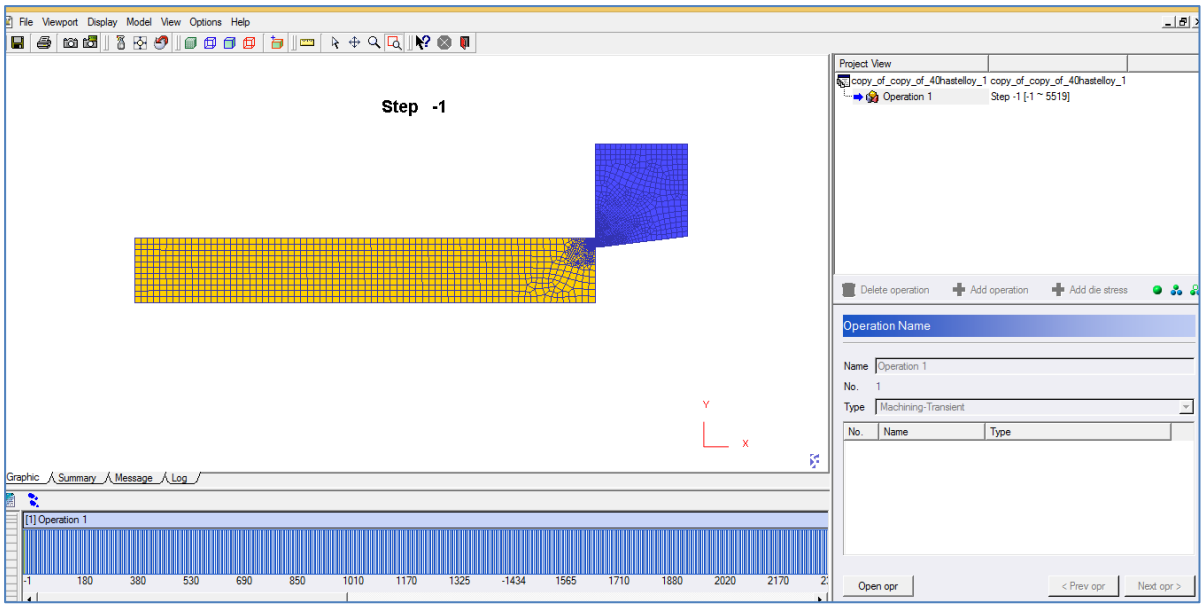

Figure 1. A snapshot from DEFORM-2D

The initial temperature of the workpiece is set as 20 ° C. The Johnson Cook (JC) material model is used to model the workpiece. In high strain situations, JC model produces reasonable results. This model shows the precision of the strain rate in the material. Equations for this model are given in Eq. 1-2. Table 1 shows the coefficients of this model.

$$\sigma = \left(A + B\varepsilon^{n}\right)\left(1 + C\ln\left(\frac{\dot{\varepsilon}}{\dot{\varepsilon}_0}\right)\right)\left(1 - T^{*}\right)^{m} \quad (1)$$

$$T^{*} = \frac{\left(T - T_{room}\right)}{\left(T_{melt} - T_{room}\right)} \quad (2)$$

$\frac{\dot{\varepsilon}}{\dot{\varepsilon}_0}$: strain rate / reference strain rate

n : strain rate sensitivity for the material

T_{room}: Room temperature

T_{melt}: Melting temperature of workpiece

A, B, C, m : Material constants

Table 1. Johnson Cook coefficients for materials used in simulations

	A(MPa)	B(MPa)	C	n	m	$\dot{\varepsilon}_0$
Hastelloy-X	380	1200	0.012	0.55	2.5	0.001

Johnson Cook material models are based on many tests and coefficients are determined by curve fitting techniques. Split Hopkinson compression tests are performed at different strain rates and temperatures in order to determine the model coefficients. The coefficients used in this study were given in Table 1. These values were reported in literature by Abotula et al. 2011.The material of the cutting tool is WC + TiAlN coating and cutting tool has a rake angle of 0° and a clearance angle of 7°. The tool tip hone radius is 0.02 mm.

Different damage models and fracture criteria have been defined in the literature in order to predict of chip shapes and cutting forces. Cockcroft & Latham fracture criterion is selected in this study. Thus, the morphology of serrated

chips could be observed. Similar approach was used before the study performed in the literature (Çakır et al., 2015).

Friction model and coefficients are determined by using different studies in the literature (Özel and Ulutan, 2012). The friction zones determined during the machining of Hastelloy-X are given in Fig 2. The friction zone is divided into two sections. The part of the tool hone radius is taken as shear friction zone and the value is 0.9. The second region is defined on the top of this region to the portion where the chips are rubbing the cutting tool. This region is determined as coulomb friction and the value is taken as 0.7.

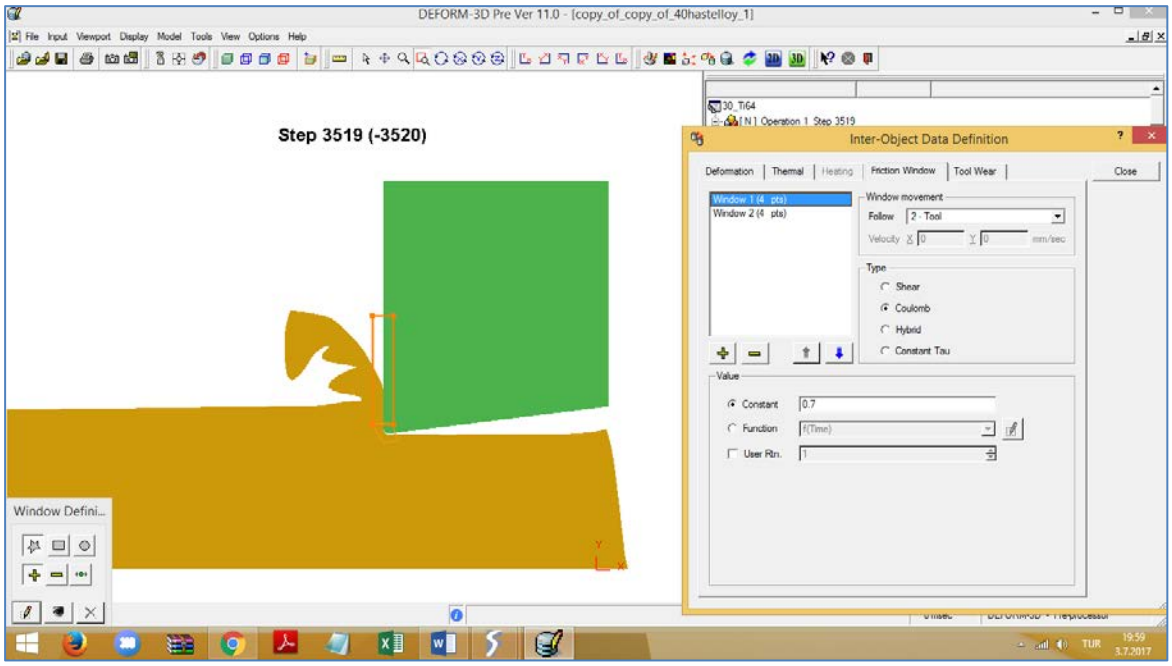

Figure 2. Friction zones determined during the machining of Hastelloy-X

Material properties for Hastelloy-X were given at Table 2. These properties have been determined with literature studies and in the producers catalogs as follows (Aghaie and Golaizi, 2008; Abotula et al., 2014).

Table 2. Mechanical and thermal properties of Hastelloy-X used in simulations

	Hastelloy-X
Modulus of Elasticity (MPa)	25^0C-205000 200^0C-198000 400^0C-187000 600^0C-173000 800^0C-157000
Thermal expansion ($mm.mm^{-1}.{}^oC^{-1}$)	20^0C-1.3e-5 200^0C-1.35e-5 400^0C-1.41e-5 500^0C-1.43e-5
Thermal conductivity ($W.m^{-1}.{}^oC^{-1}$)	25^0C-9.2 200^0C-14.1 600^0C-21.9 800^0C-24.7
Emissivity coefficient	0.85
Poisson's ratio	0.32

Results and Discussion

Mean cutting forces, maximum cutting insert temperatures and maximum effective stress values are investigated in the numerical study.

Maximum cutting insert temperatures

Numerical results have been compared to experimental study to verify the developed numerical model. Maximum insert temperatures at the cutting edge measured during machining of Hastelloy-X alloy is given in Table 3. Results of experimental study and numerical results are compared. It can be said that the developed numerical model can predict cutting insert temperature within a range of 20% error. In this context, it is observed that the numerical model satisfies the experimental results.

Table 3. Maximum insert cutting temperatures

	Experimental (˚C)	Simulation (˚C)
Conventional turning	208.2	167.73

Mean cutting forces

Numerically determined mean cutting forces for Hastelloy-X are given in Figure 3. The force in the X direction is about 110 N and the force in the Y direction is about 30 N.

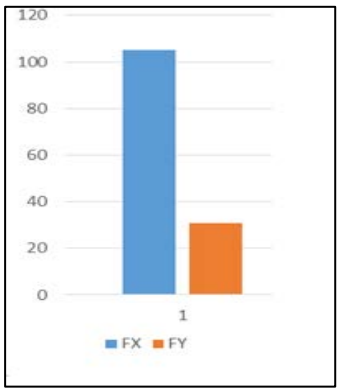

Figure 3. Cutting forces (N) for Hastelloy-X

Effective stresses

Effective stress distributions in turning of Hastelloy-X is shown in Figure 4. In conventional turning, the maximum effective stress is nearly 1600 MPa.

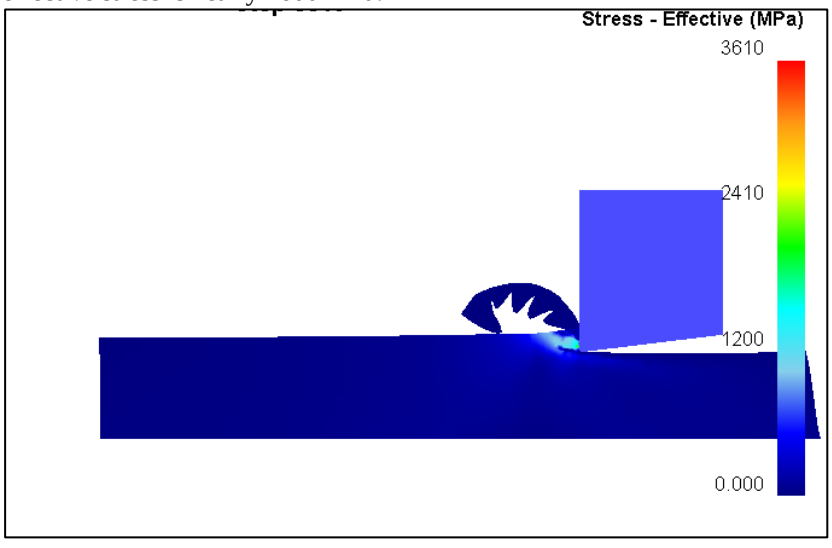

Figure 4. Effective stress distribution in turning of Hastelloy-X

Conclusion

In this study, machining of Hastelloy-X is modelled using finite element method. Mean resultant cutting force in the simulations is nearly 110 N. Maximum effective stress is approximately 1600 MPa. Maximum insert temperature is 167 ^{0}C which exhibits good agreements with the experimental results.

Acknowledgements

This work was financially supported by the Scientific and Technological Research Council of Turkey (TÜBİTAK Project #215M382) and the Research Fund of Eskişehir Osmangazi University (ESOGU BAP Project #2016-1086). The authors M.A.Sofuoğlu and S.Gürgen acknowledge the support of TÜBİTAK under programs 2228 and 2211 respectively.

References

Abotula, Sandeep, Shukla, Arun and Chona, Ravi. (2011). Dynamic Constitutive Behavior of Hastelloy X under Thermo-Mechanical Loads. *Journal of Materials Science* 46 (14): 4971–79.

Abotula, S., Heeder, N., Chona, R. and Shukla, A. (2014). Dynamic Thermo-Mechanical Response of Hastelloy X to Shock Wave Loading. *Experimental Mechanics* 54 (2): 279–91.

Aghaie-Khafri, M. and Golarzi, N.,(2008). Forming Behavior and Workability of Hastelloy X Superalloy during Hot Deformation. *Materials Science and Engineering*: A 486 (1–2): 641–47.

Akıncıoğlu, S, Gökkaya, H and Uygur, İ., (2016) The effects of cryogenic-treated carbide tools on tool wear and surface roughness of turning of Hastelloy C22 based on Taguchi method", *Int. J. Adv. Manuf. Technol.*, vol. 82, no. 1–4, pp. 303–314.

Çakır, Fatih Hayati, Gurgen, Selim, Sofuoglu, M.A. Celik, O.N. and Kushan, M.C., (2015). Finite Element Modeling of Ultrasonic Assisted Turning of Ti6Al4V Alloy. *Procedia - Social and Behavioral Sciences* 195 (Temmuz): 2839–48. doi:10.1016/j.sbspro.2015.06.404.

Choudhury, I., and El-Baradie, M., (1998) Machinability of nickel-base super alloys: a general review, *J. Mater. Process. Technol.*, vol. 77, no 1–3, pp. 278–284

Özel, Tuğrul, Sima, M. and Srivastava, A.K., (2010). Finite element simulation of high speed machining Ti-6Al-4V alloy using modified material models. *Transactions of the NAMRI/SME* 38: 49–56.

Özel, T., and Ulutan, D., (2012). Prediction of Machining Induced Residual Stresses in Turning of Titanium and Nickel Based Alloys with Experiments and Finite Element Simulations. *CIRP Annals - Manufacturing Technology* 61 (1): 547–50.

Ulutan, D. and Ozel, T., (2011) Machining induced surface integrity in titanium and nickel alloys: A review, *Int. J. Mach. Tools Manuf.*, vol. 51, no 3, pp. 250–280

PRODUCTION OF FLAME RETARDANT WOOD COMPOSITES BY USING HUNTITE AND HYDROMAGNESITE

Hüsnügül YILMAZ ATAY

İzmir Katip Çelebi University, Department of Material Science and Engineering, 35620 Çiğli İzmir Turkey

hgulyilmaz@gmail.com

Abstract: In this study, it is aimed to provide resistance to fire as seen the biggest obstacle to the wood that until 60-70 years of our lives in the almost forgotten today, even though it is frequently used in every aspect both as building material requirements of wood with furniture that we use in all areas of daily life, decorative items, in front of which is related to the use of the kitchen tools or for decoration. In this study, inorganic Turkish huntite and hydromagnesite mineral was used as an additive flame retardant material during the production of wood composite. Primarily for the production of composite material, the mineral was crushed and ground. Mineralogical structure was determined by XRF, XRD and SEM-EDS devices. Thermal behavior was observed by DTA-TG apparatus. UL-94 test apparatus was used to determine flame retardant properties of the wood composites. In the preparation of the composites, changing of the mineral additive rate was considered. In this way the additive amount dependence of fireproof composite was observed to evaluate the optimum amount of mineral.
Keywords: Wood, Composites, Flame retardant, UL-94.

Introduction

A porous, fibrous, and anisotropic material, wood is a versatile composite material containing cellulose, hemicellulose and lignin. Although it is one of the most important structural materials, it is almost forgotten in all kind of industries nowadays because of mainly its flammable property. In fact wood is an environmentally-friendly natural material and has many good properties such as good damping characteristics, thermal insulation, relatively low price and low specific gravity. In addition, wood can gain higher hardness, better weather resistance, abrasion resistance and higher strength by modification (Shah et al., 2017).

Porosity is another serious drawback of wood. The pores can interact with water due to the presence of hydrophilic groups present on its surface. Moreover the porous geometry provides channels for the flow of liquids and this which causes increased activity of microorganism in the presence of high moisture content and affects the dimensional stability of wood structures. Nevertheless, this may be converted to an advantage as the pores can be filled with the different functional materials (Shah et al, 2017; Leslaw, 2016).

The modification of wood is a topic that needs further investigations. Mostly modifications have been applied to the surface of the natural wood. This modified wood is effectively protected against degradation, has a higher life span and better mechanical properties compared to natural wood. Such as, a protective coating made of carnauba wax particles and zinc oxide was developed for the protection from both water and ultraviolet radiation (Lozhechnikova et al, 2017). In another investigation, hierarchical titania structures were constructed on wood followed by modification with perfluorodecyltriethoxysilane to produce a hydrophobic surface. Furthermore, a composite coating of titania/silica was also produced by hydrothermal process for the protection of wood (Liu et al, 2015). Shah et al. presented another method to render superhydrophobic properties to the wood (Shah et al., 2017).

In this study instead of modification of a natural wood, a wood composite was produced. This can be called engineered wood and includes a range of derivative wood products which are manufactured by binding or fixing the strands, particles, fibers, or boards of wood, together with adhesives, or other methods of fixation to form composite materials. Those products are used in a variety of applications, from home construction to commercial buildings to industrial products. They are engineered to precise design specifications which are tested to meet national or international standards (Oliveira, A.K.F. & d'Almeida, J.R.M., 2014).

Particle board is one of the engineering wood. It is manufactured from wood chips, sawmill shavings, or even sawdust, and a synthetic resin or other suitable binder, which is pressed and extruded. (Figure 1). Oriented strand board, also known as flakeboard, waferboard, or chipboard, is similar but uses machined wood flakes offering more strength. Particle board is cheaper, denser and more uniform than conventional wood and plywood and is

substituted for them when cost is more important than strength and appearance (Taramian et al, 2007).

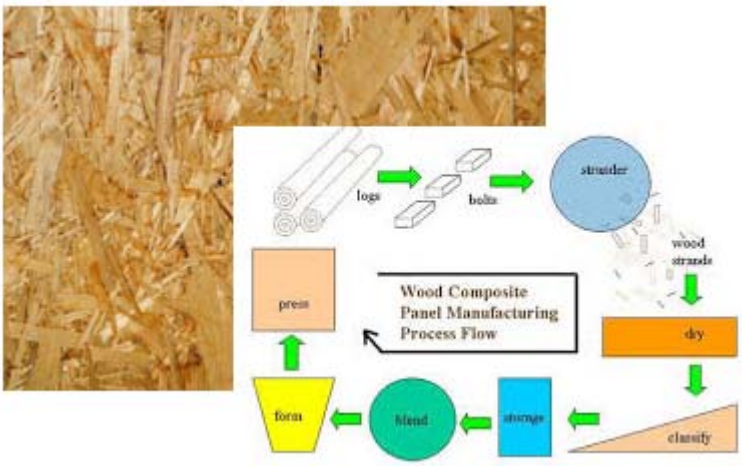

Figure 1. Particle board and munufacturing steps

As mentioned above that particle board are produced by using wood chips, sawmill shavings, or even sawdust. This is in fact an extremely important recycling process. The waste recycling covers several areas of interest such as environmental, engineering, economic and social and this is an important way to ensure sustainability in the world (Moreno, & Saron, 2017; Ng et al, 2014). The wood still is a material of expressive consumption for structural utilization for confection of furnishings, homes, buildings, among others. Packaging and pallets are also important products generated from timber industry. In Europe, around 20% of all sawnwood consumption is used for wooden pallets and packaging, while in Catalonia, northwest of Spain, 85% of the sawnwood is used to manufacture pallets. Conifers species such as pine are the main raw material for manufacture of the pallets (García-Durañona et al, 2016). The use of the pine presents an import environmental advantage due to their source from reforestation. The pine pallets are continuously submitted to high mechanical stress during use that of course lead to the usual break of the structural parts, disabling the entire pallet and generating pine waste wood (Moreno, & Saron, 2017).

A recycled wood composite was manufactured in this study by using huntite and hydromagnesite mineral additives to gain flame retardant property. The term flame retardant subsumes a diverse group of materials which are added to the materials, such as plastics and textiles, and surface finishes and coatings. Flame retardants inhibit or delay the spread of fire by suppressing the chemical or physical reactions in the flame or by the formation of a protective layer on the surface of a material. They may be mixed with the base material (additive flame retardants) or chemically bonded to it (reactive flame retardants) (Haurie et al, 2006; Le Bras et al, 2005). Both Reactive and Additive Flame retardant types can be further separated into several different classes, however two main categories can be seen as following; halogenated and halogen-free flame retardants. Halogen containing flame retardants act in the gas phase and contribute to incompletely burned substances like black smoke and toxic CO which is a highly toxic and nonirritating gas. As CO blocks the oxygen transport of the blood, it can disturb the respiration process immediately. Even though traditional solutions based on halogens have some advantages like low loadings and good retention of mechanical properties, they have also disadvantages compared to mineral flame retardants. Halogen free flame retardants are mostly inorganic fillers used to impart flame retardancy. Most used ones are alum, antimony trioxide, borax, chalk, magnesium oxide or silica. These fillers are usually cheap and in many cases help to improve the mechanical properties and surface appearance of the fabricated article (Kulshreshtha, 2002; Yılmaz Atay & Çelik, 2010).

Huntite and hydromagnesite mineral, one of the flame retardant mineral, has been used as an additive in the production of polymer composites to achieve incombustible property due to its inflammability property. The deposit normally consists of physical blends of two minerals huntite and hydromagnesite with varying ratios in between 40 and 30% huntite and 60 and 70% hydromagnesite The level of impurities is very low, the most important ones are other white carbonate minerals such as aragonite, calcite, and dolomite. Physical densities of huntite ($Mg3Ca(CO3)4$) and hydromagnesite ($Mg4(OH)2(CO3)3.3H2O$) minerals are 2.70 g/cm3 and 2.24 g/cm3, respectively (Yılmaz Atay & Çelik, 2010) . Although this mineral is said to be relatively new as it has entered into the market in 1980s, there are numbers of studies can be seen regarding huntite and hydromagnesite mineral used in polymer composites. However, there are no such studies related with the usage in wood composites.

This study investigated flame retardant behaviors of inorganic mineral huntite and hydromagnesite in wood composites. Primarily for the production of composite material, the mineral was crushed and ground. Mineralogical structure was determined by XRF, XRD and SEM-EDS devices. Thermal behavior was observed by DTA-TG apparatus. Flame retardant property of the wood composites was evaluated by UL-94 test. In the preparation of wood composites, the mineral was added to be used as additives during the production of wood materials. The samples were obtained by changing the mineral additive rate.

Materials and Methods

Fabrication of Composite Materials

The material is received from Isparta region in Turkey. Crushing and grinding steps were performed in Muğla Sıtkı Koçman University Department of Mining Engineering. Grinding was repeated in İzmir Katip Çelebi University Materials Science and Engineering Department with a ball mill to get finer particle size. Mixed and a well representative sample was drawn in each case for detail characterization and beneficiation studies.

Flame retardant wood composites were prepared by reinforcing mineral powders at different ratios into the sawdust. After well-mixing the determined amount of powders and sawdust, each mixtures were moulded under 3 tons of pressure using by a molding machine for preparation of the specimens. Each specimen has 10 mm diameter. Obtained samples and their descriptions are shown in Table 1.

Table 1. Sample codes and descriptions

Sample code	Huntite and Hydromagnesite amount in the mixture (%)
W00H	0
W20H	20
W25H	25
W30H	30
W35H	35
W40H	40
W45H	45
W50H	50
W55H	55
W60H	60

Characterization

A laser diffraction machine from Malvern Instruments, Mastersizer 2000 was used to obtain the particle size distribution of huntite hydromagnesite mineral powders. The thermal behaviors of hydromagnesite and huntite mineral and obtained composite materials were evaluated to observe decomposition and phase formation at a heating rate of 10 ^{0}C/min in the temperature range of 25–700 ^{0}C under air atmosphere by using DTA/TG machine Perkin Elmer. XRF studies were carried out for the identification of mineral phases present with an X-Ray Diffractometer (Amatek Spectro IQII) X-ray diffractometer in İzmir İnstitute of Technology. XRD analysis was performed on a Bruker D2 Phaser system with Ni-filtered Cu-K alpha radiation (k = 1.54 Å). SEM micrographs and EDS analysis were taken with Qanta Feg 250 SEM device with 3 kV accelerating voltage. Flame retardancy tests of the composites were performed by UL 94 technique with the machine of ZLT-ZYS Needle-Flame Tester. The material is conducted to the flame in a specific angle and distance. Extinguishing time of the flame and dripping ability are measured. Set-up of the experiment is shown in Figure 2.

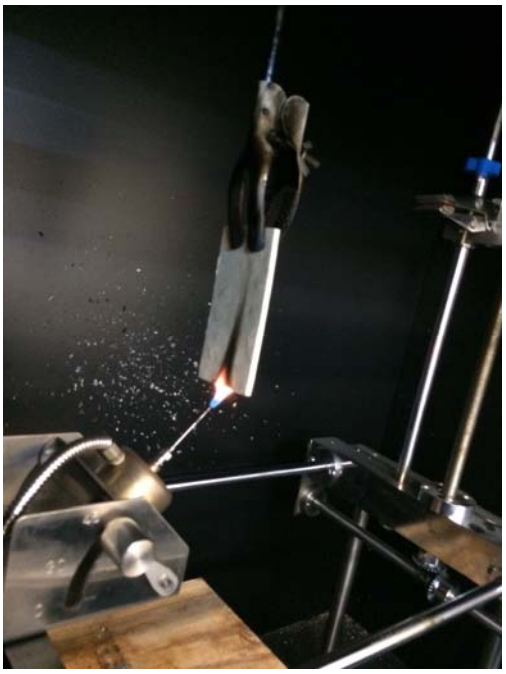

Figure 2. UL-94 flame retardant test experiment.

Results and Discussion

According to X-ray Fluorescence Spectrometry the chemical analysis of the mineral powder is as following; 53.32% Mg, 7.43% Ca, 0.53 Mn, 0.2 Al, 0.2 Ba, 0.1 Fe and 88.42% MgO, 10.4% CaO, 0.4 Al2O3, 0.07 MnO, 0.15 Fe2O3, 0.2 Ba. This results support XRD analysis and also literature information regarding chemical formula of huntite and hydromagnesite and impurities (Kirschbaum, 2001).

To determine the particle size Mastersizer 2000 the size distribution analysis is performed. The size distribution of the three particle sizes is shown in Figure 3. According to this analysis it can be said that mineral particle size is apprx. 10 µ.

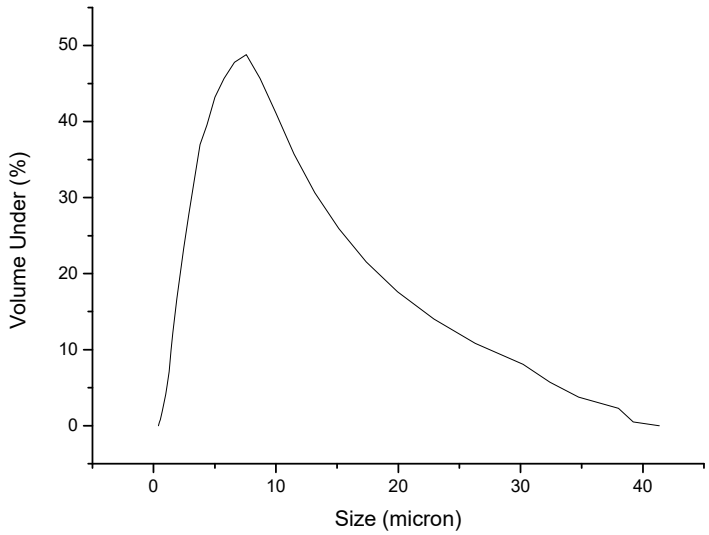

Figure 3. Size distribution of the mineral.

XRD analysis of the received material is shown in Figure 4. It is found from this result that the basic minerals are

hydromagnesite (Mg(CO3)3.3H2O) and huntite (Mg3Ca(CO3)). Magnesite exists as the main impurity in the ore. And the other impurities can be counted dolomite and calcite. The main phases with high intensity are huntite and hydromagnesite. XRD analysis result promotes literature information which stated that the impurities magnesite, aragonite, and calcite phases are accompanying with huntite and hydromagnesite (Kirschbaum, 2001).

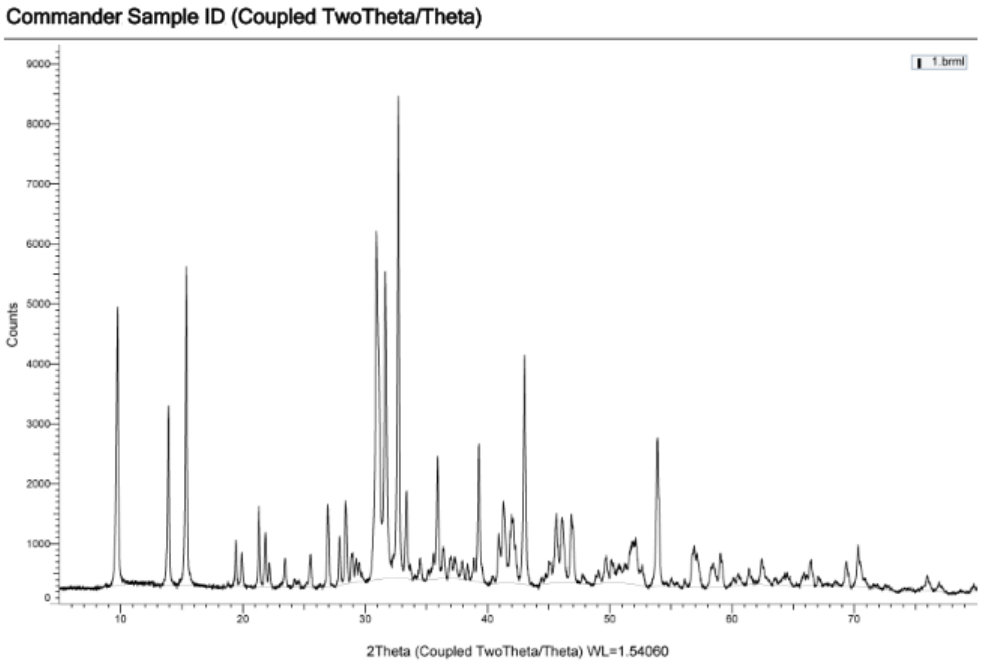

Figure 4. XRD analysis of the as-received material

Figure 5 demonstrates SEM micrographs and EDS analysis of huntite hydromagnesite mineral particles are shown in Figure 6. It is clearly seen from that the mineral particles are not circular but they are lateral with irregular shapes. EDS analysis supports XRD result as in the elemental analysis the elements of Mg, Ca, C, and O were indicated. There seem no any other elements as impurities.

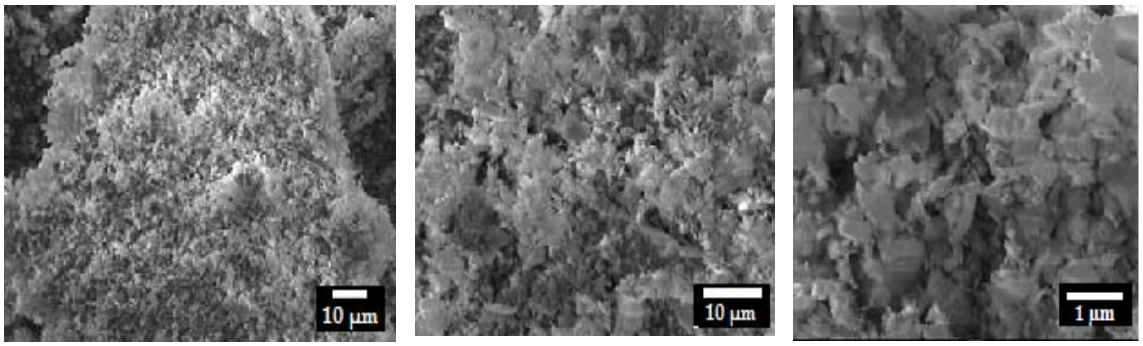

Figure 5. SEM micrographs of huntite and hydromagnesite

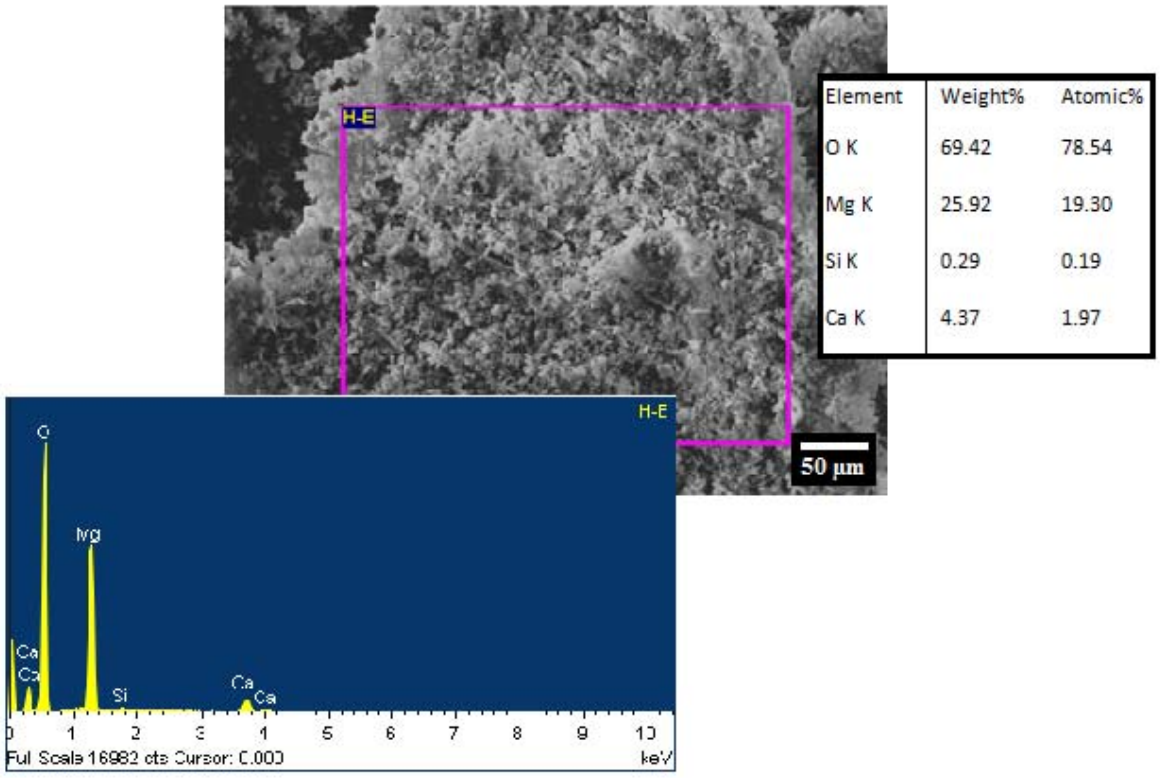

Figure 6. EDS analysis of huntite and hydromagnesite

For the flame retardant property exothermic and endothermic reactions are important, thus DTA-TG analysis are carried out to huntite hydromagnesite mineral (Figure 7). This analysis was performed by heating up at the rate of 10 ºC/min at temperatures between 25ºC and 600ºC under air. Huntite and hydromagnesite have $Mg_3Ca(CO_3)_4$ and $Mg_4(OH)_2(CO_3)_3.3H_2O$ chemical formulas, respectively. Decomposition occurred in these minerals at temperatures between 25ºC and 600ºC. The first thermal phenomenon starts at 219.86ºC and ends at 331.89ºC and then heat absorption is -3,61 J, corresponding to removal of water and OH groups. After removal of water from hydromagnesite, $Mg_4(CO_3)_3$ decomposes to MgO and CO_2. It is estimated that the decomposition of $Mg_4(CO_3)_3$ occurs at temperatures between 376.29ºC and 490,76ºC This is the second thermal behaviour and heat absorbed at -5,49 J. It is difficult to separately state decomposition phenomena of the individual components of huntite hydromagnesite because it is a mixture of $Mg_4(OH)_2(CO_3)_3.3H_2O$ and $Mg_3Ca(CO_3)_4$. Finally the third thermal effect starts at 503.94ºC and ends at 598.29ºC. In this case, heat absorption is -1,43 J. MgO and CaO are formed by the end of this process. According to Equations 1 and 2, $Mg_4(OH)_2(CO_3)_3.3H_2O$ and $Mg_3Ca(CO_3)_4$ starts to decompose at high temperatures.

$$Mg_4(CO_3)_3(OH)_2.3H_2O \rightarrow 4MgO + 3CO_2 + 4H_2O \quad (1)$$

$$Mg_3Ca(CO_3)_4 \rightarrow 3MgO + CaO + 4CO_2 \quad (2)$$

By comparing TGA analysis was to evaluate thermal stabilities of huntite/hydromagnesite mineral. It can be seen from Figure 4b that the decomposition of huntite hydromagnesite mineral occurs at temperatures between 400 ºC and 500 ºC. The weight losses were resulted at those intervals, it is indicated that weight losses of huntite hydromagnesite mineral was estimated 56 wt.%.

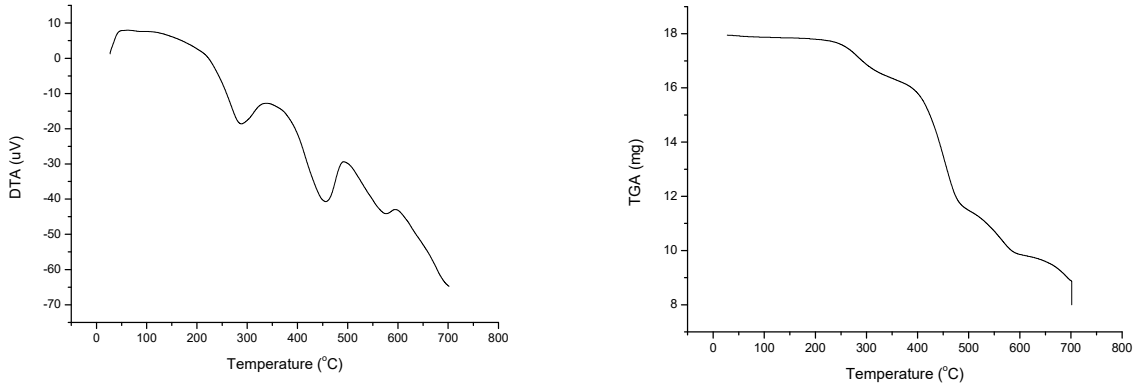

Figure 7. DTA and TGA curves of huntite hydromagnesite mineral.

Figure 8 and Figure 9 demonstrate SEM and EDS analysis of huntite hydromagnesite reinforced wood composites. In SEM micrographs cellulose fiber structures can be seen easly. They possess irregular shapes. Huntite hydromagnesite mineral particles of 10 micron size were seen in W60H sample. EDS analysis proved XRD and XRF result because C, O Mg, Al, Si and Ca elements were observed and there is any other element as impurities. It was found that by adding mineral particles denser composite structure was obtained.

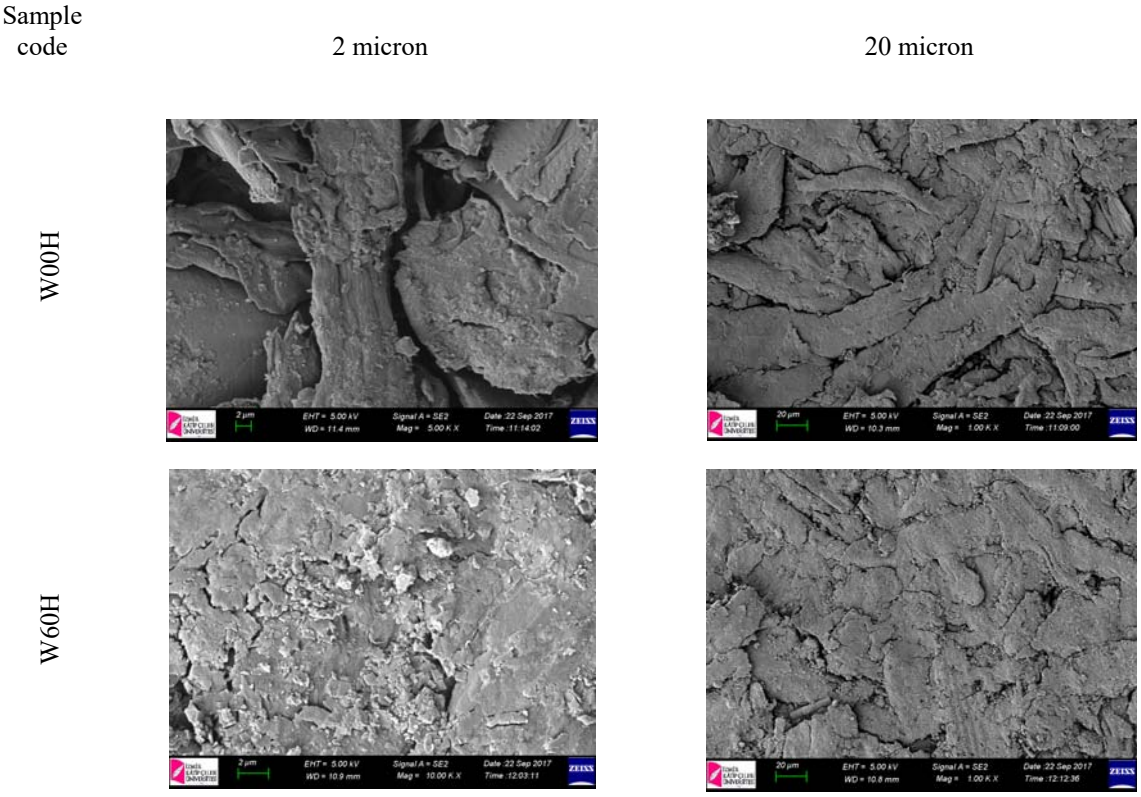

Figure 8. SEM analysis of samples of W00H and W60H

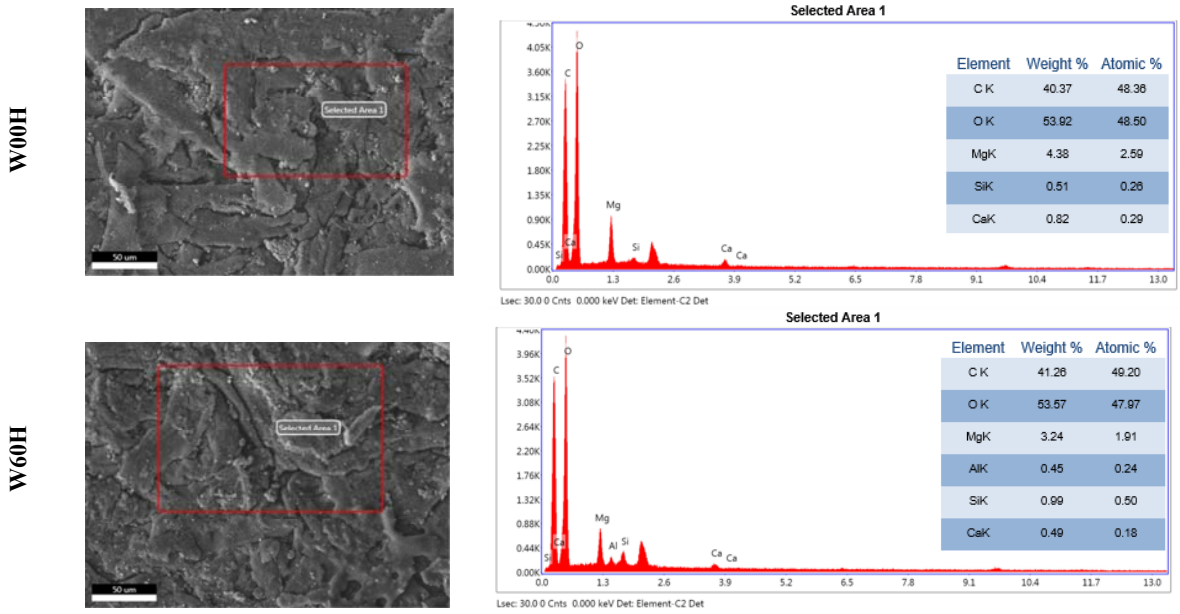

Figure 9. EDS analysis of samples of W00H and W60H

Table 2 depicts flame retardant test results. According to UL94 test, the results demonstrate the degree of flame retardant property of huntite hydromagnesite reinforced wood composite materials as a function of particle content. In between 0-45% content there was not indicated any flame retardant property, thus those samples can be defined as flammable. However, starting with 50% of mineral additive (W50H), the material became flame retardant as the flame was extinguished before 30 s according to the UL-94 standard. It can be easily seen that increasing the mineral filler amount improves the flame retardant property of the composite.

In our previous studies huntite and hydromagnesite minerals were investigated for the flame retardant property especially in polymeric composites; such as electrical cable applications, cable trays, window panels, polymeric flame retardant coatings etc (Yılmaz Atay & Çelik, 2013). In this study it is tested in wood composites and not surprisingly it was observed that the mineral was worked as flame retardant filler, too. The mechanism was similar as huntite hydromagnesite mineral undergoes an endothermic decomposition with water and carbon dioxide. By using this mineral in the wood materials, it will help to increase safety in virtually every wooden area of human existence. Therefore, this forgotten material in all kind of industries can get back its importance which it lost due to its flammable property.

Table 2. UL-94 test results of wood composite samples.

Sample Code	Flame applying time	Burning time	Result
W00H	10	30	Out of spec.
W20H	10	0	
	10	30	Out of spec.
W25H	10	30	Out of spec.
W30H	10	0	
	10	30	Out of spec.
W35H	10	30	Out of spec.
W40H	10	0	
	10	30	Out of spec.
W45H	10	30	Out of spec.
W50H	10sn	0sn	
	10sn	0sn	
	30sn	25sn	O.K.
W55H	10sn	0sn	

	10sn	0sn	
	30sn	24sn	O.K.
W60H	10sn	0sn	
	10sn	0sn	
	30sn	7sn	O.K.

Conclusion

Fighting fires depends on directly fire precautions and is directly related to the use of non-combustible material. Even if the fire started, flame retardants help to extinguish in the early stages of fire and prevent the dispersion of the flame. The flame retardant behavior of Turkish huntite hydromagnesite mineral in wood composite was investigated in this study. Wood composite was formed by using auxiliary mineral flame retardant additive introduced into the combustible product. It was found somewhat more effective by UL-94 flame retardant test. Thereby, it was depicted that by using the mineral reinforced wood composite, wood can get back its importance which it lost due to its flammable property. It was observed that increasing the loading amount of the additive increases the flame retardant property of the composite. For the further investigations mechanical behavior needs to be tested. Moreover, if different particle size of the minerals is used, it would be possible to obtain improved flame retardant properties. Therefore, to obtain the best performance, it is required to consider optimum mineral amount and the particle size. On the other hand, additive amount can be evaluated according to use conditions of wood composite; such as, where the composite will be used, what kind of load it will be applied, to what kind of environment it will be in, and so forth.

Acknowledgements

The author thanks to Scientific and Technological Research Council of Turkey (TÜBİTAK) as this work was supported by the TÜBİTAK Funds, Grant No: 216M090. Special acknowledge to Likya Minelco Madencilik Sti., Minelco Specialities Limited, Muğla Sıtkı Koçman University and Izmir Institute of Technology.

References

García-Durañona, L., Farreny, R., Navarro, P., Boschmonart-Rives, J. (2016). *Life cycle assessment of a coniferous wood supply chain for pallet production in Catalonia, Spain.* J Clean Product. 137 (pp.178–188).

Haurie, L., Fernandez, A.I., Velasco, J.I., Chimenos, J.M., Cuesta, J.-M.L., Espiell, F. (2006) *Synthetic hydromagnesite as flame retardant. Evaluation of the flame behaviour in a polyethylenematrix.* Polym. Degrad. Stabil. 91, (pp.989–994).

Kirschbaum, G. (2001). *Minerals on Fire, Flame Retardants Look to Mineral Solutions.* 3rd Minerals in Compoundings Conference, IMIL-AMI Joint Conference, April 8–10 (2001).

Kulshreshtha, A.K. (2002). Handbook of Polymer Blends and Composites, Volume 1

Le Bras, M., Bourbigot, S., Duquesne, S., Jama, C., Wilkie, C. (2005). *Fire retardancy of polymers new applications of mineral fillers.* Royal Society of Chemistry: Cambridge, UK.

Leslaw, K. (2016). *Reinforcing wood by surface modification.* Composite Structures 158 (pp.64–71).

Liu, M. Qing, Y. Wu, Y. Liang, J. Luo. (2015) S. Appl. Surf. Sci. 330 (pp.332–338) http://dx.doi.org/10.1016/j.apsusc.2015.01.024.

Lozhechnikova, A., Bellanger, H., Michen, B., Burgert, I., Österberg, M. (2017) Appl. Surf. Sci. http://dx.doi.org/10.1016/j.apsusc.2016.11.132.

Moreno, D.D.P. Saron, C. (2017). *Low-density polyethylene waste/recycled wood composites*. Composite Structures 176 (pp.1152–1157).

Ng, R., Shi, C.W.P., Tan, H.X., Song, B. (2014). *Avoided impact quantification from recycling of wood waste in Singapore: an assessment of pallet made from technical wood versus virgin softwood.* J Clean Prod. 65 (pp.447–57).

Oliveira, A.K.F. d'Almeida, J.R.M. (2014). *Description of the mechanical behavior of different thermoset composites reinforced with Manicaria saccifera fibers*. Journal of Composite Materials. 48, (pp.1189–1196). doi: 10.1177/0021998313484622

Shah, S.M., Zulfiqar, U., Hussain S.Z., Ahmad, I., Rehman, H., Hussain, I., Subhani, T. (2017). *A durable superhydrophobic coating for the protection of Wood Materials*. Materials Letters. 203, (pp.17–20).

Taramian, A. Doosthoseini, K. Mirshokraii, S. A. Faezipour, M. (2007). *Particleboard manufacturing: An innovative way to recycle paper sludge.* Waste Management. 27, (pp. 1739-1746).

Yılmaz Atay H., Çelik E. (2010). *Use of Turkish huntite/hydromagnesite mineral in plastic materials as a flame retardant.* Polymer Composites. 31 (pp 1692-1700).

Yılmaz Atay H., Çelik E. (2013). *Mechanical Properties of Flame Retardant Huntite and Hydromagnesite Reinforced Polymer Composites*. Polymer-Plastics Technology and Engineering. 52, (pp. 182-188).

STATISTICAL SIGNIFICANCE TESTING OF THE PARTICLE CIRCULARITY VALUES FROM VARIOUS PRODUCTS OF SPHALERITE COLUMN FLOTATION BENEFICIATION WITH ULTRASONIC PRE-TREATMENT

Uğur ULUSOY[a], Hülya KURŞUN[b*], İbrahim ERDOĞAN[b]
[a] Cumhuriyet University, Department of Mining Engineering, Sivas, TURKEY
uulusoy@cumhuriyet.edu.tr
[b] Cumhuriyet University, Department of Material and Metallurgical Engineering, Sivas, TURKEY
hkursun@cumhuriyet.edu.tr, ibrahim_erdogn@hotmail.com

Abstract: In this study, circularity of particles from various streams (such as feed and concentrates) of sphalerite beneficiation by column flotation with and without ultrasonic pre-treatment were measured by a recent technique; Dynamic image analysis (DIA) by counting more than 20 000 particles for each population. Then the statistical significance of mean circularity values was tested by using one way ANOVA (analysis of variance) and post hoc Tukey test. ANOVA results showed that circularity values of each particle from these product streams of column flotation with and without ultrasonic pre-treatment was statistically different from each other at the confidence level of 95%. DIA results showed that the highest circularity value was obtained in the concentrate of column flotation with ultrasonic pre-treatment which gives the highest zinc grade and recovery indicating that particle circularity has small but positive effect on the sphalerite column flotation beneficiation with ultrasonic pre-treatment.
Keywords: Zinc, circularity, column flotation, ultrasonic treatment, ANOVA

Introduction

Zinc is used by the industries such as rubber, chemical, paint, and agricultural. About three-fourths of zinc used is consumed as metal for coating, alloying metal, and zinc-based die casting applications and rolled zinc (http://www.niton.com/docs/literature/infographic_zinc3.pdf?sfvrsn=2). Zinc mine production in the world in 2014 was about 13 million tons (U.S. Geological Survey, 2015) indicating that it plays an important role in the global mineral economy.

Flotation is the most widely used separation process for the recovery of sphalerite from low grade complex Pb-Cu-Zn ores. Column flotation which is a patented process since 1962 have accomplished substantial industrial application over mechanical flotation since 1981 (Wheeler, 1988). Ameliorated concentrate grades and recoveries with decreased reagent consumption are the advantages ascribed to column cells which can operate with very deep froths and can be sprayed with wash water thus achieve high concentrate grades (Deglon, 1998).

Ultrasonic bath is a tool that uses high frequency sound waves (above the range of human hearing) to agitate an aqueous that in turn acts on contaminants adhering to substances like metals. By using ultrasonic effect with zinc column flotation our recent study has shown that ultrasound pre-treatment has improved column flotation performance with respect to zinc grade and recovery in multiple stages of column flotation (19.91 and 4.96 units, respectively) (Kursun and Ulusoy, 2015).

It is well known that flotation is a complex phenomenon in which particle shape is one of the affecting parameters of physical parameters of the particulates. Effect of particle shape on flotation has been investigated by various works regarding attachment-detachment process (Wotruba et al., 1991), the induction period for particle-bubble attachment in flotation (Verrelli et al., 2012), flotation kinetics constant of the particles (Dehghani et al., 2013; Rahimi et al., 2012), wettability (Ulusoy et al. 2004; Hiçyılmaz et al, 2004), flotation recovery (Forssberg and Zhai, 1985), and column flotation (Kursun and Ulusoy, 2006). Thus, the particle shape distribution of feed and concentrate streams of mineral flotation circuits needs to be characterized to understand how shape affects the recovery of minerals (Durney and Meloy, 1986). Dynamic Image Analysis (DIA) which is defined as image analysis methods while particles are in motion entails using techniques for dispersing particles in liquid, taking in focus, and analyzing the images using shape parameters (http://www.micromeritics.com/Repository/Files/The_Effects_of_Particle_Shape_on_Measured_Particle_Size_2011.pdf). DIA is a fast method that eradicates operator prejudice and fatigue. It brings reliability, accuracy and

reproducibility regardless who is performing the analysis. In addition, it allows statistically substantial sampling of 10 000 - 500 000 particles in one measurement.

One Way ANOVA (Analysis of variance) is an analysis of variance which is used to compare mean differences in two or more groups of measurements in image analysis. When the F-test is statistically significant, the null hypothesis is rejected. However, it is still necessary to determine which of the means were significantly different from each other. Post hoc tests are essential to determine which groups are actually different (Boslaugh and Watters, 2008; Ulusoy, 2008).

The aim of this work is to measure the particle circularity values of feed and column flotation concentrates with and without ultrasonic pre-treatment (Kursun and Ulusoy, 2015) and to corroborate the statistical significance of mean circularity values from these various column flotation streams tested by using one way ANOVA and post hoc Tukey test.

Materials and Methods

In this study, the same sphalerite ore which was taken from zinc feed of the selective zinc flotation circuit in a plant (GESOM A.Ş.) treating lead-zinc-copper complex ore (Kursun and Ulusoy, 2012; Kursun, 2014; Kursun and Ulusoy, 2015) in Turkey was used. The XRD of the ore which includes 3.23% Pb, 0.52% Cu and 2.71% Zn was already reported elsewhere (Kursun, 2014). The particle size of the sample was smaller than 74 μm (100 %) for the column flotation tests (Figure 1) which were performed by a 5 x 75 cm tubular flotation column cell (Ünal Mühendislik A.Ş., Turkey). The detailed information about the column flotation experiments by single and multistage was already described in the previous study (Kursun and Ulusoy, 2015). The pulp density was used as 30%. Flotation chemicals such as KAX (Dow Chemical), $CuSO_4$ (Merck), Aerofloat 211 (Cyanamid), 2-Ethyl hexanol (Merck) and Na_2SiO_3 (Merck) were used as collector, activator for sphalerite, collector for selective sphalerite flotation, frother and gangue depressant, respectively. Operational parameters of column flotation were optimized by single stage column flotation without ultrasonic pre-treatment. Optimized dosage values of these flotation conditions include 400 g/t of $CuSO_4$, 100 g/t of Aerofloat 211, 15 g/t of 2-ethyl hexanol, 50 g/t of Na_2SiO_3, 90 g/t of KAX, 160 rpm of stirring speed, 0.170 cm/sec of superficial wash water rate, 0.425 cm/sec of superficial feed rate, 1.5 cm/sec of superficial air rate, 4 min. of residence time, 0.437 cm/sec of tailing flow rate, 0.170 cm/sec of superficial wash water rate, 0.0123 cm/sec of bias flow rate, 0.425 cm/sec of superficial feed rate and 1.5 cm/sec of superficial air rate was. Tap water (pH: 8.2) was used for the experiments and pH was arranged as 11.5 by using lime (Merck). Collected concentrates were weighed and analyzed when the system was reached to steady state. Experiments were iterated until the consistent grade and recovery values were obtained as 3 repeats. Multiple stages (3 stages of cleaning and 3 stages of scavenging) of column flotation tests were carried out with and without ultrasonic pre-treatment after single stage column flotation experiments with and without ultrasonic pre-treatment. After column flotation tests, the feed and concentrates of multiple stages (3 stages of cleaning and 3 stages of scavenging) of column flotation tests were subjected to DIA analysis for the measurement of circularity values.

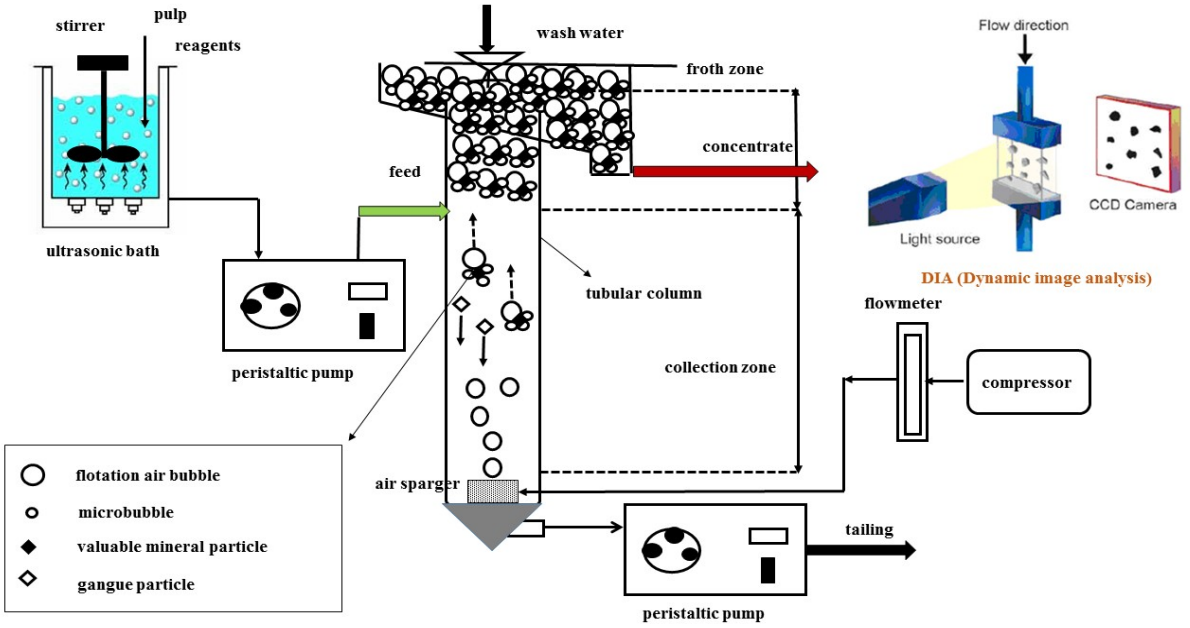

Figure 1. The experimental set-up used in this study (redrawn from Kursun and Ulusoy, 2015).

For the preparation of a few grams of representative sample to perform DIA, automatic rotary spinning riffler (Quantachrome® Instruments) was used. Then, prepared representative samples were placed in a 25 ml glass sample container added with water and hold in the ultrasonic bath for 5 min for good dispersion of the representative sample for DIA measurements.

Circularity (C) which is a fractional measure indicating shape of the particles and calculated from area (A) and bounding circle diameter (D_{BC}) as $4A/\pi D^2_{BC}$. For a spherical particle C is equal to 1 on the other hand C is lower than 1 for irregular particles such as elongated particles (Ulusoy and Yekeler, 2014).

Circularity values of sphalerite particles from three column flotation streams such as feed (C_F), concentrate with ultrasonic pre-treatment (C_{CFCUP}) and concentrate without ultrasonic pre-treatment (C_{CFC}) were determined as the average of three measurements by using a new 3D real-time dynamic image analyzer **(**Particle Insight Dynamic Image Analyzer, Micromeritics® Instrument Corp., Norcross, USA**).**

Results and Discussion

Shape results by DIA

Figure 2 illustrates the re-plotted grade and recovery results of sphalerite column flotation with and without ultrasonic pretreatment (Kursun and Ulusoy, 2015). As seen from Figure 2 ultrasonic pretreatment has increased the zinc grade and recovery obtained for both single stage and multi-stage column flotation.

Mean Circularity values of sphalerite particles from column flotation feed and concentrates with and without ultrasonic pre-treatment by DIA was shown by Figure 3 indicating that the highest circularity values obtained for concentrate with ultrasonic pre-treatment (C_{CFCUP}). Overall circularity trends were found as $C_F<C_{CFC}<C_{CFCUP}$.

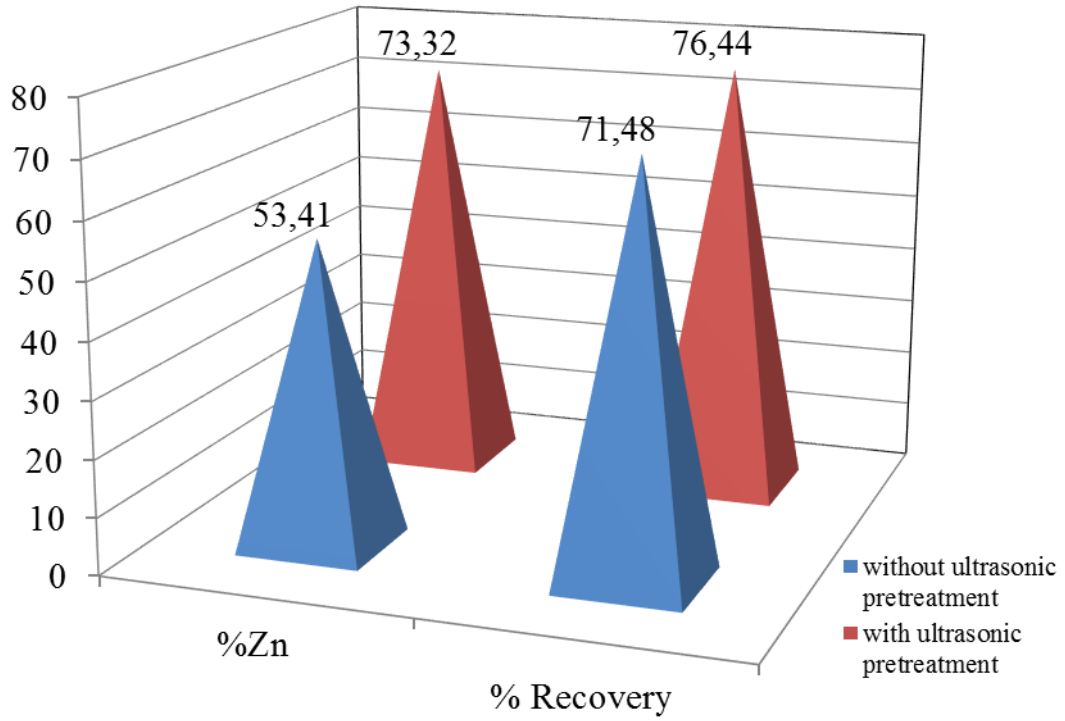

Figure 2. Zinc grade and recovery obtained for multi-stage zinc column flotation with and without ultrasonic pre-treatment (redrawn from: Kursun and Ulusoy, 2015)

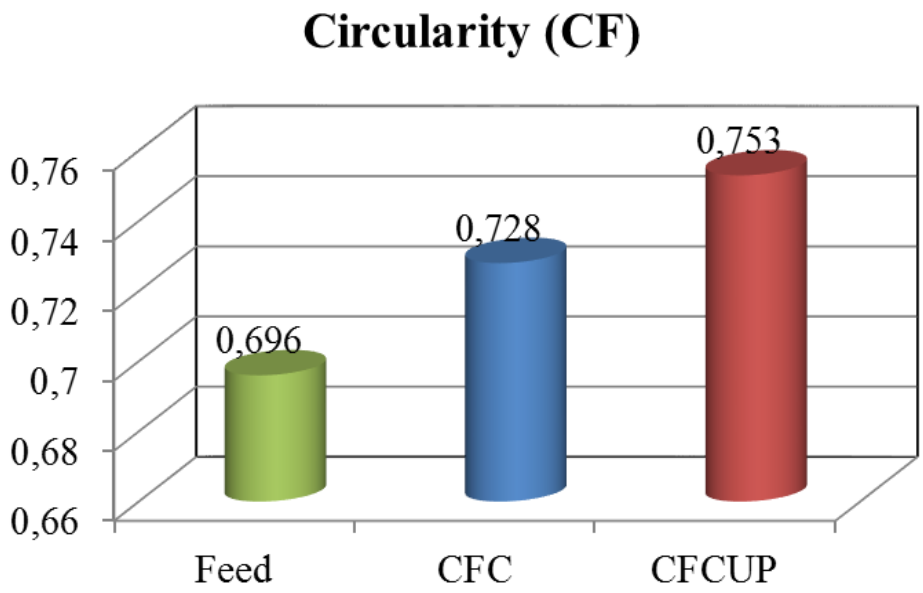

Figure 3. Circularity values measured by DIA from streams of zinc column flotation with and without ultrasonic pre-treatment (*where, F: Feed, CFC: Column flotation concentrate, CFCUP: Column flotation concentrate with ultrasonic pre-treatment)*

As seen from Figure 4 circularity values of sphalerite column flotation concentrates for multistage column flotation were increased with increased zinc grade of the concentrates. Fig. 5 illustrates the particle thumbnail images (C_F, C_{CFCUP} and C_{CFC}) from the circularity measurements by DIA. After analysis and a review of all particles in these thumbnail images which were only a small part of about 20 000 particles for each population, they consist of partly elongated particles and partly blocky (equi-dimensional) particles not represent one type of particle shape since there are small differences in circularity values of particles from each column flotation streams.

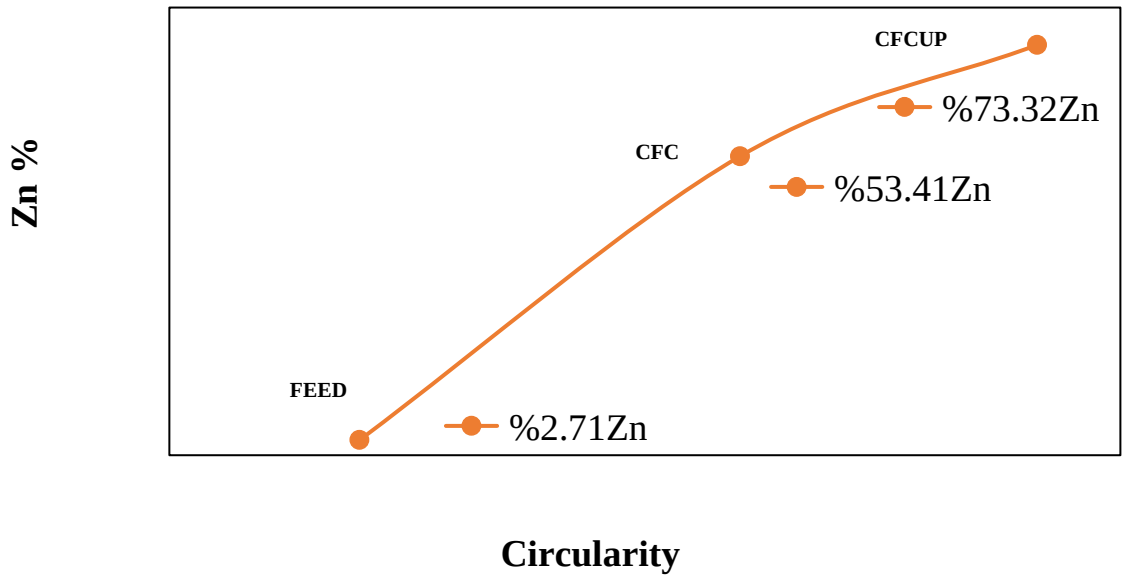

Figure 4. Changes of zinc grade with circularity values measured by DIA various streams of zinc column flotation with and without ultrasonic pre-treatment (Zn data from: Kursun and Ulusoy, 2015)

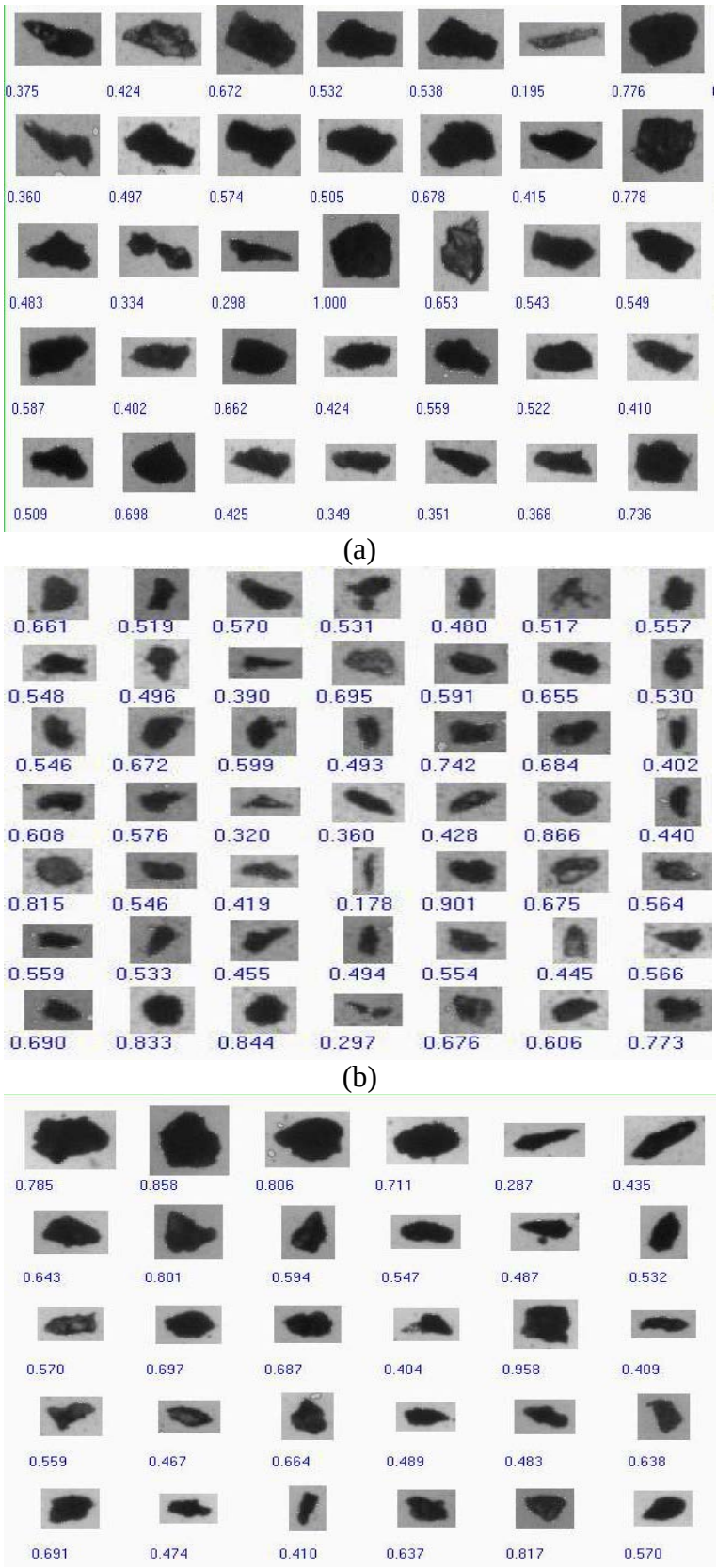

Figure 5. DIA thumbnail images of various streams of zinc column flotation with and without ultrasonic pre-teratment (a) Feed, (b) CFC, (d) CFCUP *(Where, F: Feed, CFC: Column flotation concentrate, CFCUP: Column flotation concentrate with ultrasonic pre-treatment)*

ANOVA Results

Since there is a small trend of increasing for circularity values considering the result of DIA, the significance of the circularity values of each sphalerite samples (feed, concentrate with ultrasonic pre-treatment and concentrate without ultrasonic pre-treatment) must be proved by the statistical test namely ANOVA.

The purpose of ANOVA is to assess whether the observed differences among sample means are statistically significant. ANOVA tests the null hypothesis that the population means are all equal (H_0: $\mu_1 = \mu_2 = \mu_3$) while the alternative is that they are not all equal. This alternative could be true because all the means are different or simply because one of them differs from the rest. If H_0 is not rejected, we conclude that the population means are indistinguishable based on the data given. On the other hand, if H_0 is rejected, we would like to know which pairs of means differ. Multiple-comparisons methods address this issue. It is important to keep in mind that multiple comparisons methods are used only after rejecting the ANOVA H_0 (Moore et al., 2009).

Standard Excel™ spreadsheet data from the automated DIA analyzer were imported by a software called "Statistical Package for Social Science" 22.0 (SPSS Inc., Chicago, IL, USA) to determine whether the circularity parameter of three different sphalerite column flotation streams (feed, concentrate with ultrasonic pre-treatment, concentrate without ultrasonic pre-treatment) were statistically different from each other (Fig 6). Mean values of shape parameter for these products were compared by applying one way ANOVA (Ulusoy, 2008) and post hoc Tukey's multiple comparison tests at significance level of 0.05.

(a)

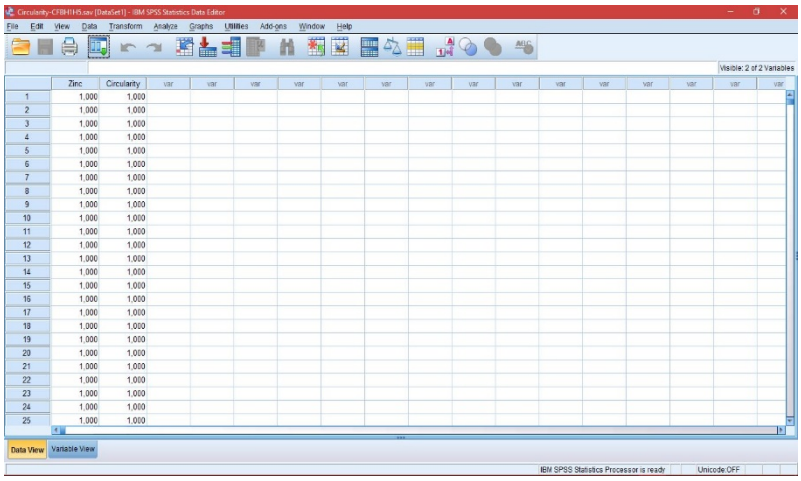

(b)

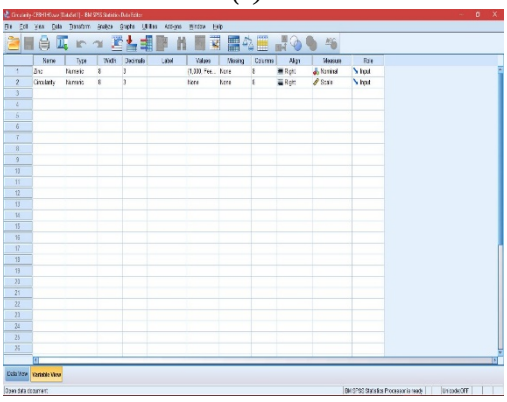

(c)

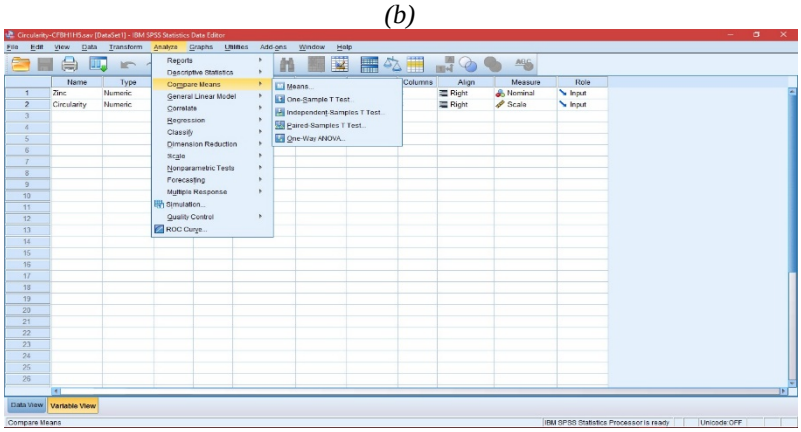

(d)

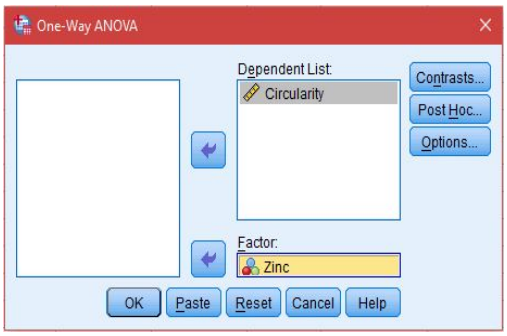

(e)

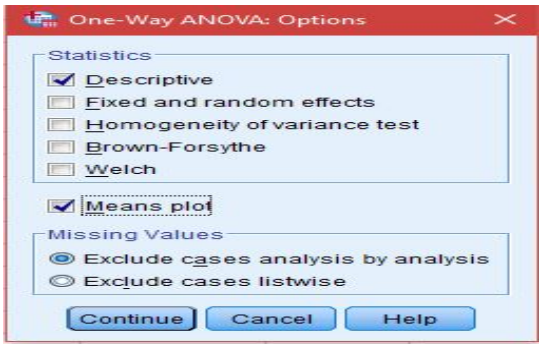

(f)

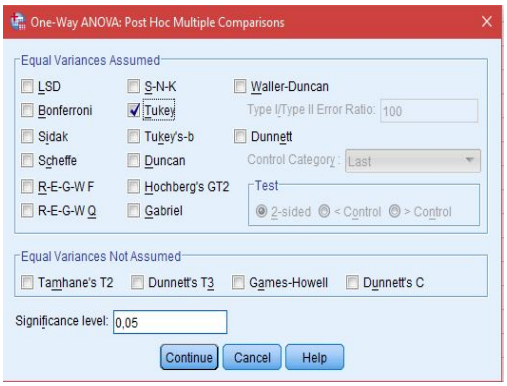

(g)

Figure 6. ANOVA study conditions by SPSS (a) version (b) data view (c) variable view (d) ANOVA menu (e) ANOVA variable (f) ANOVA options (g) Post hoc multiple comparisons.

In Table 1 there are group statistics, which provide the means and standard deviations of the groups. Table 2 shows the test of homogeneity of variances for circularity values of sphalerite column flotation streams. From Table 2, circularity results show that the test for homogeneity of variances is significant since p=.000 which is greater than 0.05. This means that (p-value is indicating not equal variances) in the homogeneity of variances assumption is not met. The One-Way ANOVA Output was given in Table 3.

Table 1. Descriptive ANOVA results of circularity values of streams of sphalerite column flotation with and without ultrasonic pre-treatment

					95% Confidence Interval for Mean			
Circularity	N	Mean	Std. Dev.	Std. Error	Lower Bound	Upper Bound	Min.	Max.
Feed	19764	.69610	.175971	.001252	.69365	.69856	.031	1.000
CFC	19514	.72368	.161446	.001156	.72141	.72594	.110	1.000
CFCUP	19452	.75422	.166987	.001197	.75187	.75656	.054	1.000
Total	58730	.72451	.169941	.000701	.72314	.72589	.031	1.000

Where, F: Feed, CFC: Column flotation concentrate, CFCUP: Column flotation concentrate with ultrasonic pre-treatment

Table 2. Test of homogeneity of variances for circularity values of streams of sphalerite column flotation with and without ultrasonic pre-treatment

Circularity			
Levene Statistic	df1	df2	Sig.
93.598	2	58727	.000

The results of the overall F test in the ANOVA summary table can be examined to determine whether group means are different. As shown in Table 3, the mean-square ratio experimentally derived (584.974) is higher than the sig. F ratio (0.00) for 95% confidence. So, it can be concluded with 95% confidence that there are significant

differences among circularity values obtained for three sphalerite column flotation streams (such as feed, concentrate without ultrasonic pre-treatment and concentrate with ultrasonic pretreatment).

If the significance value (which is usually labeled p in research reports) is less than alpha H_0 is rejected; if it is greater than alpha, H_0 is not rejected. As indicated, the overall F test is significant (i.e., p value < 0.05), indicating that means among circularity values of each groups are not equal. In other words, since the value of p value is 0.000 as shown in Table 3 there are significant difference among circularity values of each groups for at the 0.05 alpha levels. So, in this case, because the p value of .000 is less than 0.05 alpha level, the null hypothesis was rejected. The results of this ANOVA showed that there are significant differences among the groups.

Table 3. ANOVA results for circularity values of of streams of sphalerite column flotation with and without ultrasonic pre-treatment

ANOVA					
Circularity	Sum of Squares	df	Mean Square	F	Sig.
Between Groups	33.129	2	16.565	584.974	.000
Within Groups	1662.963	58727	.028		
Total	1696.093	58729			

However, it is necessary to conduct post hoc comparison tests to determine which of the group means are different. Results of Tukey post hoc tests were presented in Table 4. From the Table 4 we can see that the circularity values of each sphalerite samples (feed, concentrate with ultrasonic pre-treatment and concentrate without ultrasonic pre-treatment) are significantly different from each other. Because the p value of 0.000 is less than alpha value of 0.05.

Table 4. Results of multiple comparisons by Tukey HSD post hoc tests

		Mean			95% Confidence Interval	
(I)	(J)	Difference (I-J)	Std. Error	Sig.	Lower Bound	Upper Bound
Feed	CFC	-.027576*	.001698	.000	-.03156	-.02360
	CFCUP	-.058114*	.001700	.000	-.06210	-.05413
CFC	Feed	.027576*	.001698	.000	.02360	.03156
	CFCUP	-.030538*	.001705	.000	-.03453	-.02654
CFCUP	Feed	.058114*	.001700	.000	.05413	.06210
	CFC	.030538*	.001705	.000	.02654	.03453

*. The mean difference is significant at the 0.05 level.
Where, F: Feed, CFC: Column flotation concentrate, CFCUP: Column flotation concentrate with ultrasonic pre-treatment

The homogenous subsets table (Table 5) can help us to divide the three groups into homogenous subgroups. Within each sub-group the difference in means is statistically significant for circularity. The results also indicate that groups can be put into three subsets, based on mean differences. As the Table 5 indicates, circularity means of sphalerite particles from feed, concentrate without ultrasonic pre-treatment and concentrates with ultrasonic pre-treatment are not grouped together because their means are not similar.

Table 5. Homogeneous subsets of Tukey post hoc tests

		Subset for alpha = 0.05				
Tukey HSD[a,b]	N	1	2	3	4	5
Feed	19764	.69610				
CFC	19514			.72368		
CFCUP	19452					.75422
Sig.		1.000	1.000	1.000	1.000	1.000

Means for groups in homogeneous subsets are displayed.
a. Uses Harmonic Mean Sample Size = 19575.741.
b. The group sizes are unequal. The harmonic mean of the group sizes is used.
Where, F: Feed, CFC: Column flotation concentrate, CFCUP: Column flotation concentrate with ultrasonic pre-treatment

The mean plots (graphically displays the circularity means for the three groups) that SPSS created are an effective way to illustrate the mean differences. The difference between groups was confirmed graphically by looking at the plot of means shown in Fig 7.

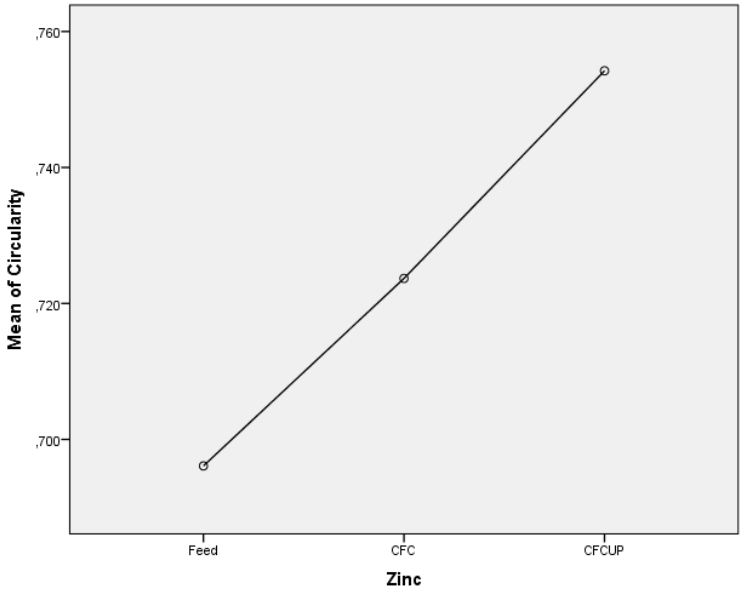

Figure 7. Mean plots for circularity of multiple comparisons for by SPSS

Conclusions

DIA results revealed that the highest mean circularity value was received in the concentrate of sphalerite column flotation with ultrasonic pre-treatment which gives the highest zinc grade and recovery pointed out that particle circularity has small but positive effect on the beneficiation by column flotation with and without ultrasonic pre-treatment.

The differences in circularity parameter of particles among the three populations from various column flotation streams were found statistically significant with a 95% confidence level. In other words, mean circularity values analyzed by counting more than 20 000 particles for each population using DIA were not identical.

Nomenclature

ANOVA	: Analysis of variance
C	: Circularity
CFC	: Column flotation concentrate
CFCUP	: Column flotation concentrate with ultrasonic pretreatment,
DIA	: Dynamic Image Analysis
F	: Feed
H_0	: Null hypothesis
p	: Significance value
μ_1	: Population mean
Alpha	: Confidence level

References

Boslaugh S.& Watters, P.A. (2008). *Statistics in a Nutshell*, 1st Edition, O'Reilly Media, Inc., c., 1005 Gravenstein Highway North, Sebastopol, (pp.238), A 95472. USA, Mary Treseler (Ed.) Inc.

Deglon, D.A. (1998). A hydrodynamic investigation of fine particle flotation in a batch flotation cell, PhD Thesis, University of Withwatersrand.

Dehghani, F., Rahimi, M. & Rezai, B. (2013). Influence of particle shape on the flotation of magnetite, alone and in the presence of quartz particles, *The Journal of the Southern African Institute of Mining and Metallurgy*, 113, (pp. 905).

Durney, T.E. & Meloy, T.P. (1986). Particle shape effects due to crushing method and size, *International Journal of Mineral Processing*, 16, (pp.109-123).

Forssberg, E. & Zhai, H., (1985). Shape and surface properties of particles liberated by autogenous grinding, *Scand. J. Metallurgy*, 14, (pp.25-32).

Hiçyılmaz, C., Ulusoy, U. & Yekeler, M. (2004). Effect of shape properties of talc and quartz particles on the wettability based separation processes, *Applied Surface Science*, 233, (pp. 204-212)

http://www.micromeritics.com/Repository/Files/The_Effects_of_Particle_Shape_on_Measured_Particle_Size_2011.pdf

http://www.niton.com/docs/literature/infographic_zinc3.pdf?sfvrsn=2

Kursun, H. (2014). A study on the utilization of ultrasonic pretreatment in zinc flotation, *Sep. Sci. Technol.* 49:18, (pp.2975-2980).

Kursun, H. & Ulusoy, U. (2006). Influence of shape characteristics of talc mineral on the column flotation behavior, *International Journal of Mineral Processing*, 78,4, (pp.262-268).

Kursun, H. & Ulusoy, U. (2012). Zinc recovery from lead-zinc-copper complex ores by using column flotation, *Miner. Process. Extr. Metall. Rev.* 33,5, (pp. 327-338).

Kursun, H. & Ulusoy, U. **(**2015). Zinc recovery from a lead-zinc-copper ore by ultrasonically assisted column flotation, *Particulate Science and Technology*, 33, 4, (pp. 349-356).

Rahimi, M., Dehghani, F., Rezai, B. & Aslani, M. R. (2012). Influence of the roughness and shape of quartz particles on their flotation kinetics, *International Journal of Minerals, Metallurgy and Materials*, 19, 4, (pp. 284).

U.S. Geological Survey (2015). Mineral commodity summaries 2015: *U.S. Geological Survey*, 196 p., Retrieved from http://minerals.usgs.gov/minerals/pubs/mcs/2015/mcs2015.pdf

Ulusoy, U. (2008). Application of ANOVA to image analysis results for talc particles produced by different milling, *Powder Technology*, 188, 2, (pp. 133-138).

Ulusoy, U., Yekeler, M. (2014). Dynamic image analysis of calcite particles created by different mills, *International Journal of Mineral Processing*, 133C (pp. 83-90).

Ulusoy, U., Hiçyılmaz, C. & Yekeler, M. (2004). Role of shape properties of calcite and barite particles on apparent hydrophobicity, *Chemical Engineering and Processing*, 43, 8, (pp.1047-1053).

Verrelli, D.I., Bruckard, W.J., Koh, P.T.L., Schwarz M.P. & Follink B. (2012). Influence of Particle Shape and Roughness on the Induction Period for Particle-Bubble Attachment, *XXVI International Mineral Processing Congress (IMPC) 2012 Proceedings* / NEW DELHI, INDIA / 24 - 28 SEPTEMBER, 05665.

Wheeler, D.A. (1988). Historical view of column flotation development. Column 88 - Proc. Int. Conf., S.M.E., Phoenix, (pp. 3-4)

Wotruba, H., Hoberg, H. & Schneider, F.U. (1991). Investigation on the separation of microlithe and zircon. The influence of particle shape on floatability. Preprints, XVII. International Mineral Processing Congress, Dresden, FRG. Polygraphischer, Bereich, Bergakademie Freiberg, Sa, (Ed: Schubert, G. Ed) vol. 4., (pp.83).

THE ANALYSIS OF A POLICY DOCUMENT: "TURKISH SCIENCE POLICY FROM 1983 TO 2003"

Ibrahim ARAP
Dokuz Eylul University, Department of Public Administration, Izmir, Turkey
ibrahim.arap@deu.edu.tr

Veysel ERAT
Bitlis Eren University, Department of Public Administration, Bitlis, Turkey
verat@beu.edu.tr

Abstract: This study aims to analyze the text entitled "Turkish Science Policy from 1983 to 2003" using the conceptual framework of public policy. Having been prepared over a period of more than two years with contributions by some 300 scientists and experts from universities, TUBITAK and other public institutions of research who come from a diversity of disciplines, this text embraces a system approach in determining a science and research policy for Turkey. For this reason, the set of concepts in the discipline of public policy will be used to analyze it. This will allow us to reveal what reasons lied behind such a text in the circumstances of the day, how successfully the text identified the issues in the system of science and technology, and how well-placed the proposed long-term solutions to these issues were. The study has been designed in four main parts. While the first part will address the conceptual framework regarding public policy, the second part will review the pre-1980 science agenda of the state. The third part will deal with the methodology and content of the document "Turkish Science Policy from 1983 to 2003" from the perspective of public policy, and finally the fourth part will investigate the reasons for its failure through comparison with similar documents that were produced later.
Keywords: Science and technology, public policy, science policy.

Introduction

The emergence of science policy comes with the Second World War when scientific research turns its focus toward strategic goals and military projects (Türkcan, 2003). The wave of research and development investments that begins with the Manhattan Project, the clearest example of strong government intervention in science policy, continues throughout the Cold War (Conner, 2003: 461). The increased importance of science leads to its use not only in the military but also in other public policy domains (Erat & Arap, 2016a). In this regard, science policy starts to spread in developed and developing nations in the '60s owing to a new understanding of the power of science, a search for rationality in all public policy domains, and initiatives by international actors like the OECD.

Science policy first appears in Turkey around the same time. It emerges in the era of planned development that opens in the '60s since, first, planning is a research-driven product and requires research institutions, and second, science itself makes part of the policy agenda (Erat & Arap, 2016b). From 1960 to 1980, however, no comprehensive science policy emerges, and even the goals in the much-emphasized issues of research staff and research areas cannot be achieved. For this reason, the country lags behind other countries working on science policy during the same period.

Turkish Science Policy from 1983 to 2003 was produced following a detailed study to meet the desired level of progress. The document bears significance in three aspects. First, while some development plans and other earlier documents involves elements that can be interpreted as science policy, this has been the first study to carry out serious analyses, propose long-term solutions to issues, and formulate policy in clear terms. Second, it was prepared using a systems approach. Third, no such study had hitherto been encountered in the formulation of other public policies, either. *Turkish Science Policy from 1983 to 2003* is not only a reference document for all scientific work in this area but also an object of study by itself. Elmacı's work focuses on particular policies in the document rather than its methodology (Elmacı, 2015).

The present study will analyze *Turkish Science Policy from 1983 to 2003* using the conceptual framework of public policy. Thus, it will cover the systems approach as used in the document and the methods it resorts to in policy formulation. The study has been designed in four parts. While the first part will address the systems approach, the second part will review the pre-1980 state science policy. The third part will deal with the methodology and content of *Turkish Science Policy from 1983 to 2003* from the perspective of public policy, and the last part will put the document in a comparison with similar later documents.

Policy As a System

A system is a set of interdependent or interrelated parts that make up an organized or complex collective whole. The systems approach in political science works to account for the entire political process, including the functions of fundamental political actors, through a systems analysis (Heywood, 2012: 45). The systems approach rests on the 1937 work *General Systems Theory* by the biologist Ludwig Von Bertalanffy (Altan, 2016: 306). According to Bertalanffy, the origin of the concept *system* dates back to the pre-Socratic era, and the Aristotelian statement that *the whole is more than the sum of its parts* is an important expression of the ongoing problematic of system. While advancements in Western science did away with the Aristotelian worldview, he argues, the problems concerning the organization of living systems were largely ignored rather than solved. Bertalanffy tries to justify his theory by referring to some particular advancements in science. Modern science is characterized by a tremendous availability of data, technical complexity, and an increase in specialization in every area required by theoretical structures. As a result, physicists, biologists, psychologists, and social scientists have each reverted to their own universe, and it is hard to transition from one area to another. Strikingly, however, similar problems and concepts exist in different areas that evolve independently of each other. Parallel developments occur in different areas within mutual independence and often without knowledge of what is going on elsewhere. For instance, there is a similarity in procedure between a biological theory, which works with concepts such as individuals, species, and competition coefficients, and quantitive economics or econometrics. On the other hand, the impact of new advancements in biological, behavioral, and social sciences requires us to expand our conceptual schema where physics applications fall short. For instance, while living organisms exchanging matter with their environment are open systems, conventional physics and physical chemistry deal with closed systems only.

Bertalanffy argues that such new developments point to the need for generalized systems and make it legitimate to work on a theory of universal principles. He proposes the General Systems Theory as a discipline, which deals with the formulation of principles that hold true for systems. According to him, this indicates the major aims of general systems theory: (1) There is a general tendency towards integration in the various sciences, natural and social. (2) Such integration seems to be centered in a general theory of systems. (3) Such theory may be an important means for aiming at exact theory in the nonphysical fields of science. (4) Developing unifying principles running "vertically" through the universe of the individual sciences, this theory brings us nearer to the goal of the unity of science. (5) This can lead to a much-needed integration in scientific education.

Bertalanffy uses his theory in biology and psychology and suggests that it can be used in all scientific fields. David Easton is the first to adapt the theory to political science and thus to contribute to the development of basic concepts in contemporary policy analysis (Jr, Hedge & Lester, 2008: 95; Knoepfel, Larrue, Frédéric & Hill, 2007: 7). While it is not originally intended for public policy, Easton's work is used in conceptualizing the relationship between policymaking, policy outputs, and the environment, and it influences public policy work produced in the '60s (Parsons, 2001: 23-24). According to Easton, political inquiry concerns itself with how decision-making takes place in society and how decisions are implemented, and considering political life as a system of activities must be key in any approach to analyze the working of this system. Taking the system of political activity as a whole, Easton states that different inputs (demands and supports) exist that sustain the working of the system, that these inputs are transformed into outputs (decisions or policies) by the system processes, and that these outputs bear consequences for the system and the environment both (Easton, 1957: 383-384).

Public policy is viewed as the reaction of the system to demands from the environment. The political system as defined by Easton involves interrelated institutions and processes that generate binding decisions on society and are generally considered to be governmental institutions and political processes. The environment, on the other hand, involves all phenomena such as the social system, the economic system, and the biological environment that lie outside the boundaries of the political system. Thus, the political system differs from all other components of society. The demands that enter the political system as inputs from the environment are actions by individuals and groups to fulfill their interests and values. The "supports" part of the inputs consists of the agreement of individuals and groups to respect election results, pay tax, abide by law, and accept decisions and actions the political system offers as responses to demands. Legislations, rules, court decisions etc., on the other hand, make up the system's outputs (Anderson, 1994: 27). These outputs generate feedback, which, in turn, shapes later demands and supports (Heywood, 2013: 41). The main condition for the system to succeed is to process inputs in the political system and to generate outputs that can meet demands and draw majority support. Therefore, the assessment of how outputs impact the environment and the political system is highly crucial for the system (Saybaşılı, 1985: 25-26).

The systems approach is seen to be helpful in organizing policymaking research and also illuminating in other important aspects of the political process. How do demands from the environment affect the content of public policy and the functioning of the political system? How does public policy affect the environment or consequent policy demands? How good is the political system at converting demands into public policy and preserving itself over time? (Anderson, 1994: 27) Nonewithstanding, the most important critique brought up to Easton's systems approach is that it takes the system as a black box, leaving the internal functioning of the political system unexplained (Birkland, 2011: 27; Birkland, 2005: 188). Since it fails to talk about decision-making procedures and processes in length and treats policy as the product of a black box called the political system, the use of his approach in public policy is believed to be restricted with general and abstract qualities (Anderson, 1994: 27). This is not an issue from the viewpoint of policymakers, however. The fundamental elements of the political system do not bother to open up the black box, and they may often be quite unwilling for any such action. In this regard, judging from the perspective of the actors of the political system, the systems analysis seems to be a good approach since it responds well to questions such as the nature of inputs that enable the sustenance of the system, the challenging pressure conditions brought about by inputs, environmental and systemic problems that constitute such pressure, and the place of outputs in problem solving (Saybaşılı, 1985: 26). It has certain shortcomings for social scientists, however, who want to open up the black box and look into the conditions under which policymaking takes place, that is, the events inside the political system. As a result, the attempts to open up the black box that begin in the '70s continue throughout the '80s and '90s (Jr, Hedge, & Lester, 2008: 96; Parsons, 2001: 77).

The Pre-1980 State Science Policy

In Turkey, the state has always resorted to science in certain areas, both before and during the Republican days. On the other hand, it is only in early '60s that science becomes a policy domain itself. Science policy is nothing more than a concept in many countries around that period. In the OECD's first Ministerial Meeting on Science, only four of the participating ministers actually represent a ministry relating to science and research. Science policy becomes more widespread in time, and in the third meeting, which takes place in 1968, all but a few countries are represented by a minister of science (Türkcan, 1981: 46). In Turkey's science policy move, the introduction of planned development plays a part along with an international trend. After all, science is not only part of the planning agenda or a policy headline but also an important instrument for good planning. Rational planning requires detailed research. The formation of staff and institutions to conduct research for public policy depends on the existence of a science policy. In this regard, important steps in science policy in Turkey include the emergence of science as a policy headline in the plans by the State Planning Organization (DPT), founded in 1960, and the establishment of the Scientific and Technical Research Council of Turkey (TÜBİTAK) to assume an active role in scientific work by the Institution's first five-year development plan (Göker, 2002: 2).

The first five-year development plan (1963 to 1967) sees research as the most efficient way to solve problems in the areas in which development is planned and covers the question of science under the "research" headline. It identifies the numbers of research staff present in higher education and the public sector at the time and offers calculations of research spending. It also lays down objectives to form a proper research environment, train staff, engage in building and equipment investments, and centralize the management of research activities (DPT, 1963). It is significant that in a country that has not been industrialized yet and is still developing, science policy aims to establish infrastructure needed for advanced research (Türkcan, 2009: 496). The single most important development in science policy around this time is the setting of the goal to found TÜBİTAK and the Social and Economic Research Institute to lead any research effort in technology and make relevant policy. While the Institute never comes to life, TÜBİTAK continues to enjoy its place as the main actor in science policy in the country today.

The second five-year development plan (1968 to 1972) identifies that many objectives in the previous plan could not be accomplished. Thus, it states the main goal in science policy to be eliminating structural shortcomings in research and building up manpower. Other important headlines include international collaboration to benefit from other countries' knowhow and collaboration between universities, industries, and the public sector to achieve technical sophistication required for domestic development (DPT, 1968).

By the third five-year development plan (1973 to 1977), neither international collaboration nor domestic inter-institutional coordination reaches the desired level. In addition, while the goal set by the first two plans is to send 6000 students abroad for graduate study, only 1181 (19.7 %) of them can eventually be sent. The budget share of research and development spending falls from 0.41 % in 1964 to 0.35 % in 1970. Therefore, the third five-year development plan diagnoses the main problem in science policy to be the inability to build research infrastructure and proposes new objectives accordingly (DPT, 1973). On the other hand, the fourth five-year development plan (1970-1983) states that the problems previously identified continue to trouble the scientific

field and puts forward the criticism that TÜBİTAK fails to establish the necessary connections between the development plans and the science and technology system and to shift the domain of activity to industry (DPT, 1979). Indeed, TÜBİTAK has been founded to support research activities that would be the engine of development. In its first twenty-five years, however, it supports 2868 projects through its Research Groups, 2385 of which are eventually finalized, but only 180 ever come to life (TÜBİTAK, 1989). While it shares the goals specified in the previous plans, the fourth plan is a more critical text, but upon the changes in Turkish economic thinking introduced by the decisions of January the 24th, 1980, and the military intervention of September 12th, 1980, it loses all prospects of being implemented. One critical point suggested by the plan is that ambiguities exist in science policy (DPT, 1979: 48). In other words, it makes clear that setting goals relating to the budget share and the number of researchers only is an inadequate approach to science and technology. Thus, it is safe to argue that this period does not display systematic or consistent policy thinking but merely consists of the beginning of science policymaking. *Turkish Science Policy 1983 to 2003* (Şenses & Taymaz, 2003), which attempts to formulate science in the light of a certain system and is considered to be the first science policy document in Turkey, is born under such circumstances.

The Document *Turkish Science Policy from 1983 to 2003*

Turkish Science Policy from 1983 to 2003 consists of five main parts: (i) the importance of science policy, (ii) science history from Turkish-Islamic science to the 1980s, (iii) the systems approach, (iv) Turkey's science and research system, its problems, and international comparisons, and (v) Turkey's long-term science and research policy (The Department of State, 1983). For the purposes of this study, the document will be analyzed beginning from the part on the systems approach.

The third part of the document talks about the systems approach and the reason why it is chosen in methodology. According to this part, the main point of departure for science policymaking is that science is such an important area that we cannot afford to manage it without planning. The reason why the systems approach is embraced in science policy, on the other hand, is that this approach allows us to take science in all its aspects and circumstances. As much as science and technology, which is considered an open system, is in interaction with other policy domains, the problems resulting from this system are in interaction with the problems of society. The systems approach enables us to take the system as a whole, to focus on its parts, and to pay attention to the interaction among the parts rather than solely deal with each element individually. In other words, every output of the system can shape the actions of the system. This, in turn, makes the feedback control feature of the systems approach useful. This way, the science and technology system earns the ability to constantly adapt through feedback and develop policy accordingly. In this regard, feedback functions as a performance assessment system.

In *Turkish Science Policy from 1983 to 2003*, in the center of the science and technology system lie all research and development institutions. Close systems include industry and trade, agriculture, healthcare, higher education, physical infrastructure, and national defense. The international science and technology scene, the natural environment, and culture stand a little further in its periphery (Figure I). The document first examines Turkey's science and technology policy with its subsystems and environment and depicts it through both qualitative and quantitive indicators. Second, it diagnoses the problems and shortcomings of the current system and draws comparisons with countries that it takes as examples. Third, it sets the main goals and policies for future work. Lastly, it highlights the ways in which the science and technology system is connected with the close systems and specifies which areas should be prioritized.

Figure I: The Science and Technology System and Its Environment.

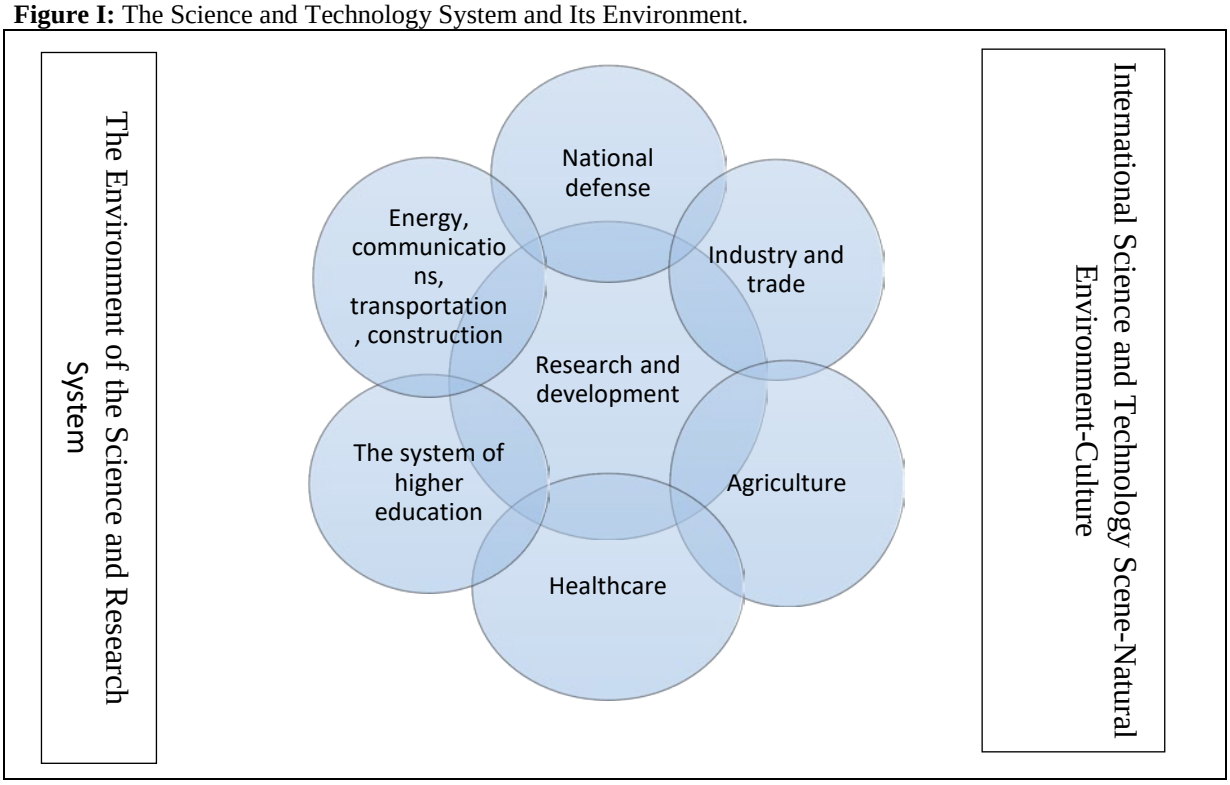

Source: Devlet Bakanlığı, 1983:29 (The Department of State, 1983: 29)

In assessing the science and technology system, six comprehensive indicators are defined, which are: institutional structure, manpower recruited in research and development, research and development spending, technological structure and sophistication, the information system, and external relations. The indicators stand in relation with one another. In other words, not only may development in one area affect other areas, but at the same time true progress is not possible without a shared development taking place in all areas. For this reason, first, the situation relating to each indicator is evaluated. As can be seen in Table I[1], these evaluations are made based on various sub-indicators. The sub-indicators, all of which are components of the science and technology system, are also each dealt with as a system by itself. This way, each subsystem provides important data concerning the indicators, based on which the problems of the science and technology system are identified using the method of international comparison. Comparisons are generally drawn with countries with sophisticated science and technology systems.

The problem assessments and the comparisons are followed by the last part, in which Turkey's long-term science policy is formulated. A detailed policy formulation is offered without breaking away from the systems approach. Before this is done, however, a general set of principles are defined for science and research policy, which apply for the entirety of the science and research system. This is important since it shows that the system has common goals. In other words, not only policies are made to eliminate the problems unique to each subsystem and move that subsystem forward, but at the same time, principles are set for the science and research system as a whole. The following are the principles defined:

- Science and research policy should constitute a dynamic system that tracks change well.
- Decisions in policy formulation and implementation should be made at the government level and have the same sanctioning force as development plans.
- Policy should be such as to contribute to national welfare and development.
- Policy should aim to deliver national technical self-sufficiency.
- Caution should be taken in seeking solutions to problems of a social nature.

[1] The table was created by the authors to show the indicators the document *Turkish Science Policy from 1983 to* 2003 uses to depict the science and research system, the evaluation criteria for these indicators, the evaluation methods and results, and the policies developed.

- Attention should be paid to make policy in agreement with economic development, put research results into application, absorb imported technology, and recruit qualified staff in fundamental and applies sciences.

In addition to these principles, five main goals are set for the entire system under the so-called "ideal to reach the level of contemporary civilization in science":

- Raising the level of scientific development, and cultural enrichment,
- Increasing the impact of science and technology in economic and social development,
- Using science and research in defense force,
- Using science and research to contribute to the infrastructure and service sectors,
- Improving healthcare and welfare, and protecting nature.

Besides these main goals, 84 subgoals are defined across industries, which we will not go into here. Table I shows the main policies for each indicator. In addition, fundamental sciences, national defense research, and science and research areas by different industries are assessed, and policies are offered accordingly. The policies are made considering the then-current situation of the country.

Science Documents after *Turkish Science Policy from 1983 to 2003*

While *Turkish Science Policy from 1983 to 2003* leads to the formation of a Supreme Council of Science and Technology (BTYK) in line with international norms to make long-term policy in the scientific domain, the document is laid aside without ever being applied (Göker, 2002). The fifth five-year development plan, dated 1984, states that the science and technology masterplan set up by *Turkish Science Policy from 1983 to 2003* should be the main point of departure in science policy (DPT, 1984). In 1988, the State Planning Organization Ad Hoc Committee issues a report entitled *The Science, Research and Technology Masterplan*. Having been prepared by over 100 members from 8 subcommittees in 13 months, the report reviews the situation in Turkey and in the world at the time, the problems that exist in science, research, and technology, and the likely remedies. It highlights that the governments, research institutions, and universities have failed to remain faithful to the policy of guiding scientific research systematically for the purposes of social welfare, specified by *Turkish Science Policy from 1983 to 2003*. The report uses the six indicators in Table I and embraces the policies in *Turkish Science Policy from 1983 to 2003*, without adding a word, in certain areas. In addition, it makes occasional references to the document and uses much of its data dated 1983 (DPT, 1988). On the other hand, the report does not take *Turkish Science Policy from 1983 to 2003* as its main point of departure, and while it displays resemblance to the document, it was prepared using no specific model.

This report never finds application, either, and in its second meeting, which takes place in 1993, the Supreme Council of Science and Technology releases a report by the name *Turkish Science and Technology Policy from 1993 to 2003*, which depicts the situation in Turkey at time relying on data concerning the number of researchers, research spending and scientific publications. The "goals" part of the report covers concepts such as competition and innovation that reflect international developments (TÜBİTAK, 1993). On the other hand, it has a poor methodology in comparison to the document *Turkish Science Policy from 1983 to 2003*. *The Project for Advancement in Science and Technology*, which comes two years later based on the seventh five-year development plan and focuses directly on goals, manages to set goals that are in tune with its day, but it still fails to reach the same level of comprehensiveness as *Turkish Science Policy from 1983 to 2003* (TÜBİTAK, 1995). Nonewithstanding, the '90s is a decade that sees more initiatives in science and technology as opposed to the '80s (Göker, 2002: 10). Finally comes *The National Science and Technology Policies 2003 to 2023 Strategy Document / Vision 2023*, which is in effect today. *Vision 2023* appears closer to *Turkish Science Policy from 1983 to 2003* in methodology. Having been prepared in a period of over two years beginning in 2002, this document is the product of 250 experts, 192 meetings, and 36 panel meetings and workshops. For its technological forecasting work, 7000 experts were sent surveys, 2400 of whom returned a response. The report portrays the existing situation and offers roadmaps for policies, strategies, and goals in the areas likely to bring the country more competitive power (TÜBİTAK, 2004). While it does not mention the systems approach or any other method, *Vision 2023* does not overlook the subsystems that make up the science and research system in *Turkish Science Policy from 1983 to 2003*. The other documents mentioned above demonstrate a similar approach as well. In other words, not only is *Turkish Science Policy from 1983 to 2003* Turkey's first comprehensive science policy, but at the same time it has invented a tradition influencing all later policy documents.

Conclusion

Turkish Science Policy from 1983 to 2003 was the product of Turkey's efforts to catch up at a time when it found itself staying behind the developments in science policy since the field's emergence in the '60s until the '80s. Previously, the development plans set goals relating to research spending and the numbers of researchers, but a comprehensive science policy never came into being. TÜBİTAK, which was founded in the '60s to be an important actor in science policy and conduct research in fundamental sciences, failed to play an active role. However, in Germany, for instance, where similar points were being made, the policy to spread an interest in fundamental sciences among youth brought about a great advancement (Altuğ et al., 1997). *Turkish Science Policy from 1983 to 2003* was prepared with the idea that the country could not afford to remain behind in the world scientific system anymore.

The document uses the systems approach to formulate science policy objectives. It considers science and research to be in connection and interaction with one another and with their environments so much so that the two make up a single whole with their structures, functioning, and relations. Departing from this, it relies on a detailed study to identify the issues particular to the country's conditions and propose different policies for each headline. *Turkish Science Policy from 1983 to 2003* aims at policies that are legitimate and up-to-date in its time. This document designates technological fields like electronic engineering, computer science, instrumentation, and telecommunications as the areas to be given first priority in development. While South Korea, which adapted the Japanese program to herself and came up with similar projections, made significant advances, Turkey eventually put aside whatever work it was planning to carry out during the same period (Göker, 2002). The policy documents could not be implemented, either, with the exception of *Vision 2023*, which is currently in place. Not only did many initiatives attempted during this period fail to be as comprehensive as *Turkish Science Policy from 1983 to 2003*, but at the same time they lacked a clear approach.

The most critical aspect of *Turkish Science Policy from 1983 to 2003* is that it has been the most detailed science policy document up to its day, and it has taken quite long for another study with such careful science policy planning to follow. Also important is that no similar work can be encountered in other public policy domains. In addition, the document has handed down an approach to science policy, which, while it has not often been used in later science policy documents, sees science and research to constitute a single system.

Table 1: The Roadmap for Science and Research Policymaking

Indicators Used In Determining the Level of the Science and Research System	**Institutional Structures and Their Current Situation**	**Manpower Employed In Research and Development and Its Current Situation**	**Research and Development Spending and Its Current Situation**	**Technological Structure and Its Current Situation**	**The Information/Documentation System**	**External Relations**
	Universities	Researcher	Research and development spending per capita	Industry	Scientific information	Bilateral collaboration
	Institutions affiliated with the Office of the Prime Minister	Technician and equivalent	Research and development spending per researcher		Technological information	Multilateral collaboration
	Agriculture, forestry, veterinary medicine, and livestock farming research	Other support personnel	Total research and development/GDP		Socioeconomic information	
	Other research structures under Ministries					
Evaluation Criteria	Private sector research institutions					
	Issues	**Issues**	**Issues**	**Issues**	**Issues**	**Issues**
	-Goals unclear. -Necessary size yet to be reached. -Insufficient collaboration. -Inadequate accumulation of knowhow. -Lack of equipment. -Administrative issues.	-7 times increase in research and development staff needed. -Low numbers of researchers in private sector. -Education system cannot meet needs. -Wrong wage policy.	-Insufficient research and development funding.	-Low levels of coordination between science and technology. -Technology transfer needed in intermediary and investment goods industry.	-Insufficient training and public awareness. -Weak government support. -No structure to coordinate. -No information network. -No connection with international system.	-Ambiguities and irregularities in collaboration.
	International Comparison	**International Comparison**	**International Comparison**	**International Comparison**	**International Comparison**	**International Comparison**
Evaluation Results and Method	Germany, France, Japan, Spain	Germany, France, Japan, Britain, USA, USSR	21 countries	USA, USSR, France, Japan	Germany, France, Japan, Spain, Brazil	
	Body to carry out judicial functions	Increasing number of staff	University research funding	Technology transfer	Informations training	To make bilateral agreements
	Body to carry out executive functions	Improving staff quality	Public sector research funding	Technological innovation incentives	Planning in national information system (scientific, technological, and socioeconomic)	Following universal developments closely
The Long-Term Science and Research Policy Determined	Body to constantly monitor science policy	Sectoral distribution to be done in situ	Private sector research incentives	Active and efficient use of technologies transferred	Connections with international information system	

References

Altan, Y. (2016). Sistem Modeli. H. Altunok, & F. G. Gedikkaya içinde, *Kamu Politikaları Ansiklopedisi* (s. 306-309). Ankara: Nobel Yayın.

Altuğ, T., Eti, Ş., Kaya, G., Akın, C., Özden, İ., Tasalı, E., . . . Hatemi, A. (1997). Ülkemiz Gençliğini doğa Bilimlerinde Bilimsel Araştırmaya Özendirmek Amacıyla Uygulanan 10 Yıllık Bir Programın sonuçları. E. akalın, H. Aydoğdu, & R. Saraoğlu içinde, *Bilim, Bilim Politikası ve Üniversiteler* (s. 91-94). İstanbul: Bağlam Yayıncılık.

Anderson, J. E. (1994). *Public Policymaking*. Boston: Houghton Mifflin Company.

Ansal, H. (1997). Bilim ve emek Süreci. E. Akalın, H. Aydoğdu, & R. Saraoğlu içinde, *Bilim, Bilim Politikası ve Üniversiteler* (s. 187-193). İstanbul: Bağlam yayıncılık.

Bertalanffy, L. v. (1968). *General System Theory*. New York: George Braziller.

Bertalanffy, L. V. (1972). The History and Status of General Systems Theory. *The Academy of Management Journal, 15*(4), 407-426.

Birkland, T. A. (2005). Models of the Policy Process. J. Rabin içinde, *Encyclopedia of Public Administration and Public Policy* (s. 188-191). Boca Raton: Taylor & Francis Group.

Birkland, T. A. (2011). *An Introduction To The Policy Process.* New York: M.E. Sharpe.

Conner, C. D. (2013). *Halkın Bilim Tarihi.* Ankara: TÜBİTAK.

Devlet Bakanlığı. (1983). Türk Bilim Politikası 1983-2003. Ankara: Devlet Bakanlığı.

DPT. (1963). *Birinci Beş Yıllık Kalkınma Planı (1963-1967).* Ankara: Devlet Personel Başkanlığı.

DPT. (1968). *İkinci Beş Yıllık Kalkınma Planı (1968-1972).* Ankara: Devlet Planlama Teşkilatı.

DPT. (1973). *Üçüncü Beş Yıllık Kalkınma Planı (1973-1977).* Ankara: Devlet Planlama Teşkilatı.

DPT. (1979). *Dördüncü Beş Yıllık Kalkınma Planı (1979-1983).* Ankara: Devlet Planlama Teşkilatı.

DPT. (1984). *Beşinci Beş Yıllık Kalkınma Planı (1984-1989).* Ankara: DPT.

DPT. (1988). *Bilim Araştırma Teknoloji.* Ankara: T. C. DPT Müsteşarlığı.

Easton, D. (1957). An Approach to the Analysis of Political Systems. *World Politics, 9*(3), 383-400.

Elmacı, İ. (2015). Bilim Politikası Çalışmalarında Bütünsellik Arayışı ve "Türk Bilim Politikası 1983-2003". *Ankara Üniversitesi Dil ve Tarih-Coğrafya Fakültesi Dergisi, 55*(1), 55-68.

Erat, V. (2016). Bir Kamu Politikasının Analizi: Türkiye'de Bilim. İzmir: İzmir Dokuz Eylül Üniversitesi (Yayımlanmamış Doktora Tezi).

Erat, V., & Arap, İ. (2016a). Bilimin Devlet İçin Önemi: Bilim-Devlet İlişkisi Üzerine Bir Çözümleme. *Eğitim Bilim toplum, 14*(53), 10-45.

Erat, V., & Arap, İ. (2016b). *Dünyada ve Türkiye'de Bilim-İktidar İlişkisinin Evrimi.* Ankara: Notabene.

Göker, A. (2002). Türkiye'de 1960'lar ve Sonrasındaki Bilim ve Teknoloji Politikası Tasarımları Niçin [Tam] Uygula[ya]madık? *Ulusal Bilim Politikası Paneli.* Ankara: ODTÜ Öğretim Elemanları Derneği.

Heywood, A. (2012). *Siyasetin Temel Kavramları.* Ankara: Adres Yayınları.

Heywood, A. (2013). *Siyaset.* Ankara: Adres Yayınları.

Jr, J. S., Hedge, D., & Lester, J. P. (2008). *Public Policy*. Boston: Thomson Wadsworth.

Knoepfel, P., Larrue, C., Frédéric, V., & Hill, M. (2007). *Public Policy Analysis.* Bristol: The Policy Press.

Parsons, W. (2001). *Public Policy*. Cheltenham: Edward Elgar Publishing.

Saybaşılı, K. (1985). *Siyaset Biliminde Temel Yaklaşımlar.* Ankara: Birey ve Toplum Yayınları.

Şenses, F., & Taymaz, E. (2003). Unutulan Bir Toplumsal Amaç: Sanayileşme Ne Oluyor? Ne Olmalı? *ERC Working Papers in Economics, 3*(1-23). 02 26, 2017 tarihinde http://erc.metu.edu/menu/series03/0301.pdf adresinden alındı

TÜBİTAK. (1989). *25. Yılında TÜBİTAK.* Ankara: TÜBİTAK.

TÜBİTAK. (1993). *Türk Bilim ve Teknoloji Politikası 1993-2003.* Ankara: TÜBİTAK.

TÜBİTAK. (1995). *Bilim ve Teknolojide Atılım Projesi.* Ankara: TÜBİTAK.

TÜBİTAK. (2004). *Ulusal Bilim ve Teknoloji Politikaları 2003-2023 Strateji Belgesi.* Ankara: TÜBİTAK.

Türkcan, E. (1977). Örgütsel Oluşum ve İşlev Arayışı: TÜBİTAK Olayı. *Amme İdaresi Dergisi, 10*(4), 46-64.

Türkcan, E. (1981). Ekonomi Politiğin Bir Aracı Olarak Bilim Politikası. *Ekonomik Yaklaşım, 2*(5), 34-77.

Türkcan, E. (2003). Teknoloji Seçimi Olarak Bilim ve Teknoloji Politikaları. A. H. Köse, F. Şenses, & e. Yeldan içinde, *İktisadi Kalkınma, Kriz ve İstikrar* (s. 153-169). İstanbul: İletişim Yayınları.

Türkcan, E. (2009). *Dünyada ve Türkiye'de Bilim, Teknoloji ve Politika.* İstanbul: Bilgi Üniversitesi Yayınları.

THE EFFECT OF ROAD ROUGHNESS ON THE HALF VEHICLE MODEL AT DIFFERENT SPEEDS

Yusuf Alptekin TÜRKKAN[1], Gürsel ŞEFKAT[2]
[1, 2] Uludag University, Mechanical Engineering Department, Bursa, Turkey
turkkan@uludag.edu.tr, sefkat@uludag.edu.tr

Abstract: In this study, equations of motion have been obtained through different methods used in mathematical model of system based on car physical models. To determine system behavior in variable road inputs, half car and seat mounted half car models have been constituted. Using the method of Lagrange which is one of the mathematical modeling method responses to system's all physical models, mathematical models have been established. SIMULINK modeling program worked in MATLAB package has been used for computer solutions of system. Simulations have been made to the response to half car model hard road roughness and seat mounted half car model the to the road roughness at different speeds. As a result of made simulations, transmitted vibrations to seat and driver have been obtained.
Keywords: Half-car, Simulink, Lagrange, Road Roughness, Ride Comfort

Introduction

While important of motor vehicles in our life is known to all, effect of human health is not known exactly. Vehicles, beyond the damage to people due to accident, there may also be some effect on human health outside accident. For this purpose, a lot of scientist has made study about what can be this damage and they have published these studies.

In this study, using MATLAB and Simulink programs semi vehicle and seat entrained semi vehicle models have been constituted from equations obtained using Lagrange method. In created models to simulate, bump input has been given in step and model of seat entrained semi vehicle in addition to other models, vibrations which has been given of the same bump input on seat and chassis in different speeds have been obtained

Modeling and Solutions

Primarily, equation of motion has been taken for analytical solutions of suspension systems. Equation of motion has been derived by Lagrange method. The motion equation are given below according to figure 1.

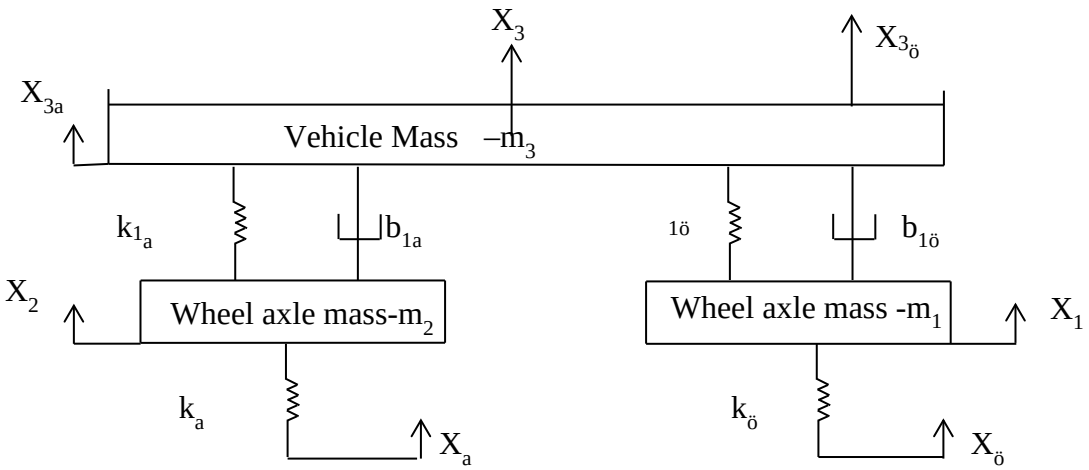

Figure 1. Semi Vehicle Model

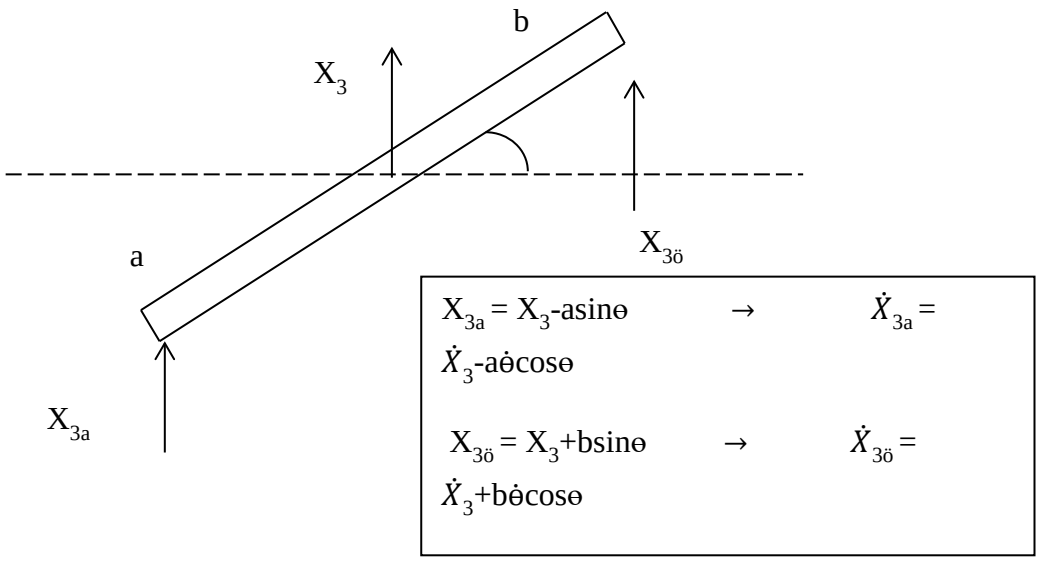

Figure 2. Motion of Inertia

$$\ddot{x}_1 = (b_{1ö}(\dot{x}_3 + b\dot{\theta} - \dot{x}_1) + k_{ö}(x_{ö} - x_1) + k_{1ö}(x_3 + b - x_1))\frac{1}{m_1} \quad (1)$$

$$\ddot{x}_2 = (b_{1a}(\dot{x}_2 + \dot{\theta}a - \dot{x}_3) + k_a(x_a - x_2) + k_{1a}(x_3 - a - x_2))\frac{1}{m_2} \quad (2)$$

$$\ddot{x}_3 = (k_{1ö}(x_1 - b - x_3) + k_{1a}(x_2 + a - x_3) + b_{1ö}(\dot{x}_1 - b\dot{\theta} - \dot{x}_3) + b_{1a}(\dot{x}_2 + \dot{\theta}a - \dot{x}_3))\frac{1}{m_3} \quad (3)$$

$$\ddot{\theta} = (b_{1ö}b(\dot{x}_1 - b\dot{\theta} - \dot{x}_3) + b_{1a}a(\dot{x}_3 - \dot{\theta}a - \dot{x}_2) + k_{1ö}b(x_1 - b - x_3) + k_{1a}a(x_3 - a - x_2))\frac{1}{I} \quad (4)$$

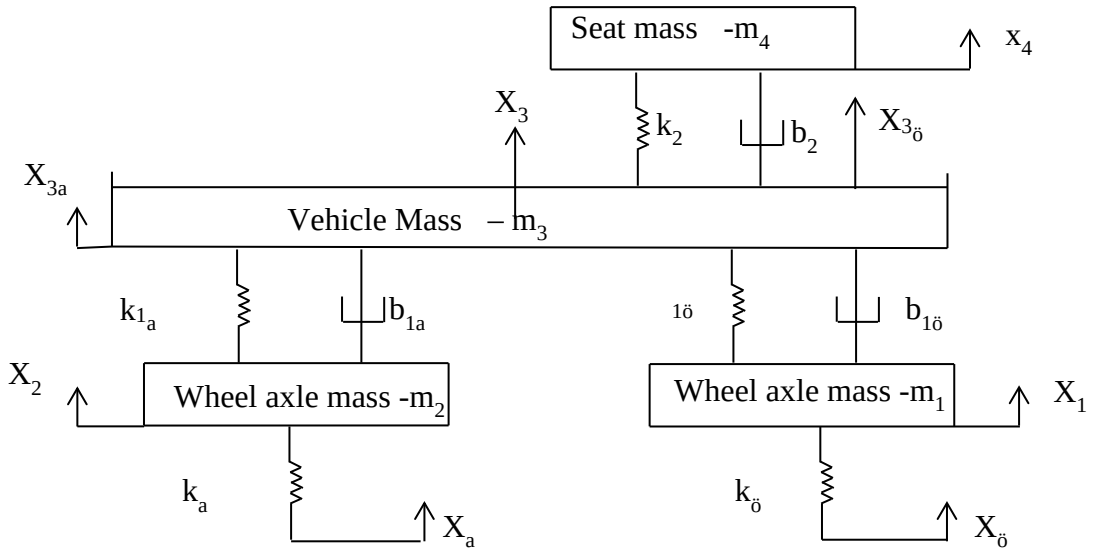

Figure 3. Seat Entrained Semi Vehicle Model

The inertia movement that occurs when the car brakes or accelerates is shown in figure 2. Seat entered semi vehicle model is shown in figure 3.

$$\ddot{x}_1 = (b_{1\ddot{o}}(\dot{x}_3 + b\dot{\theta}cos\theta - \dot{x}_1) + k_{\ddot{o}}(x_{\ddot{o}} - x_1) + k_{1\ddot{o}}(x_3 + bsin\theta - x_1))\frac{1}{m_1} \quad (5)$$

$$\ddot{x}_2 = (b_{1a}(\dot{x}_3 + \dot{\theta}acos\theta - \dot{x}_2) + k_a(x_a - x_2) + k_{1a}(x_3 - asin\theta - x_2))\frac{1}{m_2} \quad (6)$$

$$\begin{aligned}\ddot{x}_3 = (&k_{1\ddot{o}}(x_1 - bsin\theta - x_3) + k_{1a}(x_2 + asin\theta - x_3) + k_2(x_4 - bsin\theta - x_3) \\ &+ b_{1\ddot{o}}(\dot{x}_1 - b\dot{\theta}cos\theta - \dot{x}_3) + b_{1a}(\dot{x}_2 + \dot{\theta}acos\theta - \dot{x}_3) \\ &+ b_2(\dot{x}_4 - \dot{\theta}bcos\theta - \dot{x}_3))\frac{1}{m_3}\end{aligned} \quad (7)$$

$$\ddot{x}_4 = (b_2(\dot{x}_3 + \dot{\theta}bcos\theta - \dot{x}_4) + k_2(x_3 + bsin\theta - x_4))\ \frac{1}{m_4} \quad (8)$$

$$\begin{aligned}\ddot{\theta} = (&b_{1\ddot{o}}bcos\theta(\dot{x}_1 - b\dot{\theta}cos\theta - \dot{x}_3) + b_{1a}acos\theta(\dot{x}_3 - \dot{\theta}acos\theta - \dot{x}_2) \\ &+ b_2bcos\theta(\dot{x}_4 - \dot{\theta}bcos\theta - \dot{x}_3) + k_{1\ddot{o}}bcos\theta(x_1 - bsin\theta - x_3) \\ &+ k_{1a}acos\theta(x_3 - asin\theta + x_2) + k_2bcos\theta(x_4 - bsin\theta - x_3))\frac{1}{I}\end{aligned} \quad (9)$$

Case to effect the simultaneous on two wheels was examined in semi vehicle simulation applied bump model. However, this simulation just can be viable in theory. In practice, the first vehicle's leading wheel would enter bumps; rear wheel depending on the speed would enter after a certain time. In figure 4, figure 5 and figure 6, simulation of seat entrained semi vehicle model exposed to h=0.1m bumps is made at different speeds.

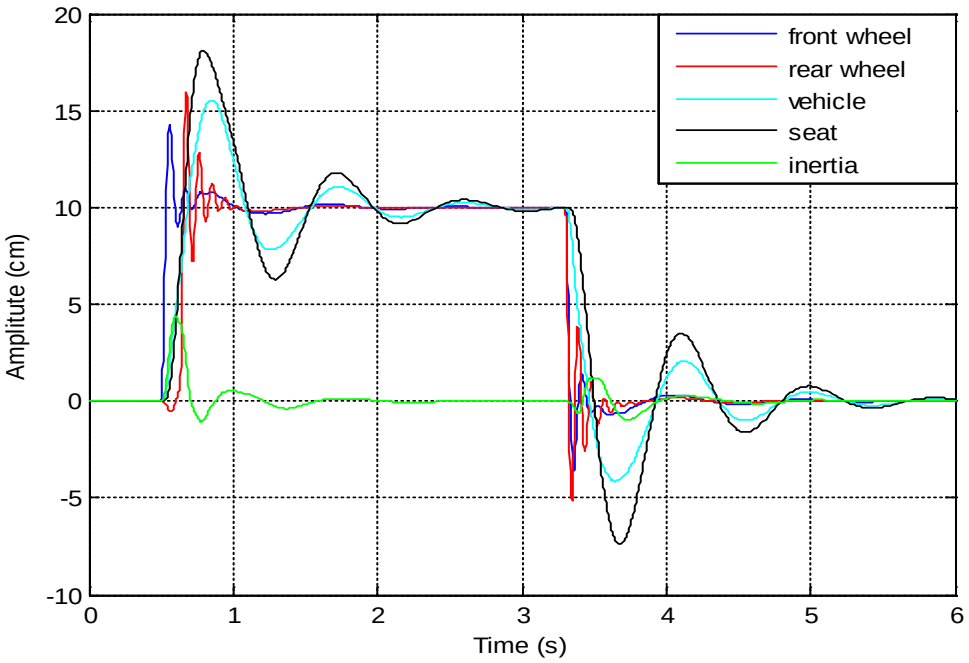

Figure 4. Step input Position-Time Graph For V= 75,6 km/h ve h=0.10m

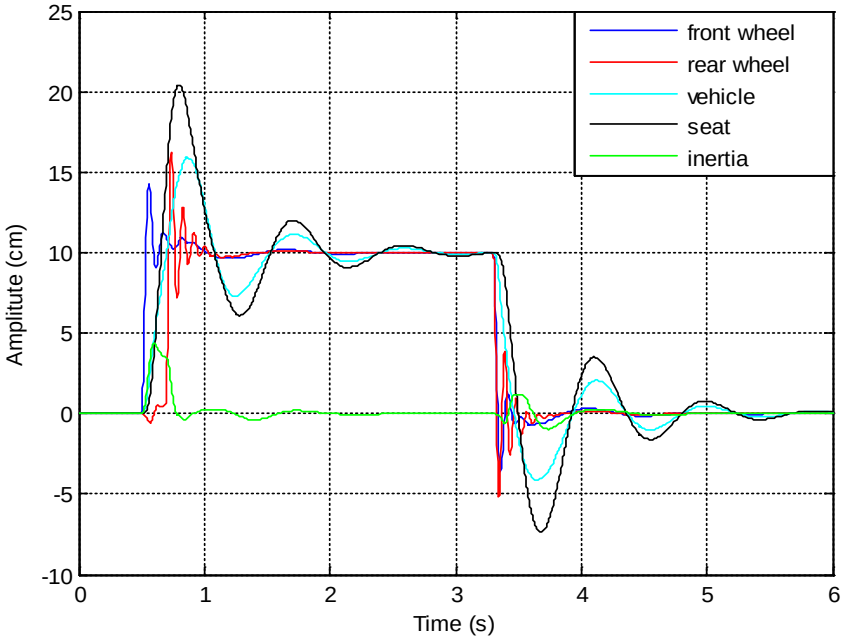

Figure 5. Step input Position-Time Graph For V= 50,4 km/h ve h=0.10m

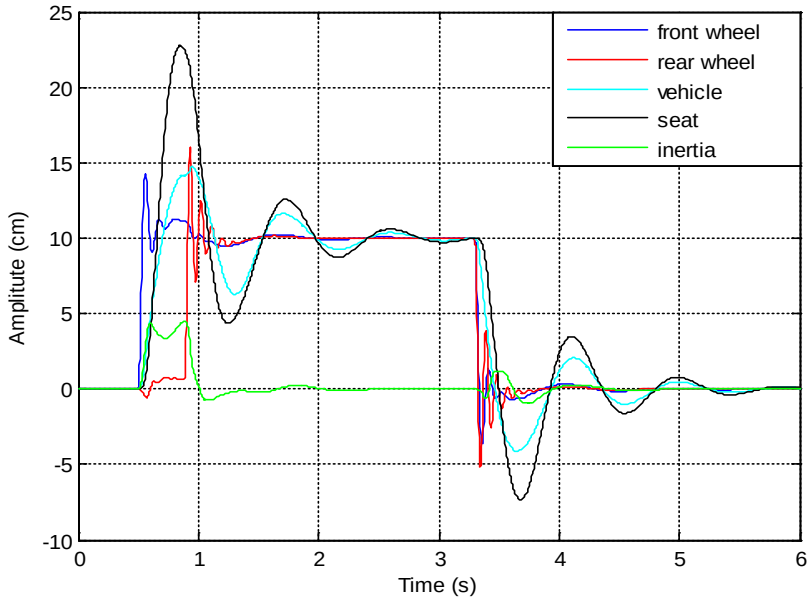

Figure 6. Step input Position-Time Graph For V= 25,2 km/h ve h=0.10m

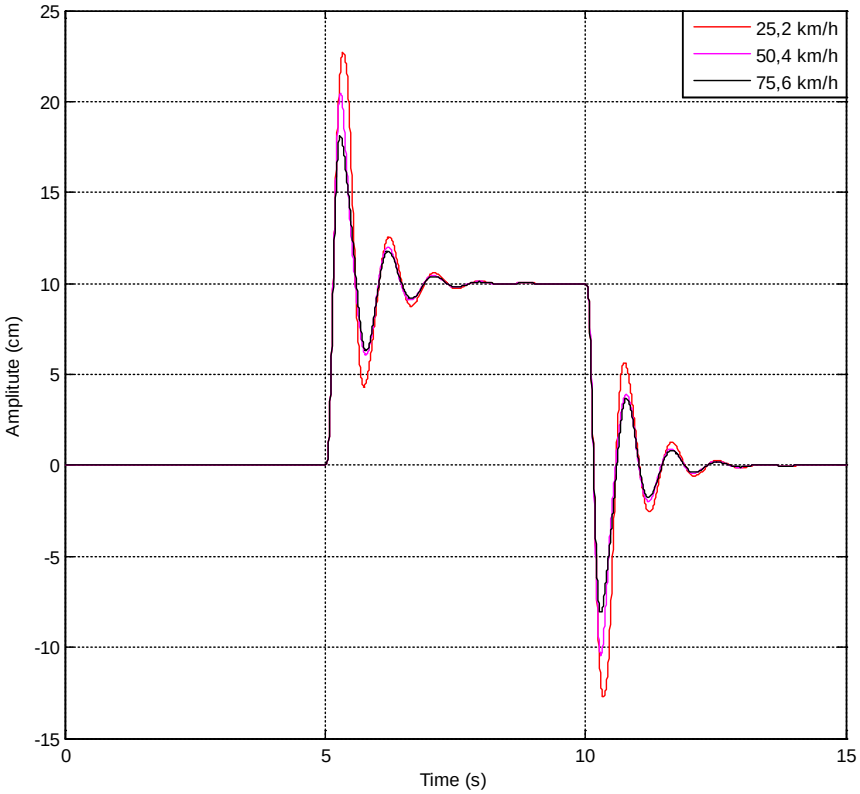

Figure 7. Seat Entrained semi-vehicle model at different speeds time dependent displacement graph

Results and Discussions

As a result of analysis, semi vehicle and seat entered semi vehicle models, motion of inertia is less about %27 in with seat models.

In this study, semi-vehicle model, phase difference occurring in the front and rear wheels depend on vehicle axle length and speed staking the route entry has been applied and effect of speed on system has been tried to scrutinize. According to the simulation results, it is noted that changing the location of the seat decreases with increasing speed but the front and rear suspension with increased displacement.

Conclusion

The results of this analysis, the value of these positions that vary depending on the system parameters have been shown to occur inevitably in the passive suspension system. This study conducted has a basis for analysis through passive suspension system of full vehicle and seat entrained full vehicle models. It was observed that vehicle comfort of a semi-active or active suspension can be improved by controlling the dynamic comfort systems and condition of comfort can be improved in limited circumstances in the passive suspension system with fixed-valued parameters.

In next studies, it is recommended that Conducting research about suspension characteristics and the structure will be developed implementation on a real vehicle for improvement of vehicle dynamics and safer driving at high speeds.

References

Rane S. (2008), Real Time Ride Comfort Development and Validation of a Methodology. Department of Mechanical Engineering., Indian Institute of Technology, Delhi.

Tuncel, H.O.(2008), Kamyon Kabin Süspansiyonun İncelenmesi ve Konfor Optimizasyonu. İTÜ Fen Bilimleri Enstitüsü Makine Mühendisliği Anabilim Dalı, İstanbul.

Hacıoğlu, Y. (2009), Mekanik Sistemlerin Geri Adımlamalı Kontrolü. İÜ Fen Bilimleri Enstitüsü Makine Mühendisliği Anabilim Dalı, İstanbul.

Kim M. S. Kim K. W. ve Yoo W. S.. (2011), Method to Objectively Evaluate Subjective Ratings of Ride Comfort. International Journal of Automotive Technology. 12(6): 831−837

Türkkan Y.A.,2014. Sürüş konforu için taşit koltuk titreşimlerinin modellenmesi ve analizi. UÜ Fen Bilimleri Enstitüsü Makine Mühendisliği Anabilim Dalı, Bursa.

